

**IST-4-027756 WINNER II**  
**D1.1.2 V1.2**  
***WINNER II Channel Models***

**Part I *Channel Models***

**Contractual Date of Delivery to the CEC:** 30/09/2007

**Actual Date of Delivery to the CEC:** 30/09/2007 (updated 04/02/2008)

**Author(s):** Pekka Kyösti, Juha Meinilä, Lassi Hentilä, Xiongwen Zhao, Tommi Jämsä, Christian Schneider, Milan Narandzić, Marko Milojević, Aihua Hong, Juha Ylitalo, Veli-Matti Holappa, Mikko Alatossava, Robert Bultitude, Yvo de Jong, Terhi Rautiainen

**Participant(s):** *EBITG, TUI, UOULU, CU/CRC, NOKIA*

**Workpackage:** *WP1 Channel Model*

**Estimated person months:** 62

**Security:** PU

**Nature:** R

**Version:** 1.1

**Total number of pages:** 82

**Abstract:**

This deliverable describes WINNER II channel models for link and system level simulations. Both generic and clustered delay line models are defined for selected propagation scenarios.

**Keyword list:** Channel modelling, radio channel, propagation scenario, channel sounder, cluster, polarisation, measurements, delay spread, angle spread, MIMO, fading

**Disclaimer:** The channel models described in this deliverable are based on a literature survey and measurements performed during this project. The authors are not responsible for any loss, damage or expenses caused by potential errors or inaccuracies in the models or in the deliverable.

## Executive Summary

This deliverable presents WINNER II channel models for link level and system level simulations of local area, metropolitan area, and wide area wireless communication systems. The models have been evolved from the WINNER I channel models described in WINNER I deliverable D5.4 and WINNER II interim channel models described in deliverable D1.1.1. The covered propagation scenarios are indoor office, large indoor hall, indoor-to-outdoor, urban micro-cell, bad urban micro-cell, outdoor-to-indoor, stationary feeder, suburban macro-cell, urban macro-cell, rural macro-cell, and rural moving networks.

The generic WINNER II channel model follows a geometry-based stochastic channel modelling approach, which allows creating of an arbitrary double directional radio channel model. The channel models are antenna independent, i.e., different antenna configurations and different element patterns can be inserted. The channel parameters are determined stochastically, based on statistical distributions extracted from channel measurement. The distributions are defined for, e.g., delay spread, delay values, angle spread, shadow fading, and cross-polarisation ratio. For each channel snapshot the channel parameters are calculated from the distributions. Channel realisations are generated by summing contributions of rays with specific channel parameters like delay, power, angle-of-arrival and angle-of-departure. Different scenarios are modelled by using the same approach, but different parameters. The parameter tables for each scenario are included in this deliverable.

Clustered delay line (CDL) models with fixed large-scale and small-scale parameters have also been created for calibration and comparison of different simulations. The parameters of the CDL models are based on expectation values of the generic models.

Several measurement campaigns provide the background for the parameterisation of the propagation scenarios for both line-of-sight (LOS) and non-LOS (NLOS) conditions. These measurements were conducted by seven partners with different devices. The developed models are based on both literature and extensive measurement campaigns that have been carried out within the WINNER I and WINNER II projects.

The novel features of the WINNER models are its parameterisation, using of the same modelling approach for both indoor and outdoor environments, new scenarios like outdoor-to-indoor and indoor-to-outdoor, elevation in indoor scenarios, smooth time (and space) evolution of large-scale and small-scale channel parameters (including cross-correlations), and scenario-dependent polarisation modelling. The models are scalable from a single single-input-single-output (SISO) or multiple-input-multiple-output (MIMO) link to a multi-link MIMO scenario including polarisation among other radio channel dimensions.

WINNER II channel models can be used in link level and system level performance evaluation of wireless systems, as well as comparison of different algorithms, technologies and products. The models can be applied not only to WINNER II system, but also any other wireless system operating in 2 – 6 GHz frequency range with up to 100 MHz RF bandwidth. The models supports multi-antenna technologies, polarisation, multi-user, multi-cell, and multi-hop networks.

This report is divided into two parts. The first part defines the channel model structure and parameters. The second part (separate volume) contains more detailed information about channel measurements and analysis.

**Authors**

<b>Partner</b>	<b>Name</b>	<b>Phone / Fax / e-mail</b>
----------------	-------------	-----------------------------

EBITG	Pekka Kyösti	Phone: +358 40 344 2000 Fax: +358 8 551 4344 e-mail: firstname.lastname@elektrobit.com
-------	--------------	--

EBITG	Juha Meinilä	Phone: +358 40 344 2000 Fax: + e-mail: firstname.lastname@elektrobit.com
-------	--------------	--

EBITG	Tommi Jämsä	Phone: +358 40 344 2000 Fax: +358 8 551 4344 e-mail: firstname.lastname@elektrobit.com
-------	-------------	--

EBITG	Xiongwen Zhao	Phone: +358 40 344 2000 Fax: +358 9 2561014 e-mail: firstname.lastname@elektrobit.com
-------	---------------	---

EBITG	Lassi Hentilä	Phone: +358 40 344 2000 Fax: +358 8 551 4344 e-mail: firstname.lastname@elektrobit.com
-------	---------------	--

UOULU/EBITG	Juha Ylitalo	Phone: +358 40 344 3352 Fax: +358 8 551 4344 e-mail: firstname.lastname@elektrobit.com
-------------	--------------	--

UOULU	Mikko Alatossava	Phone: +358 8 814 7638 Fax: +358 8 553 2845 e-mail: mikko.alatossava@ee.oulu.fi
-------	------------------	---

UOULU	Veli-Matti Holappa	Phone: +358 8 814 2890 Fax: +358 8 553 2845 e-mail: crimson@ee.oulu.fi
TUI	Milan Narandžić	Phone: + 49 3677 69 3722 Fax: + 49 3677 69 1113 e-mail: milan.narandzic@tu-ilmenau.de
TUI	Aihua Hong	Phone: + 49 3677 69 1157 Fax: + 49 3677 69 1113 e-mail: aihua.hong@tu-ilmenau.de
TUI	Marko Milojević	Phone: + 49 3677 69 2673 Fax: + 49 3677 69 1195 e-mail: marko.milojevic@tu-ilmenau.de
TUI	Christian Schneider	Phone: + 49 3677 69 1157 Fax: + 49 3677 69 1113 e-mail: christian.schneider@tu-ilmenau.de
TUI	Gerd Sommerkorn	Phone: + 49 3677 69 1115 Fax: + 49 3677 69 1113 e-mail: gerd.sommerkorn@tu-ilmenau.de
CRC	Robert Bultitude	Phone: 1-613-98-2775 Fax: 1-613-990-7987 e-mail: robert.bultitude@crc.ca
CRC	Yvo de Jong	Phone: 1-603-990-9235 Fax: 1-613-990-6339 e-mail: yvo.dejong@crc.ca
NOK	Terhi Rautiainen	Phone: +358 50 4837218 Fax: + 358 7180 36857 e-mail: terhi.rautiainen@nokia.com

## Table of Contents

<b>1. Introduction .....</b>	<b>7</b>
<b>2. Definitions .....</b>	<b>9</b>
2.1 Terminology .....	9
2.2 List of Symbols .....	12
2.3 Propagation Scenarios .....	14
2.3.1 A1 – Indoor office.....	16
2.3.2 A2 – Indoor to outdoor.....	16
2.3.3 B1 – Urban micro-cell.....	17
2.3.4 B2 – Bad Urban micro-cell .....	17
2.3.5 B3 – Indoor hotspot.....	17
2.3.6 B4 – Outdoor to indoor .....	17
2.3.7 B5 – Stationary Feeder.....	17
2.3.8 C1 – Suburban macro-cell.....	19
2.3.9 C2 – Urban macro-cell.....	19
2.3.10 C3 – Bad urban macro-cell .....	19
2.3.11 C4 – Urban macro outdoor to indoor .....	19
2.3.12 D1 – Rural macro-cell.....	20
2.3.13 D2 – Moving networks.....	20
2.4 Measurement Tools .....	20
2.4.1 Propsound (EBITG, UOULU, Nokia).....	21
2.4.2 TUI sounder .....	22
2.4.3 CRC sounder .....	24
<b>3. Channel Modelling Approach .....</b>	<b>26</b>
3.1 WINNER Generic Channel Model.....	27
3.1.1 Modelled parameters.....	27
3.2 Modelling process .....	27
3.3 Network layout .....	28
3.3.1 Correlations between large scale parameters .....	30
3.4 Concept of channel segments, drops and time evolution.....	33
3.4.1 Basic method for time-evolution.....	33
3.4.2 Markov process based method of time evolution.....	34
3.5 Nomadic channel condition .....	34
3.6 Reduced complexity models.....	35
3.6.1 Cluster Delay Line models for mobile and portable scenarios.....	36
3.6.2 Cluster Delay Line models for fixed feeder links .....	36
3.6.3 Complexity comparison of modelling methods .....	36
<b>4. Channel Models and Parameters.....</b>	<b>37</b>
4.1 Applicability .....	37
4.1.1 Environment dependence .....	37
4.1.2 Frequency dependence.....	37
4.2 Generation of Channel Coefficients .....	37
4.2.1 Generation of bad urban channels (B2, C3).....	42
4.3 Path loss models .....	43

4.3.1	Transitions between LOS/NLOS .....	46
4.4	Parameter tables for generic models.....	46
4.4.1	Reference output values .....	48
4.5	CDL Models .....	49
<b>5.</b>	<b>Channel Model Usage.....</b>	<b>50</b>
5.1	System level description.....	50
5.1.1	Coordinate system.....	50
5.1.2	Multi-cell simulations .....	51
5.1.3	Multihop and relaying .....	53
5.1.4	Interference .....	54
5.2	Space-time concept in simulations .....	55
5.2.1	Time sampling and interpolation.....	55
5.3	Radio-environment settings.....	55
5.3.1	Scenario transitions .....	55
5.3.2	LOS\NLOS transitions .....	55
5.4	Bandwidth/Frequency dependence .....	55
5.4.1	Frequency sampling .....	55
5.4.2	Bandwidth down scaling .....	55
5.4.3	FDD modeling.....	56
5.5	Comparison tables of WINNER channel model versions.....	56
5.6	Approximation of Channel Models .....	60
<b>6.</b>	<b>Parameter Tables for CDL Models.....</b>	<b>61</b>
6.1	A1 – Indoor small office.....	61
6.2	A2/B4 – Indoor to outdoor / outdoor to indoor .....	62
6.3	B1 – Urban micro-cell .....	63
6.4	B2 – Bad Urban micro-cell.....	64
6.5	B3 – Indoor hotspot.....	64
6.6	C1 – Urban macro-cell .....	66
6.7	C2 – Urban macro-cell .....	67
6.8	C3 – Bad urban macro-cell.....	68
6.9	C4 – Outdoor to indoor (urban) macro-cell .....	69
6.10	D1 – Rural macro-cell .....	70
6.11	D2a – Moving networks .....	71
6.12	Fixed feeder links - Scenario B5 .....	72
6.12.1	Scenario B5a .....	72
6.12.2	Scenario B5b.....	73
6.12.3	Scenario B5c .....	75
6.12.4	Scenario B5f.....	75
<b>7.</b>	<b>References.....</b>	<b>77</b>

## 1. Introduction

The goal of WINNER is to develop a single ubiquitous radio access system adaptable to a comprehensive range of mobile communication scenarios from short range to wide area. This will be based on a single radio access technology with enhanced capabilities compared to existing systems or their evolutions. WINNER II is a continuation of the WINNER I project, which developed the overall system concept. WINNER II has developed and optimised this concept towards a detailed system definition. [WINNERII]

The radio interface supports the challenging requirements of systems beyond 3G. It is scalable in terms of carrier bandwidth and carrier frequency range. The system concept supports a wide range of radio environments providing a significant improvement in performance and Quality of Service (QoS). The radio interface optimises the use of spectral resources, e.g. through the exploitation of actual channel conditions and multiple antenna technology. New networking topologies (e.g. relaying) supports cost-effective deployments. Support of advanced resource management and handover eases the deployment of the WINNER system concept enabling seamless service provision and global roaming. [WINNERII]

It has been widely understood that radio propagation has a significant impact on the performance of wireless communication systems. The impact on future broadband systems is even more important due to increased data rate, bandwidth, mobility, adaptivity, QoS, etc. Because of the major influence on the system performance and complexity, radio channel models and simulations have to be more versatile and accurate than in earlier systems.

WINNER I work package 5 (WP5) focused on wideband multiple-input multiple-output (MIMO) channel modelling at 5 GHz frequency range. Totally six partners were involved in WP5 during 2004 – 2005, namely Elektrobit, Helsinki University of Technology, Nokia, Royal Institute of Technology (KTH) in Stockholm, Swiss Federal Institute of Technology (ETH) in Zurich, and Technical University of Ilmenau. In the beginning of Phase I, existing channel models were explored to find out channel models for the initial use in the WINNER I project. Based on the literature survey, two standardised models were selected, namely 3GPP/3GPP2 Spatial Channel Model [3GPPSCM] and IEEE 802.11n. The former is used in outdoor simulations and the latter in indoor simulations. Because the bandwidth of the SCM model is only 5 MHz, wideband extension (SCME) was developed in WINNER I. However, in spite of the modification, the initial models were not adequate for the advanced WINNER I simulations. Therefore, new measurement-based models were developed. WINNER I generic model was created in Phase I. It allows creating of arbitrary geometry-based radio channel model. The generic model is ray-based double-directional multi-link model that is antenna independent, scalable and capable of modelling channels for MIMO connections. Statistical distributions and channel parameters extracted by measurements at any propagation scenarios can be fitted to the generic model. WINNER I channel models were based on channel measurements performed at 2 and 5 GHz bands during the project. The models covered the following propagation scenarios specified in WINNER I: indoor, typical urban micro-cell, typical urban macro-cell, sub-urban macro-cell, rural macro-cell and stationary feeder link.

In the WINNER II project work package 1 (WP1) continued the channel modelling work of WINNER I and extended the model features, frequency range (2 to 6 GHz), and the number of scenarios. Five partners were involved, namely Elektrobit, University of Oulu / Centre for Wireless Communications (CWC), Technical University of Ilmenau, Nokia, and Communication Research Centre (CRC) Canada. WINNER I models were updated, and a new set of multidimensional channel models were developed. They cover wide scope of propagation scenarios and environments, including indoor-to-outdoor, outdoor-to-indoor, bad urban micro-cell, bad urban macro-cell, feeder link base station (BS) to fixed relay station (FRS), and moving networks BS to mobile relay station (MRS), MRS to mobile station (MS). They are based on generic channel modelling approach, which means the possibility to vary number of antennas, the antenna configurations, geometry and the antenna beam pattern without changing the basic propagation model. This method enables the use of the same channel data in different link level and system level simulations and it is well suited for evaluation of adaptive radio links, equalisation techniques, coding, modulation, and other transceiver techniques. Models have been developed in two steps, WINNER II Interim Channel Models [WIN2D111] and the final WINNER II Channel Models (this deliverable, D1.1.2).

This deliverable describes the (final) WINNER II Channel Models. The models are based on WINNER I models [WIN1D54] and WINNER II interim models [WIN2D111]. This deliverable covers new features and new scenarios, such as outdoor-to-indoor urban macro-cell and line-of-sight (LOS) urban macro-cell. Some scenarios have been updated. The indoor part of the moving network scenario has been determined

and whole the scenario has been updated considerably, as well as the model for indoor hot-spot. Bad urban scenarios have also been updated. New features of the WINNER II Channel Models include modelling of the elevation of rays, treating the LOS component of the channel model as a random variable, and moving scatterers in fixed connections. The differences in the scenarios Indoor-to-Outdoor and Outdoor-to-Indoor were noticed to be negligible. Therefore these two scenarios have been merged.

Model parameters have been revised in the cases, where new results have pointed this necessary. Valuable comments have been received also via standardisation work in various standardisation bodies, especially in IEEE802.16m and ITU-R/8F. We have taken into account several such change proposals. Probably most important of them is the tuning of our path-loss models.

During the projects WINNER I and WINNER II the models have been evolved, mainly by adding new scenarios in the models, but also by including new features. In this process we have tried to conserve the model parameters from changes as much as possible. However, some changes have been inevitable. Therefore the models are not exactly the same in this and the earlier deliverables. The propagation scenarios from WINNER Phase I have been included in this document, partly updated. In WINNER Phase II the following new propagation scenarios have been created and documented in this document: indoor-to-outdoor, outdoor-to-indoor, bad urban micro-cell, bad urban macro-cell and moving network scenario. All the propagation scenarios have been listed and introduced in section 2.3. WINNER I, WINNER II interim, and WINNER II final models are compared in section 5.5.

The deliverable is divided into two major parts. This first part is the main part and defines the channel model structure and parameters. The second part contains more detailed information about channel measurements and analysis performed during projects WINNER I and II. The two parts are published in separate volumes to keep the size of each part reasonable.

SCM, SCME, and WINNER I channel models have been implemented in Matlab, and are available via WINNER web site. WINNER II channel model implementation is planned to be available by the end of the year 2007.

Sections 1 - 7 cover the following topics. Section 1 introduces this deliverable. Section 2 expresses some definitions, like the propagation scenarios and introduces the used measurement tools. Section 3 defines the channel modelling approach. Section 4 explains the generation of channel coefficients and describes path loss models as well as parameters for generic models. Section 5 discusses how the channel models are used in system level (multi-link) simulations, sampling, transition scenarios, bandwidth/frequency dependence of the models. Parameter tables for reduced variability (CDL) models can be found from Section 6. Reference list is in Section 7.



## 2. Definitions

### 2.1 Terminology

3GPP	3rd Generation Partnership Project
3GPP2	3rd Generation Partnership Project 2
ACF	Auto-Correlation Function
ADC	Analog-to-Digital Converter
AN	Antenna Array
AoA	Angle of Arrival
AoD	Angle of Departure
AP	Access Point (BS)
APP	A Posteriori Probability
APS	Angle Power Spectrum
AS	Azimuth Spread
ASA	Azimuth Spread at Arrival
ASD	Azimuth Spread at Departure
AWGN	Additive White Gaussian Noise
B3G	Beyond 3G
BER	Bit Error Rate
BRAN	Broadband Radio Access Networks
BS	Base Station
C/I	Carrier to Interference ratio
CDF	Cumulative Distribution Function
CDL	Clustered Delay Line
CG	Concept Group
CIR	Channel Impulse Response
CRC	Communications Research Centre Canada
CW	Continuous Wave
DoA	Direction of Arrival
DoD	Direction of Departure
DS/DES	Delay Spread
EBITG	Elektrobit
ECDF	Experimentally determined cumulative probability distribution function
ESA	Elevation Spread at Arrival
ESD	Elevation Spread at Departure
ESPRIT	Estimation of Signal Parameters via Rotational Invariance Techniques
ETHZ	Eidgenössische Technische Hochschule Zürich (Swiss Federal Institute of Technology Zurich)
ETSI	European Telecommunications Standards Institute
FDD	Frequency Division Duplex
FIR	Finite Impulse Response
FL	Floor Loss, loss between different floors
FRS	Fixed Relay Station
FS	Fixed Station
GPS	Global Positioning System
HIPERLAN	High Performance Local Area Network
HUT	Helsinki University of Technology (TKK)
IR	Impulse Response

---

ISIS	Initialization and Search Improved SAGE
KTH	Kungliga Tekniska Högskolan (Royal Institute of Technology in Stockholm)
LA	Local Area
LNS	Log-Normal Shadowing
LOS	Line-of-Sight
LS	Large Scale
MA	Metropolitan Area
MCSSS	Multi-Carrier Spread Spectrum Signal
METRA	Multi-Element Transmit and Receive Antennas (European IST project)
MIMO	Multiple-Input Multiple-Output
MPC	Multi-Path Component
MRS	Mobile Relay Station
MS	Mobile Station
MUSIC	Multiple Signal Classification
NLOS	Non Line-of-Sight
NOK	Nokia
OFDM	Orthogonal Frequency-Division Multiplexing
OLOS	Obstructed Line-of-Sight
PAS	Power Azimuth Spectrum
PDF	Probability Distribution Function
PDP	Power-Delay Profile
PL	Path Loss
PLO	Phase-locked oscillator
PN	Pseudo Noise
RIMAX	Maximum likelihood parameter estimation framework for joint superresolution estimation of both specular and dense multipath components
RF	Radio Frequency
RMS	Root Mean Square
RT	Roof-top
RX	Receiver
SAGE	Space-Alternating Generalized Expectation-maximization
SCM	Spatial Channel Model
SCME	Spatial Channel Model Extended
SF/SHF	Shadow Fading
SIMO	Single-Input Multiple-Output
SISO	Single-Input Single-Output
SoS	Sum of Sinusoids
std	Standard deviation
SW	Software
TDD	Time Division Duplex
TDL	Tapped Delay-Line
TUI	Technische Universität Ilmenau
TX	Transmitter
UE	User Equipment (MS)
UOULU	University of Oulu
UT	User Terminal (MS)
WA	Wide Area
WINNER	Wireless World Initiative New Radio
WPx	Work Package x of WINNER project

---

---

XPR	Cross-Polarisation power Ratio
XPRH	Horizontal Polarisation XPR
XPRV	Vertical Polarisation XPR

## 2.2 List of Symbols

$\Delta(\bullet)$	Change in parameter value
$(\bullet)^T$	Transpose
$(\bullet)^H$	Hermitian transpose
$(\bullet)^*$	Complex conjugate
$A$	Pairing matrix
$C$	Correlation matrix
$F_{tx}$	Tx antenna array response matrix
$F_{rx}$	Rx antenna array response matrix
$H$	MIMO channel transfer matrix
$N$	Normal distribution
$U$	Uniform Distribution
$\varphi$	Azimuth arrival angle AoA
$\phi$	Azimuth departure angle AoD
$\gamma$	Elevation arrival angle (EAoA)
$\psi$	Elevation departure angle (EAoD)
$\tau$	Delay
$\sigma_t$	RMS delay spread
$\sigma_\varphi$	RMS angle spread of AoA
$\sigma_\phi$	RMS angle spread of AoD
$c_{AoA}$	cluster-wise RMS angle spread of AoA
$c_{AoD}$	cluster-wise RMS angle spread of AoD
$\sigma_{SF}$	Shadow fading standard deviation
$\sigma^2$	Variance
$\zeta$	Per cluster shadowing standard deviation
$\lambda$	Wavelength
$\lambda_0$	Wave number
$\kappa^{yh}$	Vertical-to-horizontal XPR
$\kappa^{hv}$	Horizontal-to-vertical XPR
$\nu$	Doppler frequency
$\alpha$	Complex gain of a propagation path
$c$	Speed of light
$f_c$	Central frequency
$h_{bs}$	BS antenna height
$h'_{bs}$	Effective BS antenna height
$h_{ms}$	MS antenna height
$h'_{ms}$	Effective MS antenna height
$K_R$	Ricean K-factor
$n$	Index to cluster
$P$	Power
$r_\varphi$	AoA distribution proportionality factor
$r_\phi$	AoD distribution proportionality factor
$r_b$	Break point distance
$r_t$	Delay distribution proportionality factor

---

$s$	Index to Tx antenna element
$t$	Time
$u$	Index to Rx antenna element

## 2.3 Propagation Scenarios

The propagation scenarios modelled in WINNER are shown in Table 2-1. The propagation scenarios are explained in more detail in the following paragraphs. In WINNER II the work was divided between Concept Groups (CG) according to the environment they were working at. There were CG:s Local Area (LA), Metropolitan Area (MA) and Wide Area (WA), Mapping of scenarios to Concept Groups is shown in the table Table 2-1 in column CG.

**Table 2-1. Propagation scenarios specified in WINNER.**

Scenario	Definition	LOS/ NLOS	Mob. km/h	Frequ ency (GHz)	CG	Note
A1 In building	Indoor office / residential	LOS/ NLOS	0–5	2 - 6	LA	
A2	Indoor to outdoor	NLOS	0–5	2 - 6	LA	AP inside UT outside. Outdoor environment urban
B1 Hotspot	Typical urban micro- cell	LOS  NLOS	0–70	2 - 6	LA, MA	
B2	Bad Urban micro-cell	NLOS	0–70	2 - 6	MA	Same as B1 + long delays
B3 Hotspot	Large indoor hall	LOS/ NLOS	0–5	2 - 6	LA	
B4	Outdoor to indoor. micro-cell	NLOS	0–5	2 - 6	MA	-Outdoor typical urban B1. -Indoor A1
B5a Hotspot Metropol	LOS stat. feeder, rooftop to rooftop	LOS	0	2 - 6	MA	Same channel model for hot spot and metropol.
B5b Hotspot Metropol	LOS stat. feeder, street-level to street- level	LOS	0	2 - 6	MA	
B5c Hotspot Metropol	LOS stat. feeder, below- rooftop to street-level	LOS	0	2 - 6	MA	Extended B1
B5d Hotspot Metropol	NLOS stat. feeder, above rooftop to street-level	NLOS	0	2 - 6	MA	Extended C2
B5f	Feeder link BS -> FRS. Approximately RT to RT level.	LOS/ OLOS/ NLOS	0	2 - 6	WA	Desired link: LOS or OLOS, Interfering links: LOS/(OLOS) /NLOS FRS -> MS = B1*

**Table 2-1 (continued).**

Scenario	Definition	LOS/ NLOS	Mob. km/h	Frequ ency (GHz)	CG	Note
C1 Metropol	Suburban	LOS/ NLOS	0–120	2 - 6	WA	
C2 Metropol	Typical urban macro-cell	LOS/ NLOS	0–120	2 - 6	MA WA	
C3	Bad Urban macro- cell	NLOS	0–70	2 - 6	-	Same as C2 + long delays
C4	Outdoor to indoor macro-cell	NLOS	0-5	2 - 6	MA	-Outdoor typical urban C2. -Indoor A1
D1 Rural	Rural macro-cell	LOS/ NLOS	0–200	2 - 6	WA	
D2	a) Moving networks: BS – MRS, rural	LOS	0 –350	2 - 6	WA	Very large Doppler variability.
	b) Moving networks: MRS – MS, rural	LOS / OLOS/ NLOS	0 – 5	2 - 6	LA	Same as A1 NLOS

The propagation scenarios listed above have been specified according to the requirements agreed commonly in the WINNER project [WIN1D72]. These are the environments and conditions, where all the WINNER simulations have been carried out. There are a couple of facts that need to be understood about the scenarios and channel models adapted to them:

1. The scenarios cover some typical cases. They are not intended to cover all possible environments and conditions: e.g. the mountaineous or even hilly rural environments have not been covered. Similarly the antenna heights do not cover all values that could be seen reasonable. Generally speaking, the environments are such that are found in urban areas of European and North-American countries.
2. The environments are described in two levels of details: firstly, most of the scenarios use the ordinary way placing the transmitters and receivers, so that the only location parameter is the distance between transmitter and receiver, called non-grid-based models. Secondly, the other group of the scenarios is grid-based. This means that there is a grid of streets or a building layout or both, where the transmitters and receivers can be located e.g. by Cartesian coordinates. This latter group of scenarios include A1, A2, B1, B2 and B4, see 2.3.1 to 2.3.13. Other scenarios belong to the first group.

With these selections we have been able to restrict the number of scenarios reasonable, and still presumably covered representatively the conditions encountered by radio equipment in the field. We have also been able to run some simulations in grid-based scenarios with higher precision than is possible in conventional scenarios.

### 2.3.1 A1 – Indoor office

The scenario A1 has been modelled in D5.4. The layout of the scenario is shown in Figure 2-1. Base stations (Access Points) are assumed to be in corridor, thus LOS case is corridor-to-corridor and NLOS case is corridor-to-room. In the NLOS case the basic path-loss is calculated into the rooms adjacent to the corridor where the AP is situated. For rooms farther away from the corridor wall-losses must be applied for the walls parallel to the corridors. E.g. for the UE at the bottom wall of the lay-out in the Figure 2-1 there are three walls to be taken into account. Finally, we have to model the Floor Loss (FL) for propagation from floor to floor. It is assumed that all the floors are identical. The Floor Loss is constant for the same distance between floors, but increases with the floor separation and has to be added to the path-loss calculated for the same floor.

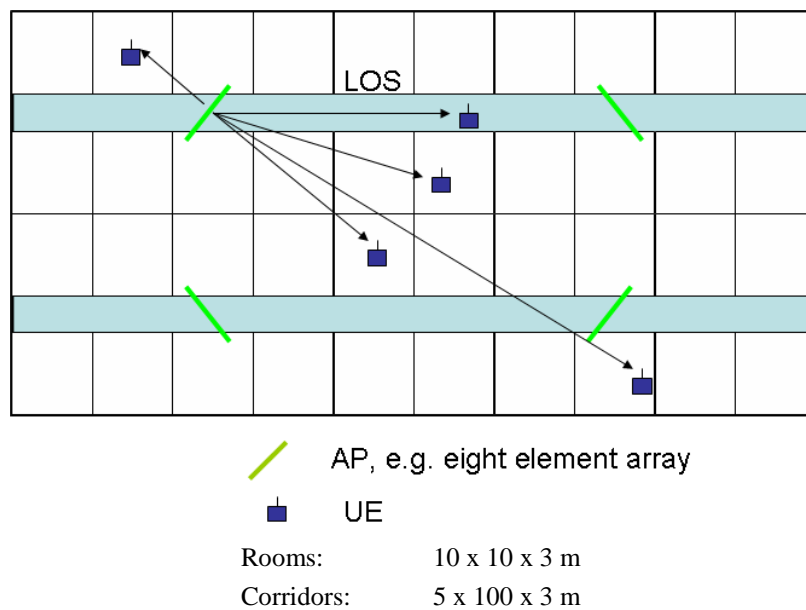


Figure 2-1. Layout of the A1 indoor scenario.

### 2.3.2 A2 – Indoor to outdoor

In indoor-to-outdoor scenario (Figure 2-2) the MS antenna height is assumed to be at 1 – 2 m, and BS antenna height at 2 – 2.5 m + floor height. The corresponding outdoor and indoor environments are B1 and A1, respectively. It is assumed that the floors 1 to 3 are used in simulations, floor 1 meaning the ground floor. The parameters of this scenario have been merged with B4 and C4 in table 4-7. We explain the merging in detail in Part II of the deliverable. The comparison of Outdoor-to-Indoor and Indoor-to-Outdoor scenario characteristics is presented in [AHHM07] and in [HACK07].

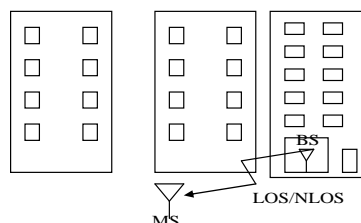


Figure 2-2. Indoor to outdoor scenario.



### 2.3.3 B1 – Urban micro-cell

In urban micro-cell scenarios the height of both the antenna at the BS and at the MS is assumed to be well below the tops of surrounding buildings. Both antennas are assumed to be outdoors in an area where streets are laid out in a Manhattan-like grid. The streets in the coverage area are classified as “the main street”, where there is the LOS from all locations to the BS, with the possible exception in cases where the LOS is temporarily blocked by traffic (e.g. trucks and busses) on the street. Streets that intersect the main street are referred to as perpendicular streets, and those that run parallel to it are referred to as parallel streets. This scenario is defined for both the LOS and the NLOS cases. Cell shapes are defined by the surrounding buildings, and energy reaches NLOS streets as a result of the propagation around corners, through buildings, and between them.

### 2.3.4 B2 – Bad Urban micro-cell

Bad urban micro-cell scenarios are identical in layout to Urban Micro-cell scenarios, as described above. However, propagation characteristics are such that multipath energy from distant objects can be received at some locations. This energy can be clustered or distinct, has significant power (up to within a few dB of the earliest received energy), and exhibits long excess delays. Such situations typically occur when there are clear radio paths across open areas, such as large squares, parks or bodies of water.

### 2.3.5 B3 – Indoor hotspot

Scenario B3 represents the propagation conditions pertinent to operation in a typical indoor hotspot, with wide, but non-ubiquitous coverage and low mobility (0-5 km/h). Traffic of high density would be expected in such scenarios, as for example, in conference halls, factories, train stations and airports, where the indoor environment is characterised by larger open spaces, where ranges between a BS and a MS or between two MS can be significant. Typical dimensions of such areas could range from 20 m × 20 m up to more than 100m in length and width and up to 20 m in height. Both LOS and NLOS propagation conditions could exist.

### 2.3.6 B4 – Outdoor to indoor

In outdoor-to-indoor urban microcell scenario the MS antenna height is assumed to be at 1 – 2 m (plus the floor height), and the BS antenna height below roof-top, at 5 - 15 m depending on the height of surrounding buildings (typically over four floors high). Outdoor environment is metropolitan area B1, typical urban microcell where the user density is typically high, and thus the requirements for system throughput and spectral efficiency are high. The corresponding indoor environment is A1, typical indoor small office. It is assumed that the floors 1 to 3 are used in simulations, floor 1 meaning the ground floor. The parameters of this scenario have been merged with A2 and C4 in table 4-7. We explain the merging in detail in Part II of the deliverable. The comparison of Outdoor-to-Indoor and Indoor-to-Outdoor scenario characteristics is presented in [AHHM07] and in [HACK07].

### 2.3.7 B5 – Stationary Feeder

Fixed feeder links scenario is described in [WIN1D54] and defined as propagation scenario B5. This scenario has also been partly modelled in [WIN1D54]. In B5, both terminals are fixed. Based on this, the scenario is divided in four categories or sub-scenarios in [WIN1D54]. These are B5a (LOS stationary feeder: rooftop to rooftop), B5b (LOS stationary feeder: street level to street level), B5c (LOS stationary feeder: below rooftop to street level) and B5d (NLOS stationary feeder: rooftop to street level). Height of street level terminal antenna is assumed to be 3-5 meters. To cover the needs of CG WA one modified sub-scenario is needed in phase 2, scenario B5f: LOS/NLOS stationary feeder: rooftop-to-below/above rooftop. All the sub-scenarios will be described below.

In stationary scenarios, the Doppler shifts of the rays are not a function of the AoAs. Instead, they are obtained from the movement of the scatterers. In B5 we let one scatterer per cluster be in motion while the others are stationary. In [TPE02] a theoretical model is built where the change of phase of scattered waves between time  $t$  and  $t+\Delta t$  is given by

$$4\pi \frac{f_c}{c} \Delta t \cos(\gamma_p) \cos(\alpha_p) \quad (2.1)$$

where  $\alpha_p$  is the angle between the direction of scatterer movement and  $\gamma_p$  the direction orthogonal to the reflecting surface and the reflection angle. By proper selection of these angles different Doppler spectrums may be achieved. For B5d also an additional term in the path-loss model has to be included.

The feeder scenarios are specified here in connection of the micro-cellular environment. Actually the feeders can be used also in the macro-cellular cases. In this document it is assumed that the useful macro-cellular feeder link, C5, is identical with the feeder model B5c.

### 2.3.7.1 B5a

The signal in B5a can be assumed to consist of a strong LOS signal and single bounce reflection. Also far away reflections can occur. The connection is almost like in free space, so that the path-loss does not depend noticeably on the antenna heights. For this scenario fixed angle spread, delay spread and XPR values are applied. Directive antennas are very effective in reducing the delay spread and other multi-path impacts as explained in [PT00]. However, the model is applicable for omni-directional antennas for up to 300 meters in distance. By using directive antennas the range can be extended approximately to 8 km.

A static (non-fading) channel component is added to the impulse response. We select its power to be 10 dB. The power-delay profile (of all paths except the direct) is set as exponential, based on the results in [OBL+02] and [SCK05]. The shadow fading is Gaussian with mean zero and standard deviation of 3.4 dB based on [PT00]. B5a sub-scenario was specified and modelled in [WIN1D54]. The same channel model is used also in Phase II.

### 2.3.7.2 B5b

In B5b it is assumed that both the transmitter and receiver have many scatterers in their close vicinity similar as theorized in [Sva02]. In addition there can also be long echoes from the ends of the street. There is a LoS ray between the transmitter and receiver and when this path is strong, the contribution from all the scatters is small. However, beyond the breakpoint distance the scatterers start to play an important role.

In papers e.g. [Bul02], [SBA+02] the results for different carrier frequencies are very similar. Therefore, in B5b model the frequency is disregarded. The principle adopted for the WINNER phase 1 model allows for various correlations between different parameters such as angle-spread, shadow-fading and delay-spread. In this case, dependency between path loss and delay-spread [MKA02] is applied. This dependence is handled by selecting one of three different CDL models given in [WIN1D54]. Based on the delay-spread formula in [MAS02] we select the delay spread to be 30 ns when the path loss is less than 85 dB, 110 ns when the path loss is between 85 dB and 110 dB, and finally 380 ns when the path loss is greater than 110 dB. With these settings the delay-spread used here is a factor 40%-156% of the delay-spread formula of [MAS02] for path losses up to 137 dB. We call these path-loss intervals range1, range2 and range3 and different clustered-delay line models will be provided for the three cases.

In terms of path loss, the break point distance calculated as

$$r_b = 4 \frac{(h_b - h_0)(h_b - h_0)}{\lambda} \quad (2.2)$$

becomes important leading to so called two slope -model. The power delay profile (of all paths except the direct) is set as exponential, based on the results in [SMI+00]. A per-path shadow fading of 3 dB is used to obtain some variation in the impulse responses. A static (non-fading) channel component is added to the impulse response. Based on [FDS+94] we select this parameter to be 10 in range1, 2 in range2, and 1 in range3. Also K-factor changes according to range. B5b sub-scenario was specified and modelled in [WIN1D54]. The same channel model is used also in Phase II.

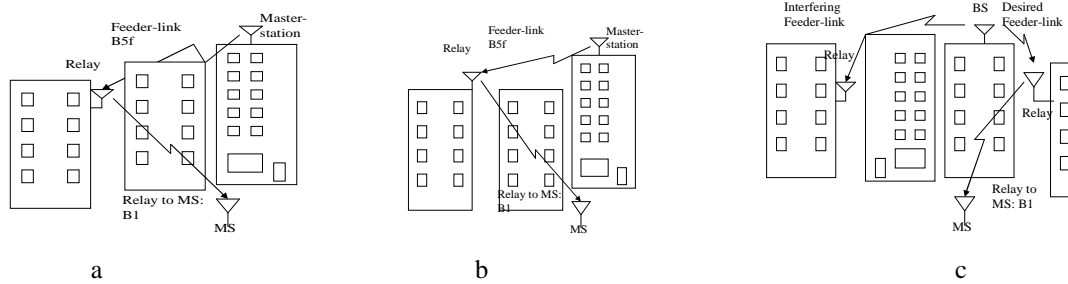
### 2.3.7.3 B5c and B5d

Scenarios B5c and B5d can be considered as LOS of B1 and NLOS of C2 respectively. Only support for Doppler spectrum of stationary cases has to be introduced. B5c is probably the most important feeder link scenario, because it will be used in urban micro-cell relay scenario. B5c is almost identical to the B1 micro-cellular LOS scenario. The only difference in environment is the assumed antenna height of the mobile/relay. Same channel model will cover both of the cases, except the difference in Doppler spectrum (mobility). Feeder link ends are stationary and the Doppler frequency results from motion of the environment. In scenario B5c some clusters represent vehicles with speed of ~50 km/h and the rest of the clusters represent stationary objects like walls and building corners.

Actually B5d seems less useful for a feeder link scenario. Therefore it is not discussed here further.

### 2.3.7.4 B5f

The sub-scenario is shown in the figure below.



**Figure 2-3 B5f scenario for three cases: a) NLOS (OLOS) b) LOS c) Combined interference case.**

B5f scenario consists of the cases with relay antennas some meters over the roof-top or some meters below the roof-top. Critical information is, if the link is LOS or NLOS: It is possible to create LOS links with the antennas below roof-tops. As well it is possible to implement NLOS links with antennas above the average roof-top level. Our approach is that the desired BS to FRS links can be planned to be LOS or OLOS, or at least “good” links. It is assumed that the interfering links from undesired BS to FRS can be LOS or NLOS. (Although in practice this can be also affected by careful planning.) It should be pointed out that the link FRS to MS is covered by the model B1. Interference to undesired feeder link may occur.

In B5f it is assumed that the relay station is shadowed due to some obstacle. The proposed model is based on literature and formed from the B5a LOS fixed relay model by attenuating artificially its direct component by 15 dB in average and summing to it a normally distributed random decibel number with standard deviation 8 dB. The path loss formula is based on the references [ZEA99] and [GEA03]. The other model parameters are the same as in B5a. The model B5f can also be understood as NLOS part of the model B5a.

### 2.3.8 C1 – Suburban macro-cell

In suburban macro-cells base stations are located well above the rooftops to allow wide area coverage, and mobile stations are outdoors at street level. Buildings are typically low residential detached houses with one or two floors, or blocks of flats with a few floors. Occasional open areas such as parks or playgrounds between the houses make the environment rather open. Streets do not form urban-like regular strict grid structure. Vegetation is modest.

### 2.3.9 C2 – Urban macro-cell

In typical urban macro-cell mobile station is located outdoors at street level and fixed base station clearly above surrounding building heights. As for propagation conditions, non- or obstructed line-of-sight is a common case, since street level is often reached by a single diffraction over the rooftop. The building blocks can form either a regular Manhattan type of grid, or have more irregular locations. Typical building heights in urban environments are over four floors. Buildings height and density in typical urban macro-cell are mostly homogenous.

### 2.3.10 C3 – Bad urban macro-cell

Bad urban environment describes cities with buildings with distinctly inhomogeneous heights or densities, and results to a clearly dispersive propagation environment in delay and angular domain. The inhomogenities in city structure can be e.g. due to large water areas separating the built-up areas, or the high-rise skyscrapers in otherwise typical urban environment. Increased delay and angular dispersion can also be caused by mountains surrounding the city. Base station is typically located above the average rooftop level, but within its coverage range there can also be several high-rise buildings exceeding the base station height. From modelling point of view this differs from typical urban macro-cell by an additional far scatterer cluster.

### 2.3.11 C4 – Urban macro outdoor to indoor

The Outdoor-to-Indoor scenario is specified here as follows: The outdoor environment is the same as in urban macrocellular case, C2, and the indoor environment is the same as in indoor case, A1. The base station antenna is clearly above the mean building height. This means that there will be quite long LOS paths to the walls penetrated by the signals, mainly in the higher floors of the buildings. On the other hand there is often quite a severe shadowing, especially in the lower floors. The propagation in the macrocellular outdoor scenario is different from the corresponding microcellular case in that the outdoor

environment produces higher delay spreads and higher path-losses than the indoor environment. Propagation through building walls and inside the building is assumed to be quite similar in both cases.

The parameters of this scenario have been merged with A2 and B4 in table 4-7.

### 2.3.12 D1 – Rural macro-cell

Propagation scenario D1 represents radio propagation in large areas (radii up to 10 km) with low building density. The height of the AP antenna is typically in the range from 20 to 70 m, which is much higher than the average building height. Consequently, LOS conditions can be expected to exist in most of the coverage area. In case the UE is located inside a building or vehicle, an additional penetration loss is experienced which can possibly be modelled as a (frequency-dependent) constant value. The AP antenna location is fixed in this propagation scenario, and the UE antenna velocity is in the range from 0 to 200 km/h.

In WINNER Phase I, measurements were conducted in a flat rural environment near Oulu in Finland, at both 2.45 and 5.25 GHz, and with an AP antenna height of 18 - 25 m. A channel model derived from these measurements is available and has been reported in [WIND54]. The channel model from Phase I for propagation scenario D1 is generalised for the frequency range 2 – 6 GHz and different BS and MS antenna heights.

### 2.3.13 D2 – Moving networks

Propagation scenario D2 (“Rural Moving Network”) represents radio propagation in environments where both the AP and the UE are moving, possibly at very high speed, in a rural area. A typical example of this scenario occurs in carriages of high-speed trains where wireless coverage is provided by so-called moving relay stations (MRSs) which can be mounted, for example, to the roof. The link between the fixed network and the moving network (train) is typically a LOS type. Later we call this link as D2a. In addition there is a link from the MRS to the UE. It is assumed that the indoor part of the MRS is mounted in the ceiling in the middle of the carriage. Later on we call this link D2b.

#### 2.3.13.1 D2a

The scenario for D2a is specified as follows:

- There is a track accompanied with base stations in the intervals of 1000 - 2000 m.
- The base stations are
  - 50 m away from the tracks and the antenna heights are 30 m, or alternatively
  - 2 m away from the tracks and the antenna heights are 5 m.
- Height of the train (and MRS) is 2.5 m
- Speed of the train is nominally 350 km/h.

No tunnels are assumed in the route, but the lower BS antenna height can be used to simulate situations compatible with the ones encountered in tunnels as regards high change rate in Doppler frequencies.

#### 2.3.13.2 D2b

D2b model is applicable in an environment inside the fast train carriage. The carriage is assumed to consist of one floor, but this should not make big difference, because one floor of a double floor carriage is quite similar as a single floor carriage. The MRS indoor part is assumed to be located in the ceiling of the carriage. It is assumed that there are chairs and tables densely as usual in train carriages. This makes that typically there is NLOS connection between the MRS and UE. Finally, it is assumed that the windows of the carriage are made of heat protective glass. This is important, because then we can assume that the relatively very fast moving scatterers do not affect considerably to the propagation. The reason is that such heat protective glass attenuates radio waves about 20 dB in both directions giving a total attenuation of 40 dB to the signals transmitted out from the carriage, scattered in the outside environment and penetrated back to the interior of the carriage.

## 2.4 Measurement Tools

Five different radio channel measurement systems have been used in the propagation measurements during Phase I and II. Main characteristics of the channel sounders used in Phase II are summarised in this section. Measuring equipment used in Phase I have been described in [WIN1D54].

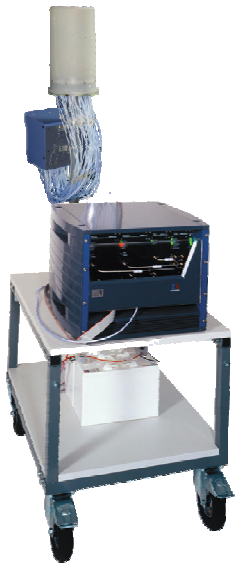

### 2.4.1 Propsound (EBITG, UOULU, Nokia)

The Propsound™ multi-dimensional radio channel sounder is a product of Elektrobit, Finland [PSound]. Propsound has been designed to enable realistic radio channel measurements in both the time and spatial domains. It is based on the spread spectrum sounding method in the delay domain. The other domains, including polarization, FDD frequency and the spatial domain, are covered using an advanced time-domain switching technique. Together with optional super-resolution techniques (based on the SAGE algorithm), this allows accurate measurements of SISO, SIMO, MIMO, geolocation and multi-user propagation channels. Some key features of Propsound are presented in Table 2-2.


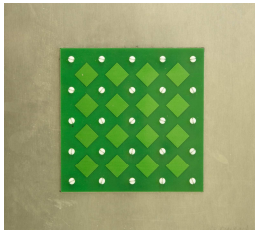
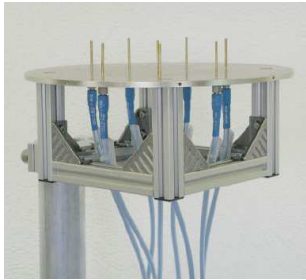
**Table 2-2 Propsound™ characteristics**


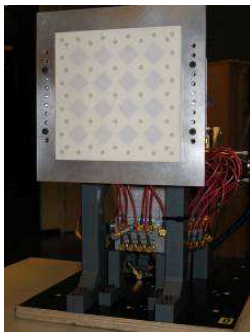
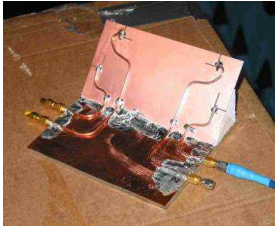
Propsound Property	Range of values
RF bands	1.7 - 2.1, 2.0 - 2.7, 3.2 - 4.0, 5.1 - 5.9 GHz
Sustained measurement rate	Up to 30,000 CIR/s (code length: 255 chips)
Maximum cycle (snapshot) rate	1500 Hz
Chip frequency	up to 100 Mchips/s
Available code lengths	31 - 4095 chips (M-sequences)
Number of measurement channels	up to 8448
Measurement modes	SISO, SIMO, MIMO
Receiver noise figure	better than 3 dB
Baseband sampling rate	up to 2 GSamples/s
Spurious IR free dynamic range:	35 dB
Transmitter output	up to 26 dBm (400 mW), adjustable in 2 dB steps
Control	Windows notebook PC via Ethernet
Post processing	MATLAB package
Synchronisation	rubidium clock with stability of $10^{-11}$

**Table 2-3 Propsound™ terminals.**

	
Transmitter with a trolley.	Receiver with a trolley.

**Table 2-4 Propsound™ antennas.**

Name	ODA_5G25	PLA_5G25	UCA_5G25
Owner	Elektrobit	Elektrobit	Elektrobit
Array structure	omnidirectional array	rectangular array	uniform circular array
Polarization	dual (+/- 45°)	dual (+/- 45°)	vertical
Center frequency [GHz]	5.25	5.25	5.25
Number of elements	50 (25 dual)	32 (16 dual)	8
Element type	patch	patch	monopole
Picture			

Name	SPH_5	PLA_5	Mockup
Owner	Radio Laboratory / Helsinki Univ. of Technology	Radio Laboratory / Helsinki Univ. of Technology	Nokia Research Center
Array structure	Semi-spherical array	Planar array	Terminal mockup
Polarization	dual (H/V)	dual (+/- 45°)	-
Center frequency [GHz]	5	5	5
Number of elements	42 (21 dual)	32 (16 dual)	4
Element type	patch	patch	-
Picture			

### 2.4.2 TUI sounder

The RUSK TUI-FAU channel sounder used at TU Ilmenau for MIMO measurements was designed by Medav, Germany [Medav]. RUSK is a real-time radio channel impulse response measurement system that supports multiple transmit and receive antenna element configurations.

The RUSK MIMO channel sounder measures the channel response matrix between all transmitting and receiving antenna elements sequentially by switching between different (Tx,Rx) antenna element pairs.

This means that the sounder uses only one physical transmitter and receiver channel, which reduces sensitivity to channel imbalance. The switched-antenna approach offers a simple way of changing the effective number of antenna elements in the array. Additionally, since antennas are not transmitting at the same time, separation of transmitted signals at the receiver side is straightforward. To accomplish synchronous switching, rubidium reference oscillators are used at both the transmitter and the receiver. Timing and switching frame synchronization is established during an initial synchronization process prior to measurement data recording and must be maintained during the entire measurement.

For channel excitation RUSK uses a multi-carrier spread spectrum signal (MCSSS) with an almost rectangular shape in the frequency domain. This approach allows precise concentration of the transmitted signal energy in the band of interest. Simultaneous sounding of multiple bands (e.g., separated up- and down-link bands in FDD) is supported by setting some spectral magnitudes to zero.

Table 2-5 summarizes the key features of the RUSK TUI-FAU channel sounder.

**Table 2-5 Key features of the Medav RUSK TUI-FAU channel sounder.**

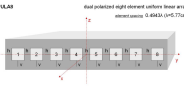
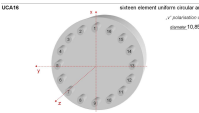
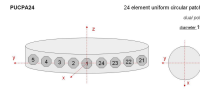

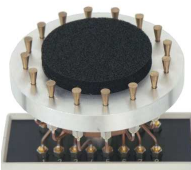


<b>RUSK TUI-FAU Sounder Property</b>	<b>Range of values</b>
RF bands	5...6 GHz
Max. meas. data storage rate	(2x)*160 Mbyte/s
Test signal	Multi Carrier Spread Spectrum Signal (MCSSS)
Sequence length (defines maximum excess delay)	256 – 8192 spectral lines, depending on IR length
Number of measurement channels	up to 65536 ( $2^{16}$ )
Measurement modes	SISO, SIMO, MIMO
Sampling frequency	640 MHz at Tx and Rx
Spurious free IR dynamic range	48 dB
Transmitter output	up to 33 dBm (2 W),
Propagation delay resolution	4.17 ns (1/bandwidth)
Impulse response length	0.8 $\mu$ s – 25.6 $\mu$ s
RF sensitivity	-88 dBm
Control	Windows PC
Post processing	MATLAB package
Synchronisation	rubidium clock with stability of $10^{-10}$

\* Rate is doubled with additional disk storage. Second storage enables shorter time gap between Tx-Rx sub-channels.

An overview of measurement-relevant technical data for the antenna arrays used in the TU-Ilmenau campaigns is given in Table 2-6.

**Table 2-6 Overview of TU-Ilmenau antenna arrays.**

Name	<b>PULA8 (PULA8@10W)</b>	<b>UCA16</b>	<b>PUCPA24</b>	<b>SPUCPA4x24</b>
Vendor	IRK Dresden	TU Ilmenau	IRK Dresden	IRK Dresden
Array structure	uniform linear array	uniform circular array	uniform circular array	stacked uniform circular array
Polarization	dual (vertical+ horizontal)	vertical	dual (vertical+ horizontal)	dual (vertical+ horizontal)

Name	PULA8 (PULA8@10W)	UCA16	PUCPA24	SPUCPA4x24
Center frequency [GHz]	5.2	5.2	5.2	5.2
Bandwidth [MHz]	120	120	120	120
Max. Power [dBm]	27 (40)	27	25	24
Number of elements	8	16	24	96
Element type	patch	disk cone	patch	patch
Dimensioning	element spacing $0.4943 \lambda$	diameter 10.85 cm	diameter 19.5 cm	diameter 19.5 cm ring spacing $0.4943 \lambda$
Element orientation				
Picture				

The monopole antenna that is mounted on the ICE roof was manufactured by Huber&Suhner, and is of type SWA 0859 – 360/4/0/DFRX30. The disc-conical antenna used for the ICE SISO measurements was designed by Kurt Blau (TU Ilmenau) for the 5.2 GHz frequency range.

### 2.4.3 CRC sounder

The sounder used for the CRC measurements is the fourth generation of a PN sounder design that was first implemented with 20 MHz bandwidth at CRC in 1981. Its construction is bread-board style, with semi-rigid cables connecting various commercially-available modules, such as phase-locked oscillators, power splitters, mixers, filter modules, and amplifiers. The bread-board style construction is maintained so as to allow easy reconfiguration and recalibration for different measurement tasks, with different operating frequencies and different bandwidths, as required. Its PN sequence generator is a CRC implementation that can generate sequences of length between 127 and 1021 chips, and it can be clocked at rates up to 65 mchips/s. Both CRC-Chanprobe's transmitter and its receiver have two RF sections with operating bandwidths centred on 2.25 GHz and 5.8 GHz. The transmitter transmits continuously in both bands. Operation at other frequencies is made possible by substituting different up-converter PLOs and bandpass filters.

The receiver front ends are connected sequentially, using an RF switch, to its IF section. Operation at other centre frequencies is accomplished via an extra, external RF section, with frequency translation to either 2.25 or 5.8 GHz. Final downconversion is from IF to baseband via quadrature downconversion circuitry. The in-phase (I) and quadrature (Q) baseband outputs can each be sampled at rates up to 100 MSamples/s. CRC-Chanprobe's operating characteristics are summarized in Table 2-7.



**Table 2-7 CRC-Chanprobe operating characteristics**

<b>CRC-Chanprobe Property</b>	<b>Range of values</b>
RF bands	0.95, 2.25, (4.9), 5.8, 30, 40, 60 GHz <sup>[1]</sup>
Sustained measurement rate	10,000 snapshots/s <sup>[2]</sup>
Maximum cycle (snapshot) rate	40,000 snapshots/s <sup>[3]</sup>
Chip rate	up to 50 Mchips/s
Useable code lengths	127 – 1021 chips (M-sequences)
Number of measurement channels	32 Switched Rx antennas, 1 Tx antenna
Measurement modes	SISO, SIMO
Receiver noise figure	< 2 dB
Baseband sampling rate	100 MSamples/s
Spurious IR free dynamic range:	40 dB
Transmitter output	up to 42 dBm at 2.25 GHz, up to 30 dBm at other frequencies
Control	Windows PC
Post processing	MATLAB package
Synchronisation	rubidium clock with stability of $10^{-11}$
Minimum Received Power level (20 dB MPSR)	-89 dBm
Linear Dynamic Range without pre-attenuation	-69 dBm to -89 dBm with 20 dB MPSR
Transmit Antenna	Vertical Quarter-Wavelength Monopole, with drooping radials
Receive Antenna	32 Element UCA of Vertical Quarter-Wavelength Monopoles with drooping radials

Note: Transfer rate specs are quoted assuming a single Rx channel, 50 Mchps m-sequence, sequence length 255 chips, 2 samples per chip, 1 sequence length per snapshot.

- 1) 0.95, 4.9 & 5.8 GHz characteristics are SISO
- 2) Based on a verified average data acquisition rate of ~20 Mbytes/S when logging data to hard disk in real time (needed for long measurement runs).
- 3) Based on a verified average data acquisition rate of ~80 Mbytes/S when not logging data to hard disk in real time (valid for short measurement runs).

CRC-Chanprobe can be operated in SISO or SIMO modes. A 32-element switched uniform circular array and a 32-element 3D cross array have been implemented for use at the receiver. Both arrays employ quarter-wavelength monopole antennas for the reception of vertically polarized waves.

### 3. Channel Modelling Approach

WINNER channel model is a geometry based stochastic model. Geometry based modelling of the radio channel enables separation of propagation parameters and antennas. The channel parameters for individual snapshots are determined stochastically, based on statistical distributions extracted from channel measurement. Antenna geometries and field patterns can be defined properly by the user of the model. Channel realisations are generated with geometrical principle by summing contributions of rays (plane waves) with specific small scale parameters like delay, power, AoA and AoD. Superposition results to correlation between antenna elements and temporal fading with geometry dependent Doppler spectrum [Cal+07].

A number of rays constitute a cluster. In the terminology of this document we equate the cluster with a propagation path diffused in space, either or both in delay and angle domains. Elements of the MIMO channel, i.e. antenna arrays at both link ends and propagation paths, are illustrated in Figure 3-1.

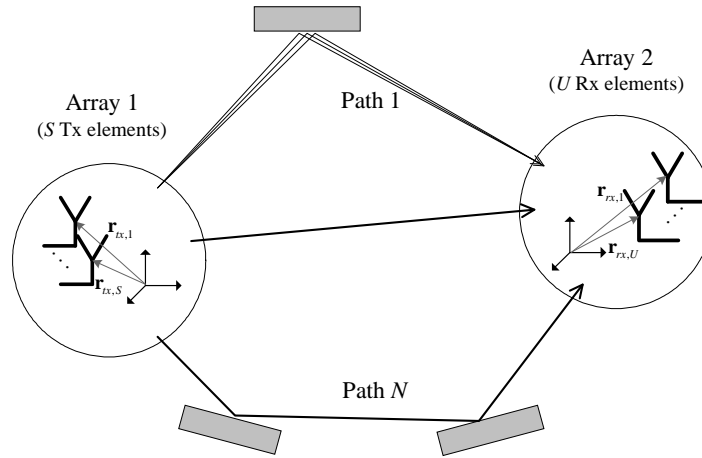


Figure 3-1 The MIMO channel

Transfer matrix of the MIMO channel is

$$\mathbf{H}(t; \tau) = \sum_{n=1}^N \mathbf{H}_n(t; \tau) \quad (3.1)$$

It is composed of antenna array response matrices  $\mathbf{F}_{tx}$  for the transmitter,  $\mathbf{F}_{rx}$  for the receiver and the propagation channel response matrix  $\mathbf{h}_n$  for cluster  $n$  as follows

$$\mathbf{H}_n(t; \tau) = \iint \mathbf{F}_{rx}(\phi) \mathbf{h}_n(t; \tau, \phi, \varphi) \mathbf{F}_{tx}^T(\phi) d\phi d\varphi \quad (3.2)$$

The channel from Tx antenna element  $s$  to Rx element  $u$  for cluster  $n$  is

$$\begin{aligned} H_{u,s,n}(t; \tau) = & \sum_{m=1}^M \begin{bmatrix} F_{rx,u,V}(\phi_{n,m}) \\ F_{rx,u,H}(\phi_{n,m}) \end{bmatrix}^T \begin{bmatrix} \alpha_{n,m,VV} & \alpha_{n,m,VH} \\ \alpha_{n,m,HV} & \alpha_{n,m,HH} \end{bmatrix} \begin{bmatrix} F_{tx,s,V}(\phi_{n,m}) \\ F_{tx,s,H}(\phi_{n,m}) \end{bmatrix} \\ & \times \exp(j2\pi\lambda_0^{-1}(\bar{\phi}_{n,m} \cdot \bar{r}_{rx,u})) \exp(j2\pi\lambda_0^{-1}(\bar{\phi}_{n,m} \cdot \bar{r}_{tx,s})) \\ & \times \exp(j2\pi\nu_{n,m}t) \delta(\tau - \tau_{n,m}) \end{aligned} \quad (3.3)$$

where  $F_{rx,u,V}$  and  $F_{rx,u,H}$  are the antenna element  $u$  field patterns for vertical and horizontal polarisations respectively,  $\alpha_{n,m,VV}$  and  $\alpha_{n,m,VH}$  are the complex gains of vertical-to-vertical and horizontal-to-vertical polarisations of ray  $n,m$  respectively. Further  $\lambda_0$  is the wave length of carrier frequency,  $\bar{\phi}_{n,m}$  is AoD unit vector,  $\bar{\phi}_{n,m}$  is AoA unit vector,  $\bar{r}_{tx,s}$  and  $\bar{r}_{rx,u}$  are the location vectors of element  $s$  and  $u$  respectively, and  $\nu_{n,m}$  is the Doppler frequency component of ray  $n,m$ . If the radio channel is modelled as dynamic, all the above mentioned small scale parameters are time variant, i.e. function of  $t$ . [SMB01]

For interested reader, the more detailed description of the modelling framework can be found in WINNER Phase I deliverable [WIN1D54].

### 3.1 WINNER Generic Channel Model

WINNER generic model is a system level model, which can describe arbitrary number of propagation environment realisations for single or multiple radio links for all the defined scenarios for desired antenna configurations, with one mathematical framework by different parameter sets. Generic model is a stochastic model with two (or three) levels of randomness. At first, large scale (LS) parameters like shadow fading, delay and angular spreads are drawn randomly from tabulated distribution functions. Next, the small scale parameters like delays, powers and directions arrival and departure are drawn randomly according to tabulated distribution functions and random LS parameters (second moments). At this stage geometric setup is fixed and only free variables are the random initial phases of the scatterers. By picking (randomly) different initial phases, an unlimited number of different realisations of the model can be generated. When also the initial phases are fixed, the model is fully deterministic.

#### 3.1.1 Modelled parameters

Parameters used in the WINNER II Channel Models have been listed and shortly explained below. Parameter values are given in a later section, see sub-section 4.4.

The first set of parameters is called large scale (LS) parameters, because they are considered as an average over a typical channel segment i.e. distance of some tens of wave-lengths. First three of the large scale parameters are used to control the distributions of delay and angular parameters.

##### Large Scale Parameters

- Delay spread and distribution
- Angle of Departure spread and distribution
- Angle of Arrival Spread and distribution
- Shadow Fading standard deviation
- Ricean K-factor

##### Support Parameters

- Scaling parameter for Delay distribution
- Cross-polarisation power ratios
- Number of clusters
- Cluster Angle Spread of Departure
- Cluster Angle Spread of Arrival
- Per Cluster Shadowing
- Auto-correlations of the LS parameters
- Cross-correlations of the LS parameters
- Number of rays per cluster

All of these parameters have been specified from the measurement results or, in some cases, found from literature. Number of rays per cluster has been selected to be 20 as in [3GPPSCM]. Analysis of the measurement data for the different parameters has been described in the Part II document of this deliverable. In the WINNER Channel Models the parameters are assumed not to depend on distance. Although this assumption is probably not strictly valid, it is used for simplicity of the model. The parameter values are given in paragraph 4.4 and represent expected values over the applicability range.

In the basic case the Angles of Arrival and Departure are specified as two-dimensional, i.e. only azimuth angles are considered. For the indoor and outdoor-to-indoor cases the angles can also be understood as solid angles, azimuth and elevation, and the modelling can be performed also as three-dimensional.

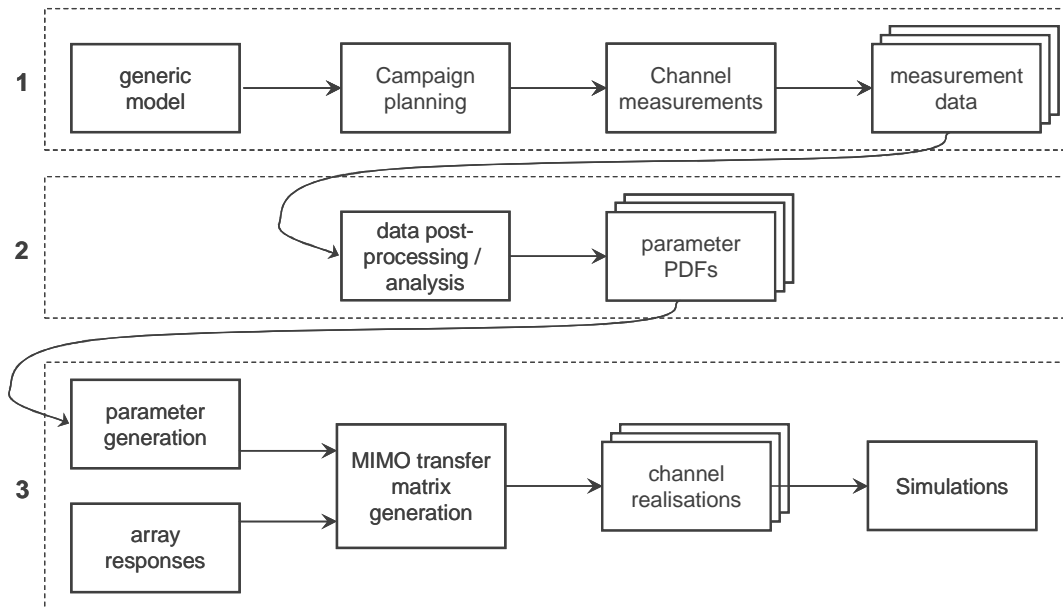
### 3.2 Modelling process

The WINNER Channel Modelling Process is depicted in Figure 3-2. The process is divided into three phases. The first phase starts from definition of propagation scenarios, which means selection of environments to be measured, antenna heights, mobility, and other general requirements. Generic model is needed to know what parameters have to be measured. Planning of measurement campaign can be started when scenarios and generic model exist. Campaign planning has to be done carefully to take into

account several aspects – e.g. channel sounder setup, measurement route, link budget. Channel measurements are done according to the campaign planning and documented accurately. Measurement data is stored onto a mass memory (e.g. magnetic tape or hard disk).

The second phase of the channel modelling process concentrates on data analysis. Depending on the required parameters, different analysis methods and items are applied. Output of data post-processing could be, e.g., a set of impulse responses, path-loss data, or extracted multidimensional propagation parameters. For the post-processed data, statistical analysis is done to obtain parameter PDFs.

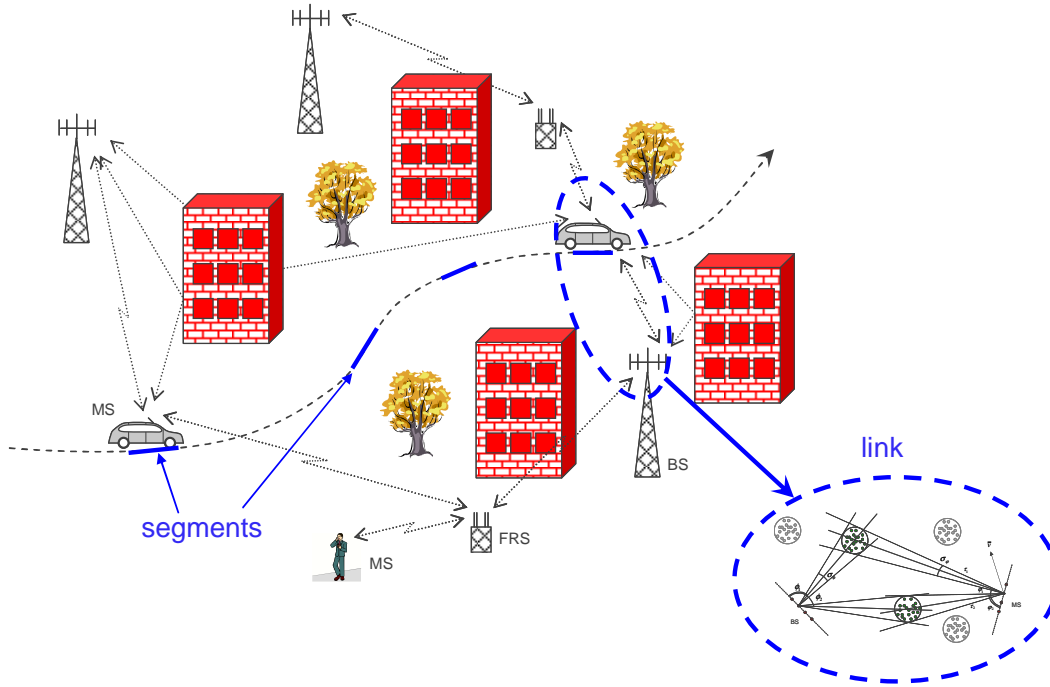
The third phase of the channel modelling process covers the items required in simulation. Parameters are generated according to the PDFs, by using random number generators and suitable filters. MIMO transfer matrix is obtained by using the generated parameters, and information about the antennas. In our approach MIMO transfer matrices are generated by using the sum-of-rays method. Generated impulse responses are called channel realisations, which are then used in simulations.



**Figure 3-2 WINNER channel modelling process**

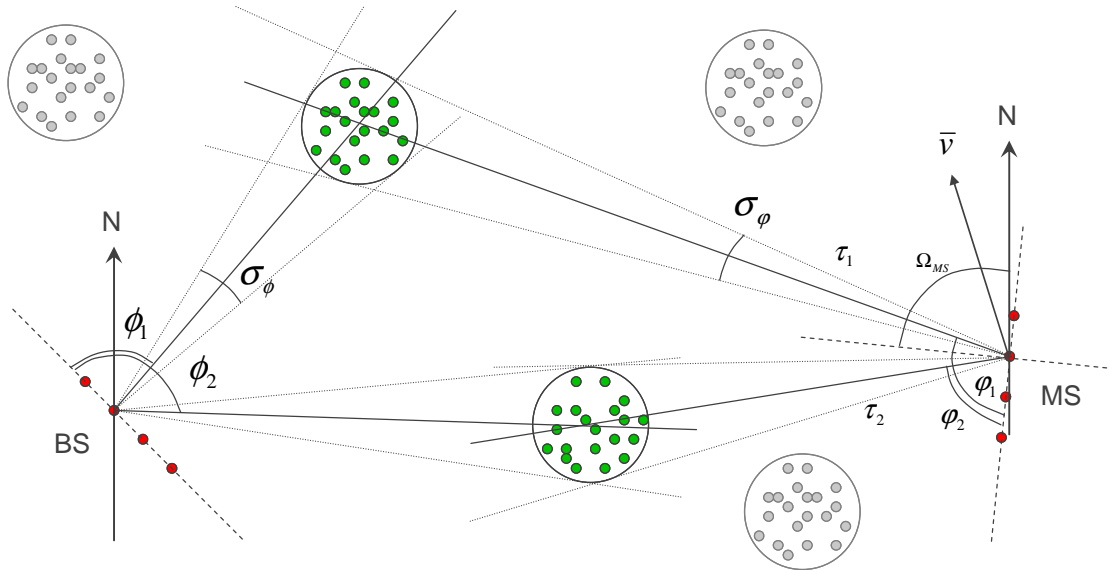
### 3.3 Network layout

WINNER MIMO radio channel model enables system level simulations and testing. This means that multiple links are to be simulated (evolved) simultaneously. System level simulation may include multiple base stations, multiple relay stations, and multiple mobile terminals as in Figure 3-3. Link level simulation is done for one link, which is shown by blue dashed ellipse. The short blue lines represent channel segments where large scale parameters are fixed. System level simulation consists of multiple links. Both link level and system level simulations can be done by modelling multiple segments, or by only one (CDL model).



**Figure 3-3. System level approach, several drops.**

A single link model is shown in Figure 3-4. The parameters used in the models are also shown in the figure. Each circle with several dots represents scattering region causing one cluster. The number of clusters varies from scenario to another.



**Figure 3-4. Single link.**

In spatial channel model the performance of the single link is defined by small-scale parameters of all MPCs between two spatial positions of radio-stations. According to this, if only one station is mobile (MS), its position in space-time is defining a single link. The more complex network topology also includes multihop links [Bap04] and cooperative relaying [Lan02], however more complex peer-to-peer connections could be easily described as collections of direct radio-links.

Large-Scale Parameters (LSP) are used as control parameters, when generating the small-scale channel parameters. If we are analyzing multiple positions of MS (many MSs or multiple positions of the single MS) we have a multiple-link model for system level simulations. It can be noted that different MSs being at the same spatial position will experience same LSP parameters.

For multi-link simulations some reference coordinate system has to be established in which positions and movement of radio-stations can be described. A term network layout is designating complete description

of the relative positions of the system elements, as well as vectored description of their movements (speeds). In general, positions (coordinates) of scatterers are unknown. Only exceptions are related to far cluster scatterers (FCS) that are actually positioned in the same coordinate system as radio-stations. In multi-link simulations spatial correlations of channel parameters are important. In order to establish correlations between links at system level the LSPs have been generated with the desired correlation properties. This has been described in the following subsection.

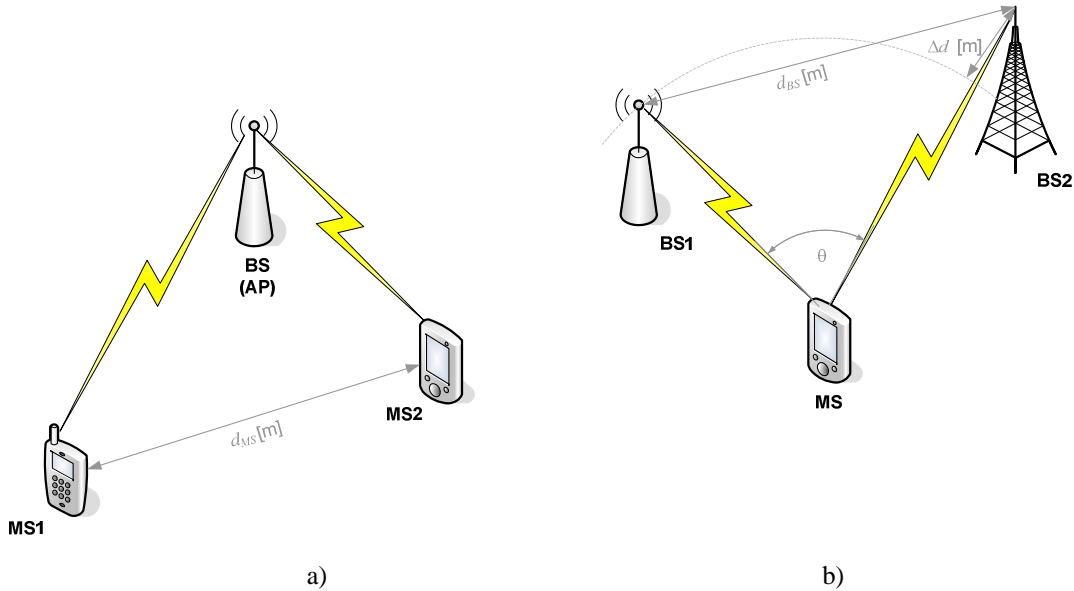
### 3.3.1 Correlations between large scale parameters

For single position of radio-stations (one link) we can describe inter-dependence of multiple control parameters (LSP) with correlation coefficient matrix. Correlations of LSPs that are observed in measured data are not reflected in joint power or probability distributions. Instead LSPs are estimated from marginal power distributions (independently for angles and delays), and necessary dependence is re-established through cross-correlation measure:

$$\rho_{xy} = \frac{C_{xy}}{\sqrt{C_{xx} C_{yy}}}, \quad (3.4)$$

where  $C_{xy}$  is the cross-covariance of LS parameters  $x$  and  $y$ .

At system level two types of correlations could be defined: a) between MSs being connected to the same BS and b) correlations of links from the same MS to multiple BSs (Figure 3-5). These correlations are mostly caused by some scatterers contributing to different links (similarity of the environment).

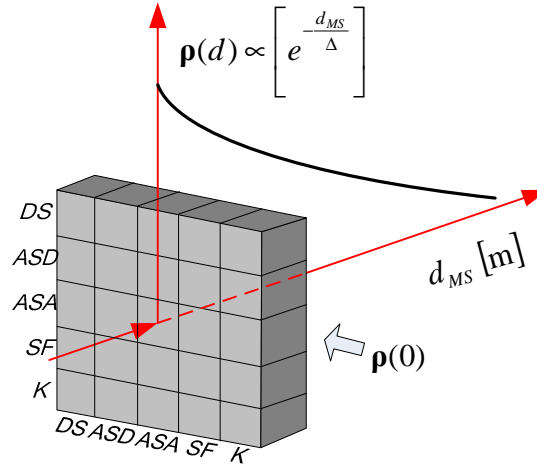


**Figure 3-5 Links toward common station will exhibit inter-correlations: a) fixed common station, b) mobile common station**

In the first case WINNER models are using exponential correlation functions to describe dependence of LSP changes over distance. In other words LSPs of two MSs links toward same BS would experience correlations that are proportional to their relative distance  $d_{MS}$ . As a consequence correlation coefficient matrices for neighbouring links (for MSs at certain distance) are not independent and they also have to reflect observed correlations over the distance dimension:

$$\rho_{xy}(d_{MS}) = \frac{C_{xy}(d_{MS})}{\sqrt{C_{xx} C_{yy}}}, \quad (3.5)$$

For this reason elements of link cross-correlations coefficient matrix should reflect exponential decay with distance, as shown in Figure 3-6



**Figure 3-6 Dependence of cross-correlation coefficient matrix over distance.**

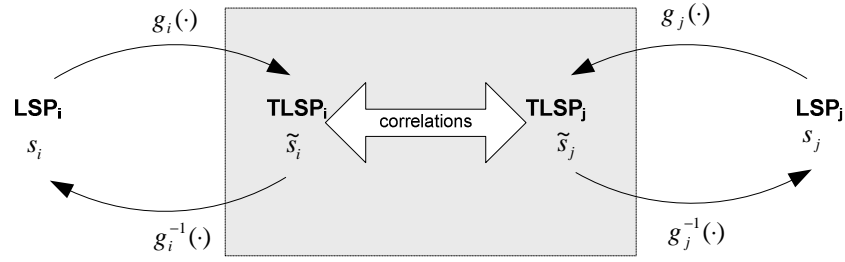
In 3GPP SCM, shadowing fading for links from one MS to different BSs exhibits constant correlation coefficient equal to 0.5. This correlation does not depend on distances between BSs or their relative angular positions as seen from MS and therefore it is not layout dependent. Additionally, this property is estimated from few measurements and therefore it is not considered as being fully representative for different WINNER scenarios. This phenomenon has also been investigated in WINNER project in some extent.

Correlation properties of links from the same MS to multiple BSs (inter-site) were investigated in Phase I of WINNER project [WIN1D54]. The results showed rather high correlation for one measurement route and quite low for another. The amount of measurement data was limited, so that we could not specify correlation other than zero.

The inter-site correlation of shadowing fading is also investigated in the literature for the outdoor macro-cell scenarios: in [Gud91],[PCH01] and [WL02], the authors proposed that the inter-site correlation is a function of the angle between BSs directions being seen from the MS ( $\theta$ ); while in [Sau99] author studied the dependence of the inter-site correlation on the distance between BSs,  $d_{BS}$ . Although some correlations could be found in the references afore, the results could not show clear correlation behaviour between different BSs. Although we also believe that such correlation most probably exists in many scenarios, at least between Base Stations near each other, at this point we decided to let the correlation be modelled as zero.

Inter-correlations between links of one MS to multiple sectors of the same BS could be analyzed in a similar way, by treating different sectors of the BS as independent one-sector BSs. As a matter of fact, the links from two different sectors to an MS are correlated so that the LS parameters for the links are the same.

Correlation of large-scale parameters (LSPs) is achieved by using weighed sums of independent Gaussian random processes (IGRP). If  $i$ -th LSP,  $s_i$ , have distribution that differs from Normal (Gauss), required distribution is generated by applying mapping from random variable  $\tilde{s}_i$  having Gaussian distribution. Random variable  $\tilde{s}_i$  will be referred as transformed LSP (TLSP). Prior of mapping  $\tilde{s}_i$  to  $s_i$ ,  $\tilde{s}_i$  is correlated with TLSPs  $\tilde{s}_j$ , belonging to other LSPs or different links (being at certain distance - for system level correlations). Process applied to introduce or to calculate correlations (from measured data) is illustrated in Figure 3-7.



**Figure 3-7 Correlations of LSP are introduced in transformed domain.**

In cases when mapping  $s_i = g_i^{-1}(\tilde{s})$  is unknown, necessary relations between LSP and transformed domain can be established using knowledge about cumulative density distribution (cdf) of  $s_i$ ,  $F_{s_i}(s)$ . In such cases  $s_i$  can be generated from  $\tilde{s}_i$  using expression:

$$s = g_i^{-1}(\tilde{s}) = F_{s_i}^{-1}(F_{\tilde{s}_i}(\tilde{s})) \quad (3.6)$$

where  $F_{\tilde{s}_i}(\tilde{s})$  is cdf of Normally distributed process that can be calculated using Q-function (or erf/erfc). In simpler cases, e.g. when LSP is log-normally distributed it is possible to use known mappings:

$$s = g_i^{-1}(\tilde{s}) = 10^{\tilde{s}} \quad (3.7)$$

$$\tilde{s} = g_i(s) = \log_{10}(s) \quad (3.8)$$

As a correlation measure cross-correlation coefficient is used, expression (3.4). Above is explained that for one link (single position of MS) inter-dependence of multiple control parameters can be described with correlation coefficient matrix. Additionally if parameters of intra-site links are correlated according to distance between MS positions, then correlation matrix gets additional dimension that describes changes in correlations over distance, Figure 3-6. This means that for each pair of TLSP we can define cross-correlation coefficient dependence over distance, as in expression (3.5):

$$\rho_{\tilde{s}_k \tilde{s}_l}(d_{k,l}) = \frac{C_{\tilde{s}_k \tilde{s}_l}(d_{k,l})}{\sqrt{C_{\tilde{s}_k \tilde{s}_k} C_{\tilde{s}_l \tilde{s}_l}}} \quad (3.9)$$

Cross-variances  $C_{\tilde{s}_k \tilde{s}_l}(d_{k,l})$  are calculated from measurement data using knowledge about positions of MS during measurement, and in general have exponential decay over distance.

If each link is controlled by M TLSPs, and we have K links corresponding to MS locations at positions  $(x_k, y_k)$ ,  $k = 1..K$ , then it is necessary to correlate values for N= M·K variables.

Generation of N Normally distributed and correlated TLSPs can be based on scaling and summation of N independent zero-mean and unit variance Gaussian random variables,  $\xi_N(x, y) = [\xi_1(x_1, y_1), \dots, \xi_N(x_N, y_N)]^T$ . Using matrix notation that can be expressed:

$$\tilde{\mathbf{s}}(x, y) = \mathbf{Q}_{N \times N} \xi_N(x, y) \quad (3.10)$$

This will ensure that final distribution is also Gaussian. Scaling coefficients have to be determined in such way that cross-variances  $C_{\tilde{s}_k \tilde{s}_l}(d_{k,l})$ ,  $d_{k,l} = \sqrt{(x_k - x_l)^2 + (y_k - y_l)^2}$  are corresponding to measured values. If element  $C_{i,j}$  of matrix  $\mathbf{C}_{N \times N}$  represents cross-variance between TLSPs  $\tilde{s}_i$  and  $\tilde{s}_j$ , then scaling matrix can be calculated as:

$$\mathbf{Q}_{N \times N} = \sqrt{\mathbf{C}_{N \times N}} \quad (3.11)$$

This approach is not appropriate for correlation of large number of parameters, since dimensions of scaling matrix are increasing proportionally to the total number of TLSPs in all links (squared dependence in number of elements). For that reason it is more convenient to generate separately the influence of LSP cross-correlation and exponential auto-correlation.



Let us assume we have  $M$  LSPs per link and  $K$  correlated links, i.e.  $K$  MSs linked to the same BS site at locations  $(x_k, y_k)$ , where  $k = 1, \dots, K$ . Auto-correlation is generated to the LSPs the following way. At first we generate a uniform grid of locations based on co-ordinates of the  $K$  MSs. Size of the grid is  $(\max(x_k) - \min(x_k) + 2D) \times (\max(y_k) - \min(y_k) + 2D)$ . To each grid node we assign  $M$  Gaussian iid  $\sim N(0,1)$  random numbers, one for each LSP. Then the grid of random numbers is filtered with a two dimensional FIR filter to generate exponential auto-correlation. Impulse response of the filter for the  $m$ th LSP is

$$h_m(d) = \exp\left(-\frac{d}{\Delta_m}\right), \quad (3.12)$$

where  $d$  is distance and  $\Delta_m$  is the correlation distance both in meters (see Table 4-5). Each of the  $M$  random numbers in nodes of the grid, representing  $M$  LSPs, is filtered with a specific filter, because the correlation distances may be different in Table 4-5. After filtering the correlated random numbers  $\xi_M(x_k, y_k)$  at grid nodes ( $K$  MS locations) are saved and the redundant grid nodes are discarded.

Cross-correlation is generated independently to the LSPs of  $K$  links by linear transformation

$$\tilde{\mathbf{s}}(x_k, y_k) = \sqrt{\mathbf{C}_{M \times M}(0)} \xi_M(x_k, y_k), \quad (3.13)$$

where elements of correlation matrix

$$\mathbf{C}_{M \times M}(0) = \begin{bmatrix} C_{\tilde{s}_1 \tilde{s}_1}(0) & \cdots & C_{\tilde{s}_1 \tilde{s}_M}(0) \\ \vdots & \ddots & \vdots \\ C_{\tilde{s}_M \tilde{s}_1}(0) & \cdots & C_{\tilde{s}_M \tilde{s}_M}(0) \end{bmatrix} \quad (3.14)$$

are defined in Table 4-5.

### 3.4 Concept of channel segments, drops and time evolution

Channel segment represents a period of quasi-stationarity during which probability distributions of low-level parameters are not changed noticeably. During this period all large-scale parameters, as well as velocity and direction-of-travel for mobile station (MS), are practically constant. To be physically feasible, the channel segment must be relatively confined in distance. The size depends on the environment, but it can be at maximum few meters. Correlation distances of different parameters describe roughly the proper size of the channel segment, see the paragraph 4.4.

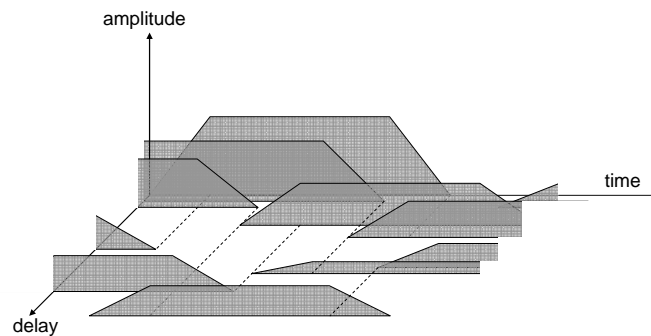
Allowing the channel segment length go to zero, we specify a drop: In a drop all parameters are fixed, except the phases of the rays. Motion within a drop is only virtual and causes fast fading and the Doppler effect by superposition of rotating phasors, rays. It can be said, that a drop is an abstract representation of a channel segment, where the inaccuracies caused by the change of the terminal location have been removed. In a simulation, the duration of a drop can be selected as desired. It is a common practice to use drops in the simulations. The main advantage is the simplicity of the simulation, because successive simulation runs do not need to be correlated. The drawback is that it is not possible to simulate cases, where variable channel conditions are needed. However, the drop-based simulation is the main method of simulations in WINNER projects I and II. In the final WINNER II Channel Models there is also an alternative for the drop-based simulation, i.e. simulation with time evolution., where correlated drops are used

In the WINNER II models the propagation parameters may vary over time between the channel segments. In the multi segment modelling two options are available, either drops (stationary channel segments like in WINNER I) or continuous channel evolution with smooth transitions between segments. There are two approaches for time evolution modelling discussed below. First is the one that is proposed to be implemented, due to the simplicity of the method. Second is a method using Markov process that can be regarded as a more advanced method and it requires parameters that have not been determined yet.

#### 3.4.1 Basic method for time-evolution

In this report time evolution of propagation parameters is modelled like depicted in Figure 3-8. The route to be modelled is covered by adjacent channel segments. The distance between segments is equal to the stationarity interval. Transition from segment to segment is carried out by replacing clusters of the “old” segment by the clusters of the “new” segment, one by one. The route between adjacent channel segments

is divided to number of sub-intervals equal to maximum number of clusters within the channel segments. During each sub-interval the power of one old cluster ramps down and one new cluster ramps up. Power ramps are linear. Clusters from the old and new segments are coupled based on their power. If number of clusters is different in the channel segments, the weakest clusters are ramped up or down without a pair from other cluster.



**Figure 3-8 Smooth transition between channel segments by power ramp-up and ramp-down of clusters.**

### 3.4.2 Markov process based method of time evolution

In [ZTL+05] the authors propose a dynamic channel model, where paths are arised and disappeared according to a Markov process. The birth and death probabilities are specified from measurements. This approach leads to a more realistic behaviour of the channel. However, to apply this approach, the birth and death parameters are needed for all the channels, which are not available at the moment. Another disadvantage is the variable number of instantaneous paths.

In spite of the drawbacks listed above this approach seems quite promising, and should be investigated and adopted in a later stage, if the benefits are deemed more important than the disadvantages. One way would be to use only the  $N$  strongest paths in the model based on the Markov process, where  $N$  is a constant.

## 3.5 Nomadic channel condition

Propagation environment is called nomadic, if the transmitter and receiver locations are normally fixed during the communication, but may have moved between different uses of the network [OVC06]. In such conditions we have to assume that some of the scatterers may move. Actually this is quite typical in many cases, like when there are people working in the vicinity of the transceiver. For the nomadic environment it is also typical that an access point and especially user terminals can change place, e.g. in the room and even go out from the room. However, the most important feature to be taken into account in channel modelling is the moving scatterers. Nomadic channels can be regarded as a special case of the WINNER generic model shown in eq. (3.3). In principle, nomadic channels can exist in all the WINNER deployment scenarios, both in indoor and outdoor. For feeder links we assume that the LOS component is strong enough, so that the reflections from moving objects can be neglected. Therefore we use nomadic modelling only for the scenarios A1 Indoor and B4 Outdoor-to-indoor.

Traditionally these scenarios have been modelled using very low speed for the User Equipment. By applying an approach using fixed links with moving scatterers, we can certainly get more accurate channel model and parameters for the generation of the channel coefficient.

The idea of modelling nomadic (or fixed) environments has been introduced in some open literature. Here we follow the approach introduced in [OP04, OC07, Erc+01, ESB+04]. Based on measurements, we can define a temporal K-factor, for both LOS and NLOS connections. Based on the temporal K-factor, pathloss model including shadow fading, cross polariztion discrimination etc., the channel coefficients can be generated [ESB+04]. In [ESB+04], 2x2 MIMO was discussed from theory, measurements, generation of channel coefficients, and validation of the channels, but without information of angular domain.

The overall procedure is roughly as follows. Assume that we have generated initial channel parameters (delays, powers, AoA/AoD etc.) for the nomadic situation. Then we draw the clusters that are moving. Next we draw the Doppler frequencies for all moving rays in all the clusters containing movement. (Note that all or only part of the rays are moving in those clusters.) Next we can simply generate the channel

coefficients for whole the channel segment. In addition it is possible to define an extra attenuation or cases, where a moving object (e.g. a person) is shadowing paths from other scatterers. However, we neglect this phenomenon for simplicity. The reasoning is as follows: The shadowing situation in the indoor environment is assumed to be statistically the same, irrespective of the position of the scatterers. Therefore we conclude that the measurements and literature results already contain this shadowed situation, precisely enough for our modelling needs.

In indoors the moving objects (called clusters) are assumed to be humans. Reflection is the main interaction with human body at WINNER target frequency range, as analysed in [VES00] and [GTD+04]. In our model only a cluster can be in linear motion for longer times, and this is modelled by an accompanying mean cluster Doppler shift. A cluster is composed of 20 rays. If the scatterer described by the cluster is assumed rigid, the relative movements come from the geometry and the movement of the cluster, and can be directly calculated from the geometric model plus the known motion. In addition, there are moving scatterers within a cluster (e.g. limbs), the parts of which are moving relatively. This phenomenon can be governed e.g. through a Doppler spectrum assigned to a cluster.

Assumptions:

1. A cluster can be either moving or static.
2. A moving cluster has a random velocity that can be zero.
3. Static cluster, contains no movement at all, moving cluster can have a random fluctuation on top of its mean movement (random velocity).
4. A moving cluster can shadow signals from other clusters. (Neglected here, as discussed afore.)

To create a model for the situation described afore, we have to fix the probabilities of static and moving clusters and the accompanying distributions of the directions of the rays and the Doppler spectra of the moving rays. The distributions for the directions of the rays, power levels etc. are all given by the ordinary random process (i.e. non-nomadic) for the creating of the channel coefficients. All that remains are the Doppler frequencies of the rays based on the virtual movement of the clusters. This means that, in addition to the ordinary process, we have to specify:

- the number of static clusters (e.g. 80% of all clusters),
- mean velocity and direction for all moving clusters, with some velocities being possibly zero (e.g. 50% zero velocity, 50% 3km/h, direction  $\sim \text{Uni}(360^\circ)$  (uniformly distributed over  $360^\circ$ )),
- additional Doppler frequency for each of the moving scatterers (e.g. calculated by ray AoA/AoD, velocity 3km/h, direction of motion  $\sim \text{Uni}(360^\circ)$ ),

The number of moving scatterer in a cluster is determined by targeted cluster-wise temporal K-factor. The temporal K-factor will be  $K_t = F/S$ , where  $F$  is the number of fixed rays and  $S$  is the total number of rays per cluster.

### 3.6 Reduced complexity models

A need has been identified for reduced-complexity channel models that can be used in rapid simulations having the objective of making comparisons between systems alternatives at link-level (e.g. modulation and coding choices). In this report, such models are referred to as reduced-complexity models, and have the character of the well-known tapped delay line class of fading channel models. However, to address the needs of MIMO channel modelling, temporal variations at the taps are determined by more detailed information than that required for the specification of relative powers, envelope fading distributions, and fading rates, which are typical inputs to traditional tapped delay line models.

Specifically, multipath AoD and AoA information is inherent in the determination of tap fading characteristics. For these reasons, the reduced complexity models reported herein are referred to as Cluster Delay Line (CDL) models. A cluster is centred at each tap. In general, each cluster is comprised of the vector sum of equal-powered MPCs (sinusoids), all of which have the same or close to same delay. Each MPC has a varying phase, but has fixed AoA and AoD offsets. The latter depend on the angular spreads at the MS and the BS, respectively, as shown in Table 4-1. The values in this table were chosen to realise a specified Laplacian PAS for each cluster, appropriate to the scenario being modelled. In cases where there is a desire to simulate Ricean-like fading, an extra MPC is added, which is given a power appropriate to the desired Rice factor, and zero angular offset. The powers and delays of the clusters can be non-uniform, and can be chosen to realise the desired overall channel rms delay spread. Parameters of all CDL models reflect the expected values of those used in the more complex models described in other sections of this report.

Doppler information is not specified explicitly for CDL models. This is because Doppler is determined by the AoAs of the MPCs, MS speed and direction, and the specified antenna patterns at the MS and BS, upon which there are no restrictions, except in fixed feeder link scenarios, as discussed in the section of feeder link models.

### 3.6.1 Cluster Delay Line models for mobile and portable scenarios

Cluster delay line (CLD) models for all mobile scenarios have been generated from the corresponding generic models by selecting typical values from a set of random channel realisations. The CLD models consist of the average power, mean AoA, mean AoD, and angle spreads at the BS and MS associated with each cluster within the cluster delay line models. Tables of CDL parameters for the above-cited scenarios can be found in Section 6. Although AoA and AoD values are fixed, it is recommended to have directional variation for e.g. beamforming simulations by adding network layout related angle parameter  $\Omega_{MS}$  and  $\Omega_{BS}$  to all tabulated angles (see Figure 5-2).

### 3.6.2 Cluster Delay Line models for fixed feeder links

Only CDL models have been created for fixed feeder links (B5 scenarios). Model parameters have mostly been derived from the literature as described in [WIN1D54], but some of them have been created by applying models generated in WINNER. CDL models for B5 scenarios are given in the tables of Section 6. As for the mobile and portable scenarios, any desired antenna patterns can be chosen. However, for scenarios B5a and B5b, at distances greater than 300 metres, the 3 dB beamwidth of the antenna at one end of the link should be less than 10 degrees, while that at the other end of the link should be less than 53 degrees. Different parameters are specified in the cited tables for scenarios B5a, b, c, and d.

For fixed link scenarios B5a, B5b, B5d and B5f, Doppler shifts are independent of AOAs. Instead, they are derived from considerations concerning the movement of interacting objects. One interacting object per cluster is modelled as having motion, while the others are fixed. Associated Doppler frequencies are specified in CDL tables. For the scenario B5c, two whole cluster are moving with random velocity.

### 3.6.3 Complexity comparison of modelling methods

Computational complexity of simulation of channel models is an important issue in system performance evaluations. Complexity comparison of WINNER modelling approach with the popular correlation matrix based method is studied in [KJ07]. A common supposition is that the correlation matrix method is simpler and computationally more effective than the geometric method. Conclusion of [KJ07] is that complexity of both methods is about the same order of magnitude. With a high number of MIMO antenna pairs (>16) correlation based method is clearly more complex.

The computation complexity is compared in terms of the number of “real operations”. With the term “real operations” is equated complexity of real multiplication, division, addition and table lookup. In Figure 3-9 the number of real operations per delay tap per MIMO channel time sample (matrix impulse response), with different MxN MIMO antenna numbers, is depicted assuming 10 or 20 rays (M in eq. 3.3) and 8<sup>th</sup> order IIR filter in correlation matrix method. It was also noted that complexity of channel realisation generation is several order of magnitudes lower than computational complexity of simulation of channel convolution.

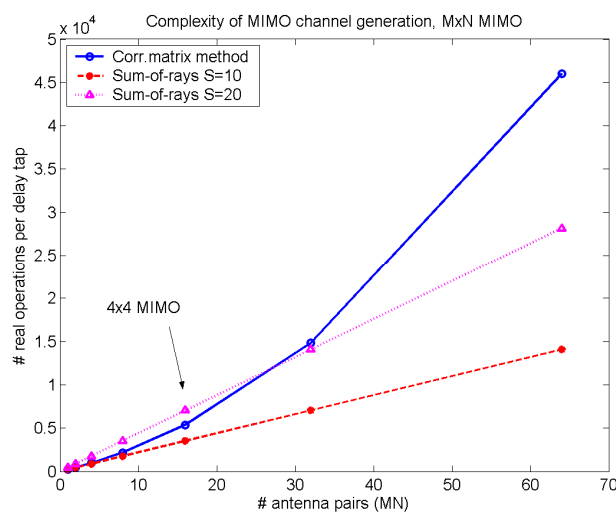


Figure 3-9. Computational complexity comparison.

## 4. Channel Models and Parameters

In this section, we summarize all the channel models and parameters. The path loss models are mainly based on 5 GHz and 2 GHz measurements. However, the frequency bands are extended for 2 – 6 GHz range.

It should be noted that the scenarios Indoor-to-Outdoor and Outdoor-to-Indoor have been combined and represented by a single channel model in this deliverable. This combining has been discussed in Part II document of this report.

### 4.1 Applicability

#### 4.1.1 Environment dependence

Different radio-propagation environment would cause different radio-channel characteristics. Instead of attempt to parameterize environment directly (e.g. street widths, average building height etc.) WINNER models are using (temporal and spatial) propagation parameters obtained from channel measurements in different environments. In this context, environments in which measurements are conducted to observe radio-channel characteristics are called propagation scenarios. For each scenario measured data is analyzed and complemented with results from literature to obtain scenario-specific parameters. After this point, same generic channel is used to model all scenarios, just by using different values of channel parameters.

Usually, even for the same scenario, existence of LOS component substantially influences values of channel parameters. Regarding to this property, most WINNER scenarios are differentiating between LOS and NLOS conditions. To enable appropriate scenario modelling, transition between LOS and NLOS cases have to be described. For this purpose distance dependent probability of LOS is used in the model.

#### 4.1.2 Frequency dependence

Dependence on carrier frequency in WINNER model is found in path-loss models. All the scenarios defined by WINNER support frequency dependent path-loss models valid for the ranges of 2 – 6 GHz. The path-loss models are based on measurements that are mainly conducted in 2 and 5 GHz frequency range. In addition the path-loss models are based on results from literature, like Okumura-Hata and other well-known models [OOK+68], [OTT+01], which have been extended to the desired frequency range. Path-loss frequency dependence has been considered in more detail in the paragraph 4.3.

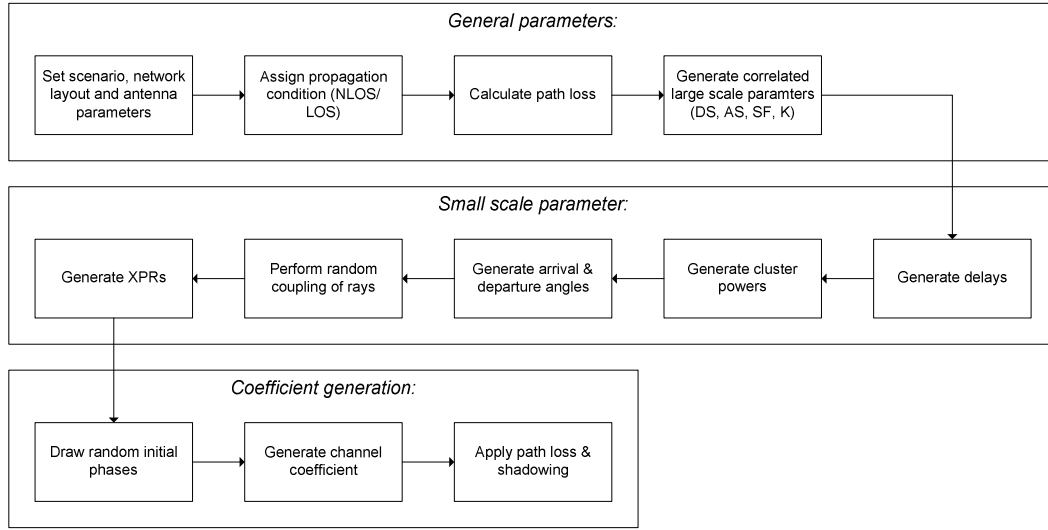
From WINNER measurement results and literature survey it was found that model parameters DS, AS and Ricean K-factor do not show significant frequency dependence [BHS05]. For that reason these parameters show only dependence on environment (scenario).

For modelling of systems with time-division-duplex (TDD) all models are using same parameters for both uplink and downlink. If system is using different carriers for duplexing (FDD), then (additionally to path loss) random phases of scatterer contributions between UL and DL are modelled as independent.

For the WINNER purposes it is required that channel model supports bandwidths up to 100 MHz. Following the approach described in [SV87] (for indoor propagation modelling) and further with SCME [BHS05] WINNER II model introduces intra-cluster delay spread as a mean to support 100 MHz bandwidth and to suppress frequency correlation. Instead of zero-delay-spread-cluster approach of Phase I model, the two strongest clusters with 20 multipath components (MPCs) are subdivided into 3 zero-delay sub-clusters. Thus we keep the total number of MPCs constant, but introduce four additional delay taps per scenario.

### 4.2 Generation of Channel Coefficients

This section gives general description of the channel coefficient generation procedure, depicted also in Figure 4-1. Steps of the procedure refer to parameter and model tables of Sections 4.2 to 4.4 give the minimum description of the system level channel model.



**Figure 4-1 Channel coefficient generation procedure**

It has to be noted, that the geometric description covers arrival angles from the last bounce scatterers and respectively departure angles to the first scatterers interacted from the transmitting side. The propagation between the first and the last interaction is not defined. Thus this approach can model also multiple interactions with the scattering media. This indicates also that e.g. the delay of a multipath component can not be determined by the geometry.

*General parameters:*

**Step 1:** Set the environment, network layout and antenna array parameters

- Choose one of the scenarios (A1, A2, B1,...)
- Give number of BS and MS
- Give locations of BS and MS, or equally distances of each BS and MS and relative directions  $\phi_{LOS}$  and  $\varphi_{LOS}$  of each BS and MS
- Give BS and MS antenna field patterns  $F_{rx}$  and  $F_{tx}$ , and array geometries
- Give BS and MS array orientations with respect to north (reference) direction
- Give speed and direction of motion of MS
- Give system centre frequency

*Large scale parameters:*

**Step 2:** Assign the propagation condition (LOS/NLOS) according to the probability described in Table 4-7.

**Step 3:** Calculate the path loss with formulas of Table 4-4 for each BS-MS link to be modelled.

**Step 4:** Generate the correlated large scale parameters, i.e. delay spread, angular spreads, Ricean K-factor and shadow fading term like explained in section 3.2.1 (Correlations between large scale parameters).

*Small scale parameters:*

**Step 5:** Generate the delays  $\tau$ .

Delays are drawn randomly from the delay distribution defined in Table 4-5. With exponential delay distribution calculate

$$\tau_n' = -r_\tau \sigma_\tau \ln(X_n), \quad (4.1)$$

where  $r_\tau$  is the delay distribution proportionality factor,  $\sigma_\tau$  is delay spread,  $X_n \sim \text{Uni}(0,1)$  and cluster index  $n = 1, \dots, N$ . With uniform delay distribution the delay values  $\tau_n'$  are drawn from the corresponding range. Normalise the delays by subtracting with minimum delay and sort the normalised delays to descending order.

$$\tau_n = \text{sort}(\tau_n' - \min(\tau_n')). \quad (4.2)$$

In the case of LOS condition additional scaling of delays is required to compensate the effect of LOS peak addition to the delay spread. Heuristically determined Ricean K-factor dependent scaling constant is

$$D = 0.7705 - 0.0433K + 0.0002K^2 + 0.000017K^3, \quad (4.3)$$

where  $K$  [dB] is the Ricean K-factor defined in Table 4-5. Scaled delays are

$$\tau_n^{LOS} = \tau_n / D, \quad (4.4)$$

they are **not** to be used in cluster power generation.

**Step 6:** Generate the cluster powers  $P$ .

The cluster powers are calculated assuming a single slope exponential power delay profile. Power assignment depends on the delay distribution defined in Table 4-5. With exponential delay distribution the cluster powers are determined by

$$P_n' = \exp\left(-\tau_n \frac{r_\tau - 1}{r_\tau \sigma_\tau}\right) \cdot 10^{\frac{-Z_n}{10}} \quad (4.5)$$

and with uniform delay distribution they are determined by

$$P_n' = \exp\left(\frac{-\tau_n}{\sigma_\tau}\right) \cdot 10^{\frac{-Z_n}{10}}, \quad (4.6)$$

where  $Z_n \sim N(0, \zeta)$  is the per cluster shadowing term in [dB]. Average the power so that sum power of all clusters is equal to one

$$P_n = \frac{P_n'}{\sum_{n=1}^N P_n'} \quad (4.7)$$

Assign the power of each ray within a cluster as  $P_n/M$ , where  $M$  is the number of rays per cluster.

**Step 7:** Generate the azimuth arrival angles  $\varphi$  and azimuth departure angles  $\phi$ .

If the composite PAS of all clusters is modelled as wrapped Gaussian (see Table 4-5) the AoA are determined by applying inverse Gaussian function with input parameters  $P_n$  and RMS angle spread  $\sigma_\varphi$

$$\varphi_n' = \frac{2\sigma_{AoA} \sqrt{-\ln(P_n / \max(P_n))}}{C}. \quad (4.8)$$

On equation above  $\sigma_{AoA} = \sigma_\varphi / 1.4$  is the standard deviation of arrival angles (factor 1.4 is the ratio of Gaussian std and corresponding "RMS spread"). Constant  $C$  is a scaling factor related to total number of clusters and is given in the table below:

# clusters	4	5	8	10	11	12	14	15	16	20
$C$	0.779	0.860	1.018	1.090	1.123	1.146	1.190	1.211	1.226	1.289

In the LOS case constant  $C$  is dependent also on Ricean K-factor. Constant  $C$  in eq. (4.10) is substituted by  $C^{LOS}$ . Additional scaling of angles is required to compensate the effect of LOS peak addition to the angle spread. Heuristically determined Ricean K-factor dependent scaling constant is

$$C^{LOS} = C \cdot (1.1035 - 0.028K - 0.002K^2 + 0.0001K^3), \quad (4.9)$$

where  $K$  [dB] is the Ricean K-factor defined in Table 4-5.

Assign a positive or negative sign to the angles by multiplying with a random variable  $X_n$  with uniform distribution to discrete set of  $\{1, -1\}$ , add component  $Y_n \sim N(0, \sigma_{AoA}/5)$  to introduce random variation

$$\varphi_n = X_n \varphi_n' + Y_n + \varphi_{LOS}, \quad (4.10)$$

where  $\varphi_{LOS}$  is the LOS direction defined in the network layout description Step1.c.

In the LOS case substitute (4.12) by (4.13) to enforce the first cluster to the LOS direction  $\varphi_{LOS}$

$$\varphi_n = (X_n \varphi_n' + Y_n) - (X_n \varphi_1' + Y_1 - \varphi_{LOS}). \quad (4.11)$$

Finally add the offset angles  $\alpha_m$  from Table 4-1 to cluster angles

$$\varphi_{n,m} = \varphi_n + c_{AoA} \alpha_m, \quad (4.12)$$

where  $c_{AoA}$  is the cluster-wise rms azimuth spread of arrival angles (cluster ASA) in the Table 4-5.

**Table 4-1 Ray offset angles within a cluster, given for 1° rms angle spread.**

Ray number $m$	Basis vector of offset angles $\alpha_m$
1,2	$\pm 0.0447$
3,4	$\pm 0.1413$
5,6	$\pm 0.2492$
7,8	$\pm 0.3715$
9,10	$\pm 0.5129$
11,12	$\pm 0.6797$
13,14	$\pm 0.8844$
15,16	$\pm 1.1481$
17,18	$\pm 1.5195$
19,20	$\pm 2.1551$

For departure angles  $\phi_n$  the procedure is analogous.

**Step 7b** *If the elevation angles are supported:* Generate elevation arrival angles  $\psi$  and elevation departure angles  $\gamma$ .

Draw elevation angles with the same procedure as azimuth angles on Step 7. Azimuth rms angle spread values and cluster-wise azimuth spread values are replaced by corresponding elevation parameters from Table 4-6.

**Step 8:** Random coupling of rays within clusters.

Couple randomly the departure ray angles  $\phi_{n,m}$  to the arrival ray angles  $\varphi_{n,m}$  within a cluster  $n$ , or within a sub-cluster in the case of two strongest clusters (see step 11 and Table 4-2).

*If the elevation angles are supported they are coupled with the same procedure.*

**Step 9:** Generate the cross polarisation power ratios (XPR)  $\kappa$  for each ray  $m$  of each cluster  $n$ .

XPR is log-Normal distributed. Draw XPR values as

$$\kappa_{m,n} = 10^{X/10}, \quad (4.13)$$

where ray index  $m = 1, \dots, M$ ,  $X \sim N(\sigma, \mu)$  is Gaussian distributed with  $\sigma$  and  $\mu$  from Table 4-5 for XPR.

*Coefficient generation:*

**Step 10:** Draw the random initial phase  $\{\Phi_{n,m}^{vv}, \Phi_{n,m}^{vh}, \Phi_{n,m}^{hv}, \Phi_{n,m}^{hh}\}$  for each ray  $m$  of each cluster  $n$  and for four different polarisation combinations (vv,vh,hv,hh). Distribution for the initial phases is uniform,  $\text{Uni}(-\pi, \pi)$ .

*In the LOS case* draw also random initial phases  $\{\Phi_{LOS}^{vv}, \Phi_{LOS}^{hh}\}$  for both VV and HH polarisations.

**Step 11:** Generate the channel coefficients for each cluster  $n$  and each receiver and transmitter element pair  $u, s$ .

*For the  $N - 2$  weakest clusters, say  $n = 3, 4, \dots, N$ , and uniform linear arrays (ULA), the channel coefficient are given by:*



$$\mathbf{H}_{u,s,n}(t) = \sqrt{P_n} \sum_{m=1}^M \begin{bmatrix} F_{tx,s,V}(\phi_{n,m}) \\ F_{tx,s,H}(\phi_{n,m}) \end{bmatrix}^T \begin{bmatrix} \exp(j\Phi_{n,m}^{vv}) & \sqrt{\kappa_{n,m}} \exp(j\Phi_{n,m}^{vh}) \\ \sqrt{\kappa_{n,m}} \exp(j\Phi_{n,m}^{hv}) & \exp(j\Phi_{n,m}^{hh}) \end{bmatrix} \begin{bmatrix} F_{rx,u,V}(\phi_{n,m}) \\ F_{rx,u,H}(\phi_{n,m}) \end{bmatrix} \cdot \exp(jd_s 2\pi\lambda_0^{-1} \sin(\phi_{n,m})) \exp(jd_u 2\pi\lambda_0^{-1} \sin(\phi_{n,m})) \exp(j2\pi v_{n,m} t) \quad (4.14)$$

where  $F_{rx,u,V}$  and  $F_{rx,u,H}$  are the antenna element  $u$  field patterns for vertical and horizontal polarisations respectively,  $d_s$  and  $d_u$  are the uniform distances [m] between transmitter elements and receiver elements respectively, and  $\lambda_0$  is the wave length on carrier frequency. If polarisation is not considered, 2x2 polarisation matrix can be replaced by scalar  $\exp(j\Phi_{n,m})$  and only vertically polarised field patterns applied.

With the fixed feeder link models (B5 scenarios) the Doppler frequency component  $v_{n,m}$  is tabulated for the first ray of each cluster. For the other rays  $v_{n,m} = 0$ . With all other models the Doppler frequency component is calculated from angle of arrival (downlink), MS speed  $v$  and direction of travel  $\theta_v$

$$v_{n,m} = \frac{\|v\| \cos(\phi_{n,m} - \theta_v)}{\lambda_0}, \quad (4.15)$$

For the two strongest clusters, say  $n = 1$  and 2, rays are spread in delay to three sub-clusters (per cluster), with fixed delay offset  $\{0, 5, 10\}$  ns (see Table 4-2). Delays of sub-clusters are

$$\begin{aligned} \tau_{n,1} &= \tau_n + 0 \text{ ns} \\ \tau_{n,2} &= \tau_n + 5 \text{ ns} \\ \tau_{n,3} &= \tau_n + 10 \text{ ns} \end{aligned} \quad (4.16)$$

Twenty rays of a cluster are mapped to sub-clusters like presented in Table 4-2 below. Corresponding offset angles are taken from Table 4-1 with mapping of Table 4-2.

**Table 4-2 Sub-cluster information for intra cluster delay spread clusters.**

sub-cluster #	mapping to rays	power	delay offset
1	1,2,3,4,5,6,7,8,19,20	10/20	0 ns
2	9,10,11,12,17,18	6/20	5 ns
3	13,14,15,16	4/20	10 ns

In the LOS case define  $\mathbf{H}'_{u,s,n} = \mathbf{H}_{u,s,n}$  and determine the channel coefficients by adding single line-of-sight ray and scaling down the other channel coefficient generated by (4.14). The channel coefficients are given by:

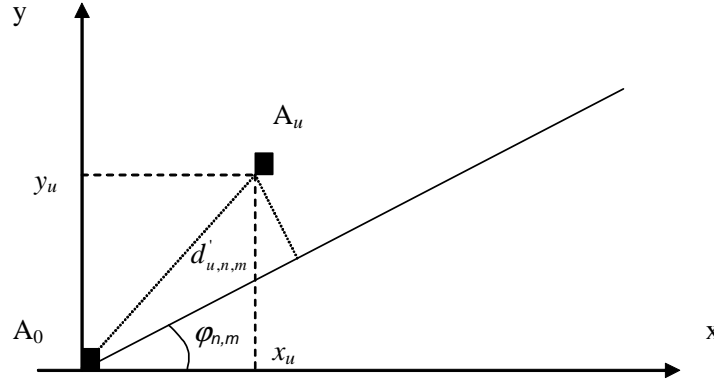
$$\begin{aligned} \mathbf{H}_{u,s,n}(t) &= \sqrt{\frac{1}{K_R + 1}} \mathbf{H}'_{u,s,n}(t) \\ &+ \delta(n-1) \sqrt{\frac{K_R}{K_R + 1}} \begin{bmatrix} F_{tx,s,V}(\phi_{LOS}) \\ F_{tx,s,H}(\phi_{LOS}) \end{bmatrix}^T \begin{bmatrix} \exp(j\Phi_{LOS}^{vv}) & 0 \\ 0 & \exp(j\Phi_{LOS}^{hh}) \end{bmatrix} \begin{bmatrix} F_{rx,u,V}(\phi_{LOS}) \\ F_{rx,u,H}(\phi_{LOS}) \end{bmatrix} \\ &\cdot \exp(jd_s 2\pi\lambda_0^{-1} \sin(\phi_{LOS})) \exp(jd_u 2\pi\lambda_0^{-1} \sin(\phi_{LOS})) \exp(j2\pi v_{LOS} t) \end{aligned} \quad (4.17)$$

where  $\delta(\cdot)$  is the Dirac's delta function and  $K_R$  is the Ricean K-factor defined in Table 4-5 converted to linear scale.

If non-ULA arrays are used the equations must be modified. For arbitrary array configurations on horizontal plane, see Figure 4-2, the distance term  $d_u$  in equations (4.14) and (4.17) is replaced by

$$d'_{u,n,m} = \frac{\sqrt{x_u^2 + y_u^2} \cos(\arctan(y_u/x_u) - \phi_{n,m})}{\sin \phi_{n,m}}, \quad (4.18)$$

where  $(x_u, y_u)$  are co-ordinates of  $u$ th element  $A_u$  and  $A_0$  is the reference element.



**Figure 4-2 Modified distance of antenna element  $u$  with non-ULA array.**

If the elevation is included (4.16) will be written as

$$\mathbf{H}_{u,s,n}(t) = \sqrt{P_n} \sum_{m=1}^M \begin{bmatrix} F_{rx,u,V}(\phi_{n,m}) \\ F_{rx,u,H}(\phi_{n,m}) \end{bmatrix}^T \begin{bmatrix} \exp(j\Phi_{n,m}^{vv}) & \sqrt{\kappa_{n,m}} \exp(j\Phi_{n,m}^{vh}) \\ \sqrt{\kappa_{n,m}} \exp(j\Phi_{n,m}^{hv}) & \exp(j\Phi_{n,m}^{hh}) \end{bmatrix} \begin{bmatrix} F_{tx,s,V}(\phi_{n,m}) \\ F_{tx,s,H}(\phi_{n,m}) \end{bmatrix} \cdot \exp(j2\pi\lambda_0^{-1} \bar{r}_s \cdot \bar{\Phi}_{n,m}) \exp(jd2\pi\lambda_0^{-1} \bar{r}_u \cdot \bar{\Psi}_{n,m}) \exp(j2\pi\nu_{n,m}t) \quad (4.19)$$

where scalar product

$$\bar{r}_s \cdot \bar{\Phi}_{n,m} = x_s \cos \gamma_{n,m} \cos \phi_{n,m} + y_s \cos \gamma_{n,m} \sin \phi_{n,m} + z_s \sin \gamma_{n,m}, \quad (4.20)$$

$\bar{r}_s$  is location vector of Tx array element  $s$ ,  $\bar{\Phi}_{n,m}$  is departure angle unit vector of ray  $n,m$  and  $x_s, y_s$  and  $z_s$  are components of  $\bar{r}_s$  to x,y and z-axis respectively,  $\phi_{n,m}$  is ray  $n,m$  arrival azimuth angle and  $\gamma_{n,m}$  is ray  $n,m$  arrival elevation angle.  $\bar{r}_u \cdot \bar{\Psi}_{n,m}$  is a scalar product of Rx antenna element  $u$  and arrival angle  $n,m$ .

Further on in the case of elevation assuming horizontal only motion, eq. (4.15) will be written as

$$\nu_{n,m} = \frac{\bar{v} \cdot \bar{\Psi}_{n,m}}{\lambda_0} = \frac{|v| \cos \theta_v \cos \gamma_{n,m} \cos \phi_{n,m} + |v| \sin \theta_v \cos \gamma_{n,m} \sin \phi_{n,m}}{\lambda_0}. \quad (4.21)$$

**Step 12:** Apply the path loss and shadowing for the channel coefficients.

#### 4.2.1 Generation of bad urban channels (B2, C3)

Bad urban channel realizations can be created as modified B1 and C2 NLOS procedures as follows:

**Step 1:**

Drop five far scatterers within a hexagonal cell, within radius [FSmin, FSmax]. For FSmin and FSmax values see Table 4-3. For each mobile user determine the closest two far scatterers, which are then used for calculating far scatterer cluster parameters.

**Table 4-3 Far scatterer radii and attenuations for B2 and C3.**

Scenario	FS <sub>min</sub>	FS <sub>max</sub>	FS <sub>loss</sub>
B2	150 m	500 m	4 dB/μs
C3	300 m	1500 m	2 dB/μs

**Step 2:**

For C3 create 20 delays as described for C2 model in section 4.2. step 5. For the shortest 18 delays create a typical urban C2 channel profile (powers and angles) as in section 4.2.

Similarly, create 16 delays for B1 NLOS, and for the shortest 14 delays create a typical B1 NLOS channel profile as in section 4.2.

The last two delays in B2 and C3 are assigned for far scatterer clusters.

**Step 3:**

Create typical urban channel powers  $P'$  for FS clusters substituting equation (4.5) of section 4.2 step 6

with  $P'_n = 10^{\frac{-Z_n}{10}}$ , where  $Z_n \sim N(0, \zeta)$  is the per cluster shadowing term in [dB].

**Step 4:**

Next create excess delays due to far scatterer clusters as

$$\tau_{\text{excess}} = \frac{d_{BS \rightarrow FS \rightarrow MS} - d_{LOS}}{c} \quad (4.22)$$

Attenuate FS clusters as FS<sub>loss</sub>, given in Table 4-3.

**Step 5:**

Select directions of departure and arrival for each FS cluster according to far scatterer locations. i.e. corresponding to a single reflection from far scatterer.

It is worth noticing that depending on the location of the mobile user within the cell the FS clusters may appear also at shorter delays than the maximum C2 or B1 NLOS cluster. In such cases the far scatterers do not necessarily result to increased angular or delay dispersion. Also the actual channel statistics of the bad urban users depend somewhat on the cell size.

### 4.3 Path loss models

Path loss models for the various WINNER scenarios have been developed based on results of measurements carried out within WINNER, as well as results from the open literature. These path loss models are typically of the form of (4.23), where  $d$  is the distance between the transmitter and the receiver in [m],  $f_c$  is the system frequency in [GHz], the fitting parameter  $A$  includes the path-loss exponent, parameter  $B$  is the intercept, parameter  $C$  describes the path loss frequency dependence, and  $X$  is an optional, environment-specific term (e.g., wall attenuation in the A1 NLOS scenario).

$$PL = A \log_{10}(d[\text{m}]) + B + C \log_{10}\left(\frac{f_c[\text{GHz}]}{5.0}\right) + X \quad (4.23)$$

The models can be applied in the frequency range from 2 – 6 GHz and for different antenna heights. The path-loss models have been summarized in Table 4-4, which either defines the variables of (4.23), or explicitly provides a full path loss formula. The free-space path loss,  $PL_{\text{free}}$ , that is referred to in the table can be written as

$$PL_{\text{free}} = 20 \log_{10}(d) + 46.4 + 20 \log_{10}(f_c/5.0) \quad (4.24)$$

The distribution of the shadow fading is log-normal, and the standard deviation for each scenario is given in the table.

#### Frequency dependencies of WINNER path-loss models

The path loss models shown in Table 4-4 are based on measured data obtained mainly at 2 and 5 GHz. These models have been extended to arbitrary frequencies in the range from 2 – 6 GHz with the aid of the path loss frequency dependencies defined below. Following various results from the open literature, as

[RMB+06, CG+99, JHH+05, Rudd03, SMI+02, KI04, YIT06], the following frequency extensions are employed for the frequency coefficient  $C$  shown in (4.23)

- (1) For all LOS deployment scenarios, and for all distances smaller than or equal to the breakpoint distance,  $d'_{BP}$ :  $C = 20$ . Beyond the breakpoint distance, the frequency dependence is defined by the formulas in Table 4-4.
- (2) For rural NLOS environments:  $C = 20$ ;
- (3) For urban and suburban NLOS macrocells:  $C = 23$ ;
- (4) For urban and suburban NLOS microcells:  $C = 23$ ;
- (5) For indoor environments:  $C = 20$ ;
- (6) For indoor-to-outdoor and outdoor-to-indoor environments:  $C$  is the same as in the corresponding outdoor scenario;
- (7) For fixed NLOS feeder scenarios: in urban and suburban scenarios  $C = 23$ , otherwise  $C = 20$ .

**Table 4-4 Summary table of the path-loss models**

Scenario	Path loss [dB]	Shadow fading std [dB]	Applicability range, antenna height default values
LOS	$A = 18.7, B = 46.8, C = 20$	$\sigma = 3$	$3\text{m} < d < 100\text{m}$ , $h_{BS} = h_{MS} = 1 \dots 2.5\text{m}$
A1	NLOS <sup>1)</sup> $A = 36.8, B = 43.8, C = 20$ and $X = 5(n_w - 1)$ (light walls) <b>or</b> $X = 12(n_w - 1)$ (heavy walls)	$\sigma = 4$	same as A1 LOS, $n_w$ is the number of walls between the BS and the MS ( $n_w > 0$ for NLOS)
	NLOS <sup>2)</sup> light walls:	$\sigma = 6$	same as A1 LOS, $n_w$ is the number of walls between BS and MS
	heavy walls:	$\sigma = 8$	
	FL For any of the cases above, add the floor loss (FL), if the BS and MS are in different floors: $FL = 17 + 4(n_f - 1), n_f > 0$		$n_f$ is the number of floors between the BS and the MS ( $n_f > 0$ )
A2 NLOS	$PL = PL_b + PL_{tw} + PL_{in}$ , $\begin{cases} PL_b = PL_{B1}(d_{out} + d_{in}) \\ PL_{tw} = 14 + 15(1 - \cos(\theta))^2 \\ PL_{in} = 0.5d_{in} \end{cases}$	$\sigma = 7$	$3\text{m} < d_{out} + d_{in} < 1000\text{m}$ , $h_{BS} = 3(n_{FI} - 1) + 2\text{m}$ $h_{MS} = 1.5$ , See <sup>3)</sup> for explanation of parameters
B1	LOS $A = 22.7, B = 41.0, C = 20$ $PL = 40.0 \log_{10}(d_1) + 9.45 - 17.3 \log_{10}(h'_{BS}) - 17.3 \log_{10}(h'_{MS}) + 2.7 \log_{10}(f_c/5.0)$	$\sigma = 3$  $\sigma = 3$	$10\text{m} < d_1 < d'_{BP}$ <sup>4)</sup>  $d'_{BP} < d_1 < 5\text{km}$ $h_{BS} = 10\text{m}, h_{MS} = 1.5\text{m}$
	NLOS $PL = \min(PL(d_1, d_2), PL(d_2, d_1))$ where $PL(d_k, d_l) =$ $PL_{LOS}(d_k) + 20 - 12.5n_j + 10n_j \log_{10}(d_l) + 3 \log_{10}(f_c/5.0)$ and $n_j = \max(2.8 - 0.0024d_k, 1.84)$ , $PL_{LOS}$ is the path loss of B1 LOS scenario and $k, l \in \{1, 2\}$ .	$\sigma = 4$	$10\text{m} < d_1 < 5\text{km}$ , $w/2 < d_2 < 2\text{km}$ <sup>5)</sup> $w = 20\text{m}$ (street width) $h_{BS} = 10\text{m}, h_{MS} = 1.5\text{m}$ When $0 < d_2 < w/2$ , the LOS PL is applied.
B2 NLOS	Same as B1.	$\sigma = 4$	

B3	LOS	$A = 13.9, B = 64.4, C = 20$	$\sigma = 3$	$5\text{m} < d < 100\text{m},$ $h_{BS} = 6\text{m}, h_{MS} = 1.5\text{m}$
	NLOS	$A = 37.8, B = 36.5, C = 23$	$\sigma = 4$	Same as B3 LOS
B4	NLOS	Same as A2, except antenna heights.		$3\text{m} < d_{out} + d_{in} < 1000\text{m},$ $h_{BS} = 10\text{m}, h_{MS} = 3(n_{FI} - 1) + 1.5\text{m}$
B5a	LOS	$A = 23.5, B = 42.5, C = 20$	$\sigma = 4$	$30\text{m} < d < 8\text{km}$ $h_{BS} = 25\text{m}, h_{RS} = 25\text{m}$
B5c	LOS	Same as B1 LOS, except antenna heights ( $h_{RS}$ is the relay antenna height).	$\sigma = 3$	$10\text{m} < d < 2000\text{m}$ $h_{BS} = 10\text{m}, h_{MS} (=h_{RS}) = 5\text{m}$
B5f	NLOS	$A = 23.5, B = 57.5, C = 23$	$\sigma = 8$	$30\text{m} < d < 1.5\text{km}$ $h_{BS} = 25\text{m}, h_{RS} = 15\text{m}$
C1	LOS	$A = 23.8, B = 41.2, C = 20$ $PL = 40.0 \log_{10}(d) + 11.65 - 16.2 \log_{10}(h_{BS})$ $- 16.2 \log_{10}(h_{MS}) + 3.8 \log_{10}(f_c/5.0)$	$\sigma = 4$ $\sigma = 6$	$30\text{m} < d < d_{BP},$ $d_{BP} < d < 5\text{km},$ $h_{BS} = 25\text{m}, h_{MS} = 1.5\text{m}$
	NLOS	$PL = (44.9 - 6.55 \log_{10}(h_{BS})) \log_{10}(d) + 31.46$ $+ 5.83 \log_{10}(h_{BS}) + 23 \log_{10}(f_c/5.0)$	$\sigma = 8$	$50\text{m} < d < 5\text{km},$ $h_{BS} = 25\text{m}, h_{MS} = 1.5\text{m}$
C2	LOS	$A = 26, B = 39, C = 20$ $PL = 40.0 \log_{10}(d) + 13.47 - 14.0 \log_{10}(h'_{BS})$ $- 14.0 \log_{10}(h'_{MS}) + 6.0 \log_{10}(f_c/5.0)$	$\sigma = 4$ $\sigma = 6$	$10\text{m} < d < d'_{BP} \text{ } ^4)$ $d'_{BP} < d < 5\text{km}$ $h_{BS} = 25\text{m}, h_{MS} = 1.5\text{m}$
	NLOS	$PL = (44.9 - 6.55 \log_{10}(h_{BS})) \log_{10}(d) + 34.46$ $+ 5.83 \log_{10}(h_{BS}) + 23 \log_{10}(f_c/5.0)$	$\sigma = 8$	Same as C1 NLOS
C3	NLOS	Same as C2 NLOS		Same as C2 NLOS
C4	NLOS	$PL = PL_{C2}(d_{out} + d_{in}) + 17.4 + 0.5d_{in} - 0.8h_{MS}$ where $PL_{C2}$ is the path-loss function of C2 LOS/NLOS scenario. (Use LOS, if BS to wall connection is LOS, otherwise use NLOS)	$\sigma = 10$	Same as C2 NLOS See <sup>3)</sup> for explanation of parameters. $h_{BS} = 25\text{m}, h_{MS} = 3n_{FI} + 1.5\text{m}$
D1	LOS	$A = 21.5, B = 44.2, C = 20$ $PL = 40.0 \log_{10}(d) + 10.5 - 18.5 \log_{10}(h_{BS})$ $- 18.5 \log_{10}(h_{MS}) + 1.5 \log_{10}(f_c/5.0)$	$\sigma = 4$ $\sigma = 6$	$10\text{m} < d < d_{BP}, \text{ } ^6)$ $d_{BP} < d < 10\text{km},$ $h_{BS} = 32\text{m}, h_{MS} = 1.5\text{m}$
	NLOS	$PL = 25.1 \log_{10}(d) + 55.4 - 0.13(h_{BS} - 25) \log_{10}(d/100)$ $- 0.9(h_{MS} - 1.5) + 21.3 \log_{10}(f_c/5.0)$	$\sigma = 8$	$50\text{m} < d < 5\text{km},$ $h_{BS} = 32\text{m}, h_{MS} = 1.5\text{m}$
D2a	LOS	Same as D1 LOS		

- 1) Actual A1 NLOS scenario (Corridor-to-Room)
- 2) Optional A1 NLOS scenario (Room-to-Room through wall)
- 3)  $PL_{B1}$  is the B1 path loss,  $PL_{C2}$  is the C2 path loss,  $d_{out}$  is the distance between the outdoor terminal and the point on the wall that is nearest to the indoor terminal,  $d_{in}$  is the distance from the wall to the indoor terminal,  $\theta$  is the angle between the outdoor path and the normal of the wall.  $n_{FI}$  is the floor index (the ground floor has index 1).
- 4)  $d'_{BP} = 4 h'_{BS} h'_{MS} f_c / c$ , where  $f_c$  is the centre frequency in Hz,  $c = 3.0 \times 10^8$  m/s is the propagation velocity in free space, and  $h'_{BS}$  and  $h'_{MS}$  are the effective antenna heights at the BS and the MS, respectively. The effective antenna heights  $h'_{BS}$  and  $h'_{MS}$  are computed as follows:  $h'_{BS} = h_{BS} - 1.0$  m,  $h'_{MS} = h_{MS} - 1.0$  m, where  $h_{BS}$  and  $h_{MS}$  are the actual antenna heights, and the effective environment height in urban environments is assumed to be equal to 1.0 m.
- 5) The distances  $d_1$  and  $d_2$  will be defined below in Figure 4-3.
- 6) The breakpoint distance,  $d_{BP}$ , is computed as follows:  $d_{BP} = 4 h_{BS} h_{MS} f_c / c$ , where  $h_{BS}$ ,  $h_{MS}$ ,  $f_c$  and  $c$  have the same definition as under item 4).

The NLOS path loss model for scenario B1 is dependent on two distances,  $d_1$  and  $d_2$ . These distances are defined with respect to a rectangular street grid, as illustrated in Figure 4-3, where the MS is shown moving along a street perpendicular to the street on which the BS is located (the LOS street).  $d_1$  is the distance from the BS to the centre of the perpendicular street, and  $d_2$  is the distance of the MS along the perpendicular street, measured from the centre of the LOS street.

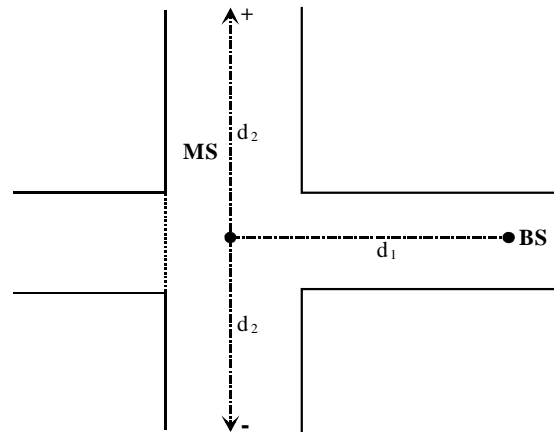


Figure 4-3 Geometry for  $d_1$  and  $d_2$  path-loss model

#### 4.3.1 Transitions between LOS/NLOS

The WINNER channel model allows transitions between different propagation conditions, the most important of which are transitions between LOS and NLOS within the same WINNER scenario. In the A1 (indoor) and B1 (urban microcell) scenarios, transitions from LOS to NLOS can occur as a result of the MS turning from the corridor or street in which the BS is located (the LOS corridor/street) into a perpendicular corridor or street. An analysis of this specific case has indicated that such transitions can be adequately modelled by using the A1 or B1 LOS and NLOS path loss models defined in Table 4-4. Let  $d_1$  and  $d_2$  denote the distances along the LOS corridor/street and the perpendicular corridor/street, respectively, as illustrated in Figure 4-3. The A1 LOS path loss model is then considered to be applicable for values of  $d_2$  smaller than  $3F_1$ , where  $F_1$  represents the radius of the first Fresnel zone (for definition of Fresnel zones see [Sau99, sec 3.3.1]). For values of  $d_2$  greater than  $3F_1$ , the A1 NLOS path loss model can be used. For the B1 scenario, a better fit to measured data was obtained by choosing the NLOS/LOS transition distance equal to  $10F_1$ . It is noted that, in most cases, reasonably good results can also be obtained by setting the transition distance equal to half the width of the LOS corridor or street, as reflected by the path loss model for B1 NLOS in Table 4-4.

#### 4.4 Parameter tables for generic models

Table 4-5 provides parameter values corresponding to the WINNER generic channel models. Parameter values related to elevation angles are provided in Table 4-6.

Table 4-5 Table of parameters for generic models.

Scenarios		A1		A2/B4/C4 #	B1		B3		C1		C2		D1		D2a
		LOS	NLOS	NLOS	LOS	NLOS	LOS	NLOS	LOS	NLOS	LOS	NLOS	LOS	NLOS	LOS
Delay spread ( <i>DS</i> ) $\log_{10}[\text{s}]$	$\mu$	-7.42	-7.60	-7.39/ -6.62 <sup>v</sup>	-7.44	-7.12	-7.53	-7.41	-7.23	-7.12	-7.39	-6.63	-7.80	-7.60	-7.4
	$\sigma$	0.27	0.19	0.36/ 0.32 <sup>v</sup>	0.25	0.12	0.12	0.13	0.49	0.33	0.63	0.32	0.57	0.48	0.2
AoD spread ( <i>ASD</i> ) $\log_{10}[\text{°}]$	$\mu$	1.64	1.73	1.76	0.40	1.19	1.22	1.05	0.78	0.90	1	0.93	0.78	0.96	0.7
	$\sigma$	0.31	0.23	0.16	0.37	0.21	0.18	0.22	0.12	0.36	0.25	0.22	0.21	0.45	0.31
AoA spread ( <i>ASA</i> ) $\log_{10}[\text{°}]$	$\mu$	1.65	1.69	1.25	1.40	1.55	1.58	1.7	1.48	1.65	1.7	1.72	1.20	1.52	1.5
	$\sigma$	0.26	0.14	0.42	0.20	0.20	0.23	0.1	0.20	0.30	0.19	0.14	0.18	0.27	0.2
Shadow fading ( <i>SF</i> ) [dB]	$\sigma$	3	4	7	3	4	3	4	4/6 <sup>+</sup>	8	4/6 <sup>+</sup>	8	4/6 <sup>+</sup>	8	4
	$\mu$	7	N/A	N/A	9	N/A	2	N/A	9	N/A	7	N/A	7	N/A	7
K-factor ( <i>K</i> ) [dB]	$\sigma$	6	N/A	N/A	6	N/A	3	N/A	7	N/A	3	N/A	6	N/A	6
Cross-Correlations *	<i>ASD</i> vs <i>DS</i>	0.7	-0.1	0.4	0.5	0.2	-0.3	-0.1	0.2	0.3	0.4	0.4	-0.1	-0.4	-0.1
	<i>ASA</i> vs <i>DS</i>	0.8	0.3	0.4	0.8	0.4	-0.4	0	0.8	0.7	0.8	0.6	0.2	0.1	0.2
	<i>ASA</i> vs <i>SF</i>	-0.5	-0.4	0.2	-0.5	-0.4	-0.2	0.2	-0.5	-0.3	-0.5	-0.3	-0.2	0.1	-0.2
	<i>ASD</i> vs <i>SF</i>	-0.5	0	0	-0.5	0	0.3	-0.3	-0.5	-0.4	-0.5	-0.6	0.2	0.6	0.2
	<i>DS</i> vs <i>SF</i>	-0.6	-0.5	-0.5	-0.4	-0.7	-0.1	-0.2	-0.6	-0.4	-0.4	-0.4	-0.5	-0.5	-0.5
	<i>ASD</i> vs <i>ASA</i>	0.6	-0.3	0	0.4	0.1	0.3	-0.3	0.1	0.3	0.3	0.4	-0.3	-0.2	-0.3
	<i>ASD</i> vs <i>K</i>	-0.6	N/A	N/A	-0.3	N/A	0.2	N/A	0.2	N/A	0.1	N/A	0	N/A	0
	<i>ASA</i> vs <i>K</i>	-0.6	N/A	N/A	-0.3	N/A	-0.1	N/A	-0.2	N/A	-0.2	N/A	0.1	N/A	0.1
	<i>DS</i> vs <i>K</i>	-0.6	N/A	N/A	-0.7	N/A	-0.3	N/A	-0.2	N/A	-0.4	N/A	0	N/A	0
	<i>SF</i> vs <i>K</i>	0.4	N/A	N/A	0.5	N/A	0.6	N/A	0	N/A	0.3	N/A	0	N/A	0
Delay distribution		Exp	Exp	Exp	Exp	Uniform ≤800ns	Exp	Exp	Exp	Exp	Exp	Exp	Exp	Exp	Exp
AoD and AoA distribution		Wrapped Gaussian													
Delay scaling parameter $r_\tau$		3	2.4	2.2	3.2	—	1.9	1.6	2.4	1.5	2.5	2.3	3.8	1.7	3.8
XPR [dB]	$\mu$	11	10	9	9	8	9	6	8	4	8	7	12	7	12
	$\sigma$	4	4	11	3	3	4	3	4	3	4	3	8	4	8
Number of clusters		12	16	12	8	16	10	15	15	14	8	20	11	10	8
Number of rays per cluster		20	20	20	20	20	20	20	20	20	20	20	20	20	20
Cluster <i>ASD</i>		5	5	8	3	10	5	6	5	2	6	2	2	2	2
Cluster <i>ASA</i>		5	5	5	18	22	5	13	5	10	12	15	3	3	3
Per cluster shadowing std $\zeta$ [dB]		6	3	4	3	3	3	3	3	3	3	3	3	3	3
Correlation distance [m]	<i>DS</i>	7	4	21/10 <sup>Δ</sup>	9	8	3	1	6	40	40	40	64	36	64
	<i>ASD</i>	6	5	15/11 <sup>Δ</sup>	13	10	1	0.5	15	30	15	50	25	30	25
	<i>ASA</i>	2	3	35/17 <sup>Δ</sup>	12	9	2	0.5	20	30	15	50	40	40	40
	<i>SF</i>	6	4	14/7 <sup>Δ</sup>	14	12	3	3	40	50	45	50	40	120	40
	<i>K</i>	6	N/A	N/A	10	N/A	1	N/A	10	N/A	12	N/A	40	N/A	40

NOTE! With arrival and departure directions we consider downlink case, i.e. departure refers to BS and arrival refers to MS.

\* The path loss models for the C1 LOS and D1 LOS scenarios contain separate shadowing standard deviations for distances smaller and greater than the breakpoint distance, respectively.

\* The sign of the shadow fading term is defined so that increasing values of *SF* correspond to increasing received power at the MS.

# AoD and AoA refer to azimuth angles at the indoor and outdoor terminals, respectively. Parameter values for the B4 and C4 scenarios are identical.

<sup>v</sup> In case column A2/B4/C4 contains two parameter values, the left value corresponds to A2/B4 microcell and the right value to C4 macrocell.

<sup>Δ</sup> In case column A2/B4/C4 contains two parameter values, the left value corresponds to A2 Indoor-to-Outdoor and the right value to B4/C4 Outdoor-to-Indoor.

**Table 4-6 Table of elevation-related parameters for generic models.**

Scenarios		A1		A2/B4 <sup>#</sup> /C4
		LOS	NLOS	NLOS
Elevation AoD spread ( <i>ESD</i> )	$\mu$	0.88	1.06	0.88
	$\sigma$	0.31	0.21	0.34
Elevation AoA spread ( <i>ESA</i> )	$\mu$	0.94	1.10	1.01
	$\sigma$	0.26	0.17	0.43
Cross-Correlations	<i>ESD</i> vs <i>DS</i>	0.5	-0.6	N/A
	<i>ESA</i> vs <i>DS</i>	0.7	-0.1	0.2
	<i>ESA</i> vs <i>SF</i>	-0.1	0.3	0.2
	<i>ESD</i> vs <i>SF</i>	-0.4	0.1	N/A
	<i>ESD</i> vs <i>ESA</i>	0.4	0.5	N/A
Elevation AoD and AoA distribution		Gaussian		
Cluster <i>ESD</i>		3	3	3
Cluster <i>ESA</i>		3	3	3

<sup>#</sup>ESD and ESA refer to elevation angle spreads at the indoor and outdoor terminals, respectively.

System level simulations require estimates of the probability of line-of-sight. For scenarios A2, B2, B4, C2 and C3, the LOS probability is approximated as being zero. For the remaining scenarios, LOS probability models are provided in Table 4-7. These models are based on relatively limited data sets and/or specific assumptions and approximations regarding the location of obstacles in the direct path, and should therefore not be considered exact.

If the terminal locations are known with respect to a street grid or floor plan, which can be the case in grid-based scenarios such as A1 (indoor) and B1 (urban microcell), the WINNER channel model provides the option to determine the existence of NLOS/LOS propagation conditions deterministically.

**Table 4-7 Line of sight probabilities**

Scenario	LOS probability as a function of distance $d$ [m]	Note
A1	$P_{LOS} = \begin{cases} 1 & , d \leq 2.5 \\ 1 - 0.9(1 - (1.24 - 0.61 \log_{10}(d))^3)^{1/3} & , d > 2.5 \end{cases}$	
B1	$P_{LOS} = \min(18/d, 1) \cdot (1 - \exp(-d/36)) + \exp(-d/36)$	
B3	$P_{LOS} = \begin{cases} 1 & , d \leq 10 \\ \exp\left(-\frac{d-10}{45}\right) & , d > 10 \end{cases}$	For big factory halls, airport and train stations.
C1	$P_{LOS} = \exp\left(-\frac{d}{200}\right)$	
C2	$P_{LOS} = \min(18/d, 1) \cdot (1 - \exp(-d/63)) + \exp(-d/63)$	
D1	$P_{LOS} = \exp\left(-\frac{d}{1000}\right)$	

#### 4.4.1 Reference output values

Table 4-8 and Table 4-9 provide median values of the large-scale parameters produced by the WINNER channel model for various scenarios. The values in Table 4-9 were computed under the



assumption that the maximum cell radii for microcells and macrocells are 200 and 500 m, respectively, and that the distribution of user terminals over the cell area is uniform. The median values are dependent on cell radii, thus the tabulated values are not universal in bad urban scenarios.

**Table 4-8: Median output values of large-scale parameters.**

Scenario		DS (ns)	AS at BS (°)	AS at MS (°)	ES at BS (°)	ES at MS (°)
A1	LOS	40	44	45	8	9
	NLOS	25	53	49	11	13
A2/B4 <sup>#</sup> /C4	NLOS	49/240 <sup>∇</sup>	58	18	10	10
B1	LOS	36	3	25		
	NLOS	76	15	35		
B3	LOS	27	17	38	21.2	
	NLOS	39	12	50	22.3	
C1	LOS	59	6	30		
	NLOS	75	8	45		
C2	LOS	41	10	50		
	NLOS	234	8	53		
D1	LOS	16	6	16		
	NLOS	37	9	33		
D2	LOS	39	5	32		

<sup>#</sup>AS at BS denotes indoor azimuth spread and AS at MS denotes outdoor azimuth spread

<sup>∇</sup> In case column A2/B4/C4 contains two parameter values, the left value corresponds to A2/B4 microcell and the right value to C4 macrocell.

**Table 4-9: Median output values of large scale parameters for bad urban scenarios.**

Scenario	DS (μs)	AS at BS (°)	AS at MS (°)	Power of the 1 <sup>st</sup> FS cluster (dB)	Power of the 2 <sup>nd</sup> FS cluster (dB)	Delay of the 1 <sup>st</sup> FS cluster (μs)	Delay of the 2 <sup>nd</sup> FS cluster (μs)
B2	0.48	33	51	-5.7	-7.7	1.1	1.6
C3	0.63	17	55	-9.7	-13.0	3.1	4.8

## 4.5 CDL Models

Although the clustered delay line (CDL) model is based on similar principles as the conventional tapped delay line model, it is different in the sense that the fading process for each tap is modelled in terms of a sum of sinusoids rather than by a single tap coefficient. The CDL model describes the propagation channel as being composed of a number of separate clusters with different delays. Each cluster, in turn, is composed of a number of multipath components (rays) that have the same delay values but differ in angle-of-departure and angle-of-arrival. The angular spread within each cluster can be different at the BS and the MS. The offset angles represent the Laplacian PAS of each cluster. The average power, mean AoA, mean AoD of clusters, angle-spread at BS and angle-spread at MS of each cluster in the CDL represent expected output of the stochastic model with parameters listed in Table 4-8. Exceptions are the fixed feeder link models in scenario B5, for which no stochastic models have been defined.

Parameter tables for the CDL models are given in Section 6 of this document.

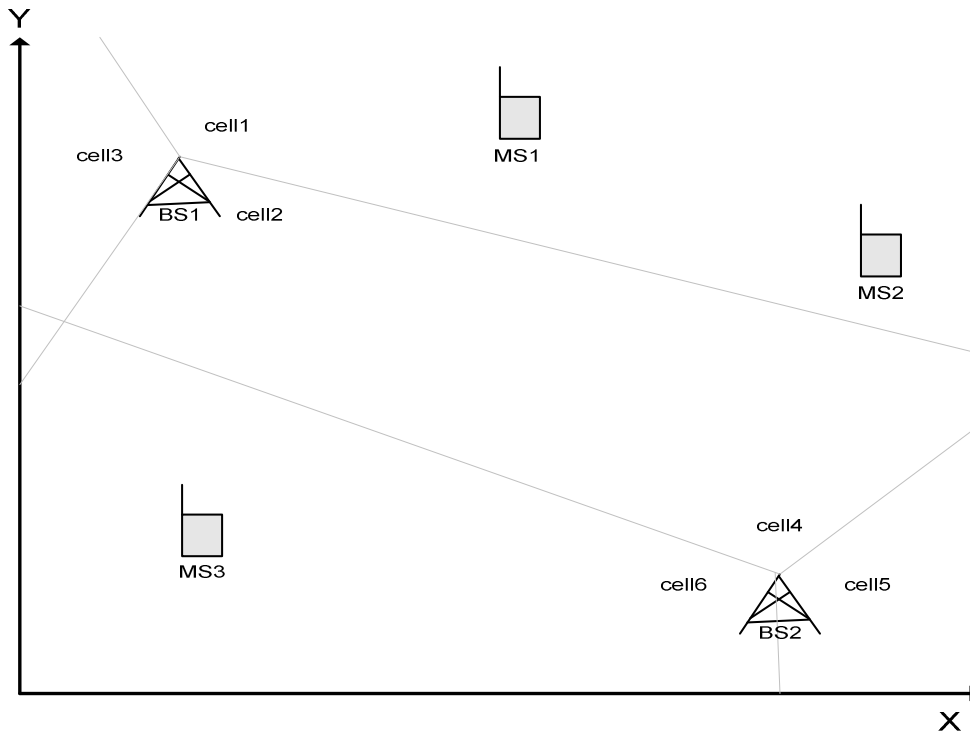
## 5. Channel Model Usage

The purpose of this chapter is to discuss issues concerning usage of the WINNER channel model for simulations.

### 5.1 System level description

#### 5.1.1 Coordinate system

System layout in the Cartesian coordinates is for example the following:



**Figure 5-1: System layout of multiple base stations and mobile stations.**

All the BS and MS have (x,y) coordinates. MS and cells (sectors) have also array broad side orientation, where north (up) is the zero angle. Positive direction of the angles is the clockwise direction.

**Table 5-1: Transceiver coordinates and orientations.**

Tranceiver		Co-ordinates	Orientation [°]
BS1	cell1	$(x_{bs1}, y_{bs1})$	$\Omega_{c1}$
	cell2	$(x_{bs1}, y_{bs1})$	$\Omega_{c2}$
	cell3	$(x_{bs1}, y_{bs1})$	$\Omega_{c3}$
BS2	cell4	$(x_{bs2}, y_{bs2})$	$\Omega_{c4}$
	cell5	$(x_{bs2}, y_{bs2})$	$\Omega_{c5}$
	cell6	$(x_{bs2}, y_{bs2})$	$\Omega_{c6}$
MS1		$(x_{ms1}, y_{ms1})$	$\Omega_{ms1}$
MS2		$(x_{ms2}, y_{ms2})$	$\Omega_{ms2}$
MS3		$(x_{ms3}, y_{ms3})$	$\Omega_{ms3}$

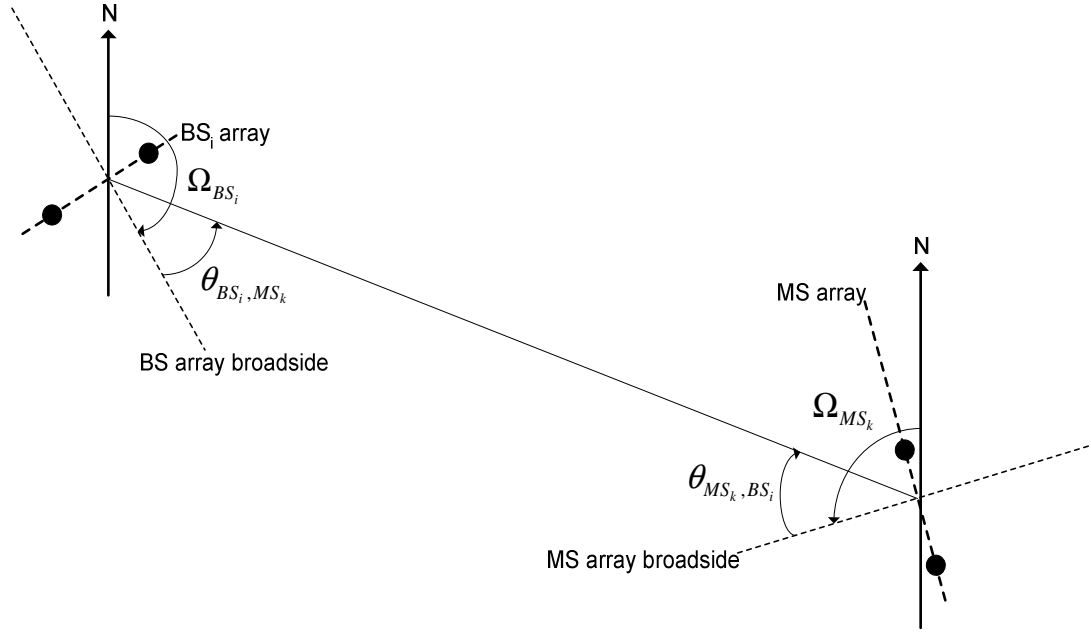
Both the distance and line of sight (LOS) direction information of the radio links are calculated for the input of the model. Distance between the  $BS_i$  and  $MS_k$  is

$$d_{BS_i, MS_k} = \sqrt{(x_{BS_i} - x_{MS_k})^2 + (y_{BS_i} - y_{MS_k})^2}. \quad (5.1)$$

The LOS direction from  $BS_i$  to  $MS_k$  with respect to BS antenna array broad side is (see Figure 5-2)

$$\theta_{BS_i, MS_k} = \begin{cases} -\arctan\left(\frac{y_{MS_k} - y_{BS_i}}{x_{MS_k} - x_{BS_i}}\right) + 90^\circ - \Omega_{BS_i}, & \text{when } x_{MS_k} \geq x_{BS_i} \\ -\arctan\left(\frac{y_{MS_k} - y_{BS_i}}{x_{MS_k} - x_{BS_i}}\right) - 90^\circ - \Omega_{BS_i}, & \text{when } x_{MS_k} < x_{BS_i} \end{cases} \quad (5.2)$$

The angles and orientations are depicted in the figure below.



**Figure 5-2: BS and MS antenna array orientations.**

Pairing matrix  $\mathbf{A}$  is in the example case of Figure 5-2 a 6x3 matrix with values  $\chi_{n,m} \in \{0,1\}$ . Value 0 stands for link cell  $n$  to  $MS_m$  is not modelled and value 1 for link is modelled.

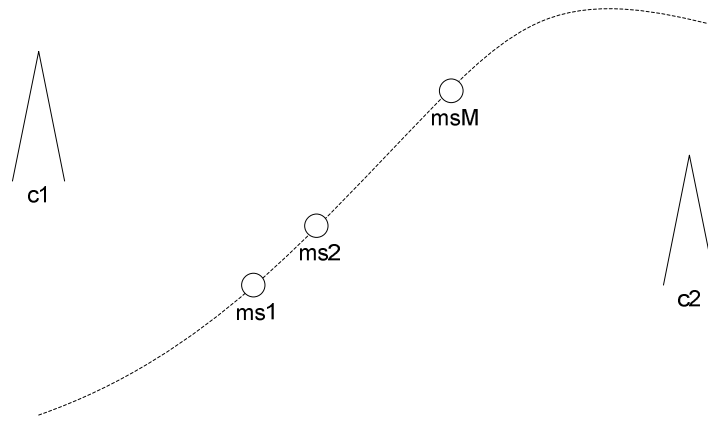
$$\mathbf{A} = \begin{bmatrix} \chi_{c1,ms1} & \chi_{c1,ms2} & \chi_{c1,ms3} \\ \chi_{c2,ms1} & \chi_{c2,ms2} & \chi_{c2,ms3} \\ \vdots & \vdots & \vdots \\ \chi_{c6,ms1} & \chi_{c6,ms2} & \chi_{c6,ms3} \end{bmatrix} \quad (5.3)$$

The pairing matrix can be applied to select which radio links will be generated and which will not.

## 5.1.2 Multi-cell simulations

### 5.1.2.1 Single user (Handover)

A handover situation is characterized by a MS moving from the coverage area of one BS to the coverage area of another BS. Figure 5-3 illustrates this setup.



**Figure 5-3: Handover scenario.**

There are two base-stations or cells denoted  $c1$  and  $c2$ , and one mobile station. Thus, while there is only one mobile station in the scenario, each location of the mobile on its path is assigned a unique label  $ms1$  to  $msM$ . This is equivalent to a scenario with multiple mobile stations at different positions  $ms1$  to  $msM$ . Path-loss will be determined according to the geometry and large-scale parameters correlate properly. The resulting procedure is as follows:

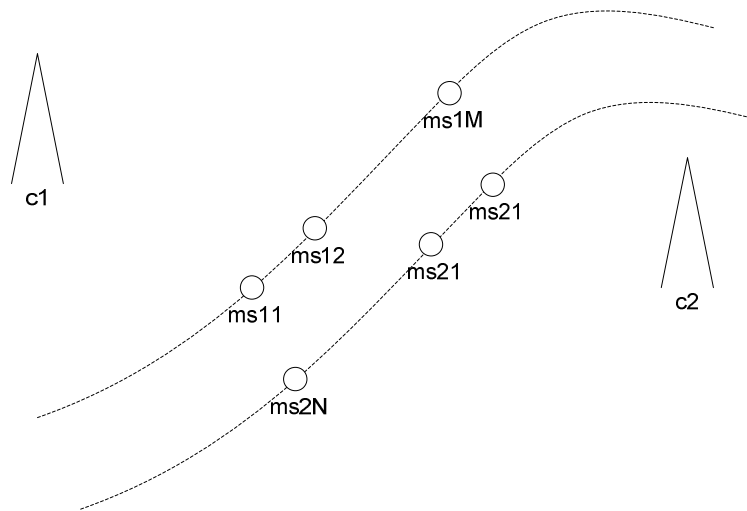
1. Set base station  $c1$  and  $c2$  locations and array orientations according to geometry.
2. Set MS locations  $ms1$  to  $msM$  and array orientations along the route. Choose the distance between adjacent locations according to desired accuracy.
3. Set all the entries of the pairing matrix to 1.
4. Generate all the radio links at once to obtain correct correlation properties. It is possible to generate more channel realizations, i.e. time samples, for each channel segment afterwards. This can be done by applying the same values of small scale parameters and restoring final phases of the rays.
5. Simulate channel segments consecutively to emulate motion along the route.

It is also possible to model even more accurate time evolution between locations as described in section 3.4. The clusters of current channel segment (location) are replaced by clusters of the next channel segment one by one.

#### 5.1.2.2 Multi-user

The handover situation from the previous section was an example of single-user multi-cell setup. Other cases of such a setup are for example found in the context of multi-BS protocols, where a MS receives data from multiple BS simultaneously.

The extension to multiple users (and one or more base stations) is straightforward. Because location and mobile station index are treated equivalently, it follows that all locations of all mobiles have to be defined. Consider the drive-by situation in Figure 5-4.



**Figure 5-4: Drive-by scenario (with multiple mobile stations).**

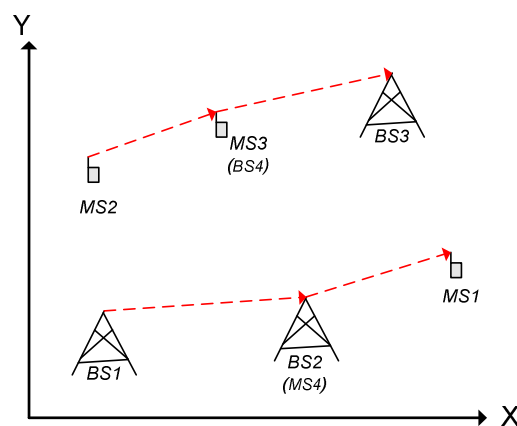
Here,  $M$  locations of mobile station 1, and  $N$  locations of mobile station 2 are defined yielding a total of  $M+N$  points or labels. The resulting procedure is as follows.

1. Set BS  $c1$  and  $c2$  locations and array orientations according to layout.
2. Set MS locations  $ms11$  to  $ms2N$  and array orientations according to layout.
3. Set the links to be modelled to 1 in the pairing matrix.
4. Generate all the radio links at once to obtain correct correlation properties. It is possible to generate more channel realizations, i.e. time samples, for each channel segment afterwards. This can be done by applying the same values of small scale parameters and restoring final phases of the rays.
5. Simulate channel segments in parallel or consecutively according to the desired motion of the mobiles.

### 5.1.3 Multihop and relaying

Typically, the links between the MSs and the links between the BSs are not of interest. Cellular systems are traditionally networks where all traffic goes through one or more BS. The BS themselves again only talk to a BS hub and not between them.

Multihop and relaying networks break with this limitation. In multihop networks, the data can take a route over one or more successive MS. Relaying networks, on the other hand, employ another level of network stations, the relays, which depending on the specific network, might offer more or less functionality to distribute traffic intelligently. The WINNER channel model can be used to obtain the channels for multihop or relaying scenarios, as described below.



**Figure 5-5: Multihop and relaying scenarios.**

In the example figure above the signal from *MS1* to *BS3* is transmitted via *MS3* and *BS2* act as a repeater for *BS1*. These scenarios can be generated by introducing a BS-MS pair into position of a single BS serving as a relay or into position of a single MS serving as a multihop repeater. In these cases one can apply path-loss models of feeder scenarios described in section 3.2.4. The resulting procedure is as follows.

1. Set base station *BS1* to *BS3* locations and array orientations according to layout.
2. Set mobile locations *MS1* to *MS3* and array orientations according to layout.
3. Add extra base station *BS4* to position of *MS3* and extra mobile *MS4* to position of *BS2* with same array orientations and array characteristics as *MS3* and *BS2* respectively.
4. Set the *BSxMS* pairing matrix to

$$\mathbf{A} = \begin{bmatrix} 0 & 0 & 0 & 1 \\ 1 & 0 & 0 & 0 \\ 0 & 0 & 1 & 0 \\ 0 & 1 & 0 & 0 \end{bmatrix}$$

5. Generate all the radio links at once.
6. Simulate the channel segments in parallel.

### 5.1.4 Interference

Interference modelling is an application subset of channel models that deserves additional consideration. Basically, communication links that contain interfering signals are to be treated just as any other link. However, in many communication systems these interfering signals are not treated and processed in the same way as the desired signals and thus modelling the interfering links with full accuracy is inefficient.

A simplification of the channel modelling for the interference link is often possible but closely linked with the communication architecture. This makes it difficult for a generalized treatment in the context of channel modelling. In the following we will thus constrain ourselves to giving some possible ideas of how this can be realised. Note that these are all combined signal and channel models. The actual implementation will have to be based on the computational gain from computational simplification versus the additional programming overhead.

#### AWGN interference

The simplest form of interference is modelled by additive white Gaussian noise. This is sufficient for basic C/I (carrier to interference ratio) evaluations when coupled with a path loss and shadowing model. It might be extended with e.g. on-off keying (to simulate the non-stationary behaviour of actual transmit signals) or other techniques that are simple to implement.

#### Filtered noise

The possible wideband behaviour of an interfering signal is not reflected in the AWGN model above. An implementation using a complex SCM or WIM channel, however, might be unnecessarily complex as well because the high number of degrees of freedom does not become visible in the noise-like signal anyway. Thus we propose something along the lines of a simple, sample-spaced FIR filter with Rayleigh-fading coefficients.

#### Pre-recorded interference

A large part of the time-consuming process of generating the interfering signal is the modulation and filtering of the signal, which has to be done at chip frequency. Even if the interfering signal is detected and removed in the communication receiver (e.g., multi-user detection techniques) and thus rendering a PN generator too simple, a method of pre-computing and replaying the signal might be viable. The repeating content of the signal using this technique is typically not an issue as the content of the interferer is discarded anyway.

#### Exact interference by multi-cell modelling

Interference situations are quite similar to multi-cell or multi-BS situations, except that in this case the other BSs transmit a non-desired signal which creates interference.

## 5.2 Space-time concept in simulations

### 5.2.1 Time sampling and interpolation

Channel sampling frequency has to be finally equal to the simulation system sampling frequency. To have feasible computational complexity it is not possible to generate channel realisations on the sampling frequency of the system to be simulated. The channel realisations have to be generated on some lower sampling frequency and then interpolated to the desired frequency. A practical solution is e.g. to generate channel samples with sample density (over-sampling factor) two, interpolate them accurately to sample density 64 and to apply zero order hold interpolation to the system sampling frequency. Channel impulse responses can be generated during the simulation or stored on a file before the simulation on low sample density. Interpolation can be done during the system simulation.

To be able to obtain the deep fades in the NLOS scenarios, we suggest using 128 samples per wavelength (parameter 'SampleDensity' = 64). When obtaining channel parameters quasi-stationarity has been assumed within intervals of 10-50 wavelengths. Therefore we propose to set the drop duration corresponding to the movement of up to 50 wavelengths.

## 5.3 Radio-environment settings

### 5.3.1 Scenario transitions

In the channel model implementation it is not possible to simulate links from different scenarios within one drop. This assumes that all propagation scenarios are the same for all simulated links. The change of the scenario in time can be simulated by changing the scenario in the consecutive drop.

Similarly, to obtain different scenarios within radio-network in the same drop, multiple drops could be simulated – one for each scenario. Afterwards, merging should be performed.

### 5.3.2 LOS\NLOS transitions

Mix of LOS and NLOS channel realizations can be obtained by first calculating a set of LOS drops and after it a set of NLOS drops. This can be done by setting the parameter 'PropagCondition' to 'LOS' and later to 'NLOS'.

## 5.4 Bandwidth/Frequency dependence

### 5.4.1 Frequency sampling

The WINNER system is based on the OFDM access scheme. For simulations of the system, channel realizations in time-frequency domain are needed. The output of WIM is the channel in time-delay domain. The time-frequency channel at any frequency can be obtained by applying next two steps:

- define a vector of frequencies where the channel should be calculated
- by use of the Fourier transform calculate the channel at defined frequencies

### 5.4.2 Bandwidth down scaling

The channel models are delivered for 100 MHz RF band-width. Some simulations may need smaller bandwidths. Therefore we describe below shortly, how the down-scaling should be performed. In doing so we assume that the channel parameters remain constant in down-scaling as indicated in our analyses.

#### 5.4.2.1 Down-scaling in delay domain

There is a need for down-scaling, if the minimum delay sample spacing in the Channel Impulse Response (CIR) is longer than 5 ns in the simulation. Five nanoseconds is the default minimum spacing for the channel model samples (taps) and defines thus the delay grid for the CIR taps. For all smaller spacings the model shall be down-scaled. The most precise way would be filtering by e.g. a FIR filter. This would, however, create new taps in the CIR and this is not desirable. The preferred method in the delay domain is the following:

- Move the original samples to the nearest location in the down-sampled delay grid.
- In some cases there are two such locations. Then the tap should be placed in the one that has the smaller delay.
- Sometimes two taps will be located in the same delay position. Then they should be summed as complex numbers.

Above it has been assumed that the CIR samples are taken for each MIMO channel separately and that the angle information has been vanished in this process. This is the case, when using the model e.g. with the WIM implementation [WIN2WIM].

#### 5.4.2.2 Down-scaling in frequency domain

If desired, the down-scaling can also be performed in the frequency domain. Then the starting point will be the original CIR specified in the delay domain. This CIR is transformed in the frequency domain for each simulation block. Then the transformed CIR can be filtered as desired, e.g. by removing the extra frequency samples, and used in the simulation as normally.

The maximum frequency sampling interval is determined by the coherence bandwidth

$$B_c = \frac{1}{C\sigma_\tau}, \quad (5.4)$$

where  $\sigma_\tau$  is the rms delay spread and  $C$  is a scaling constant related to fading distribution.

#### 5.4.3 FDD modeling

In next steps we explain how to obtain both uplink and downlink channel of an FDD system with bandwidths of 100 MHz. The center carrier frequencies are  $f_c$  and  $f_c + \Delta f_c$ :

- Define BS and MS positions, calculate the channel for one link, e.g. BS to MS at certain carrier frequency  $f_c$
- Save the small scale parameters
- Exchange the positions of the BS and MS
- Calculate the other link, in this example the MS to BS by:
  - Using saved small scale parameters
  - Randomizing the and initial phases of rays
  - Changing the carrier frequency to  $f_c + \Delta f$

### 5.5 Comparison tables of WINNER channel model versions

This section shows the main differences between the different versions of WINNER channel models (Phase I (D5.4), Phase II Interim (D1.1.1), and Phase II Final (D1.1.2) models). Note! This section is aimed as comparison of the different versions, not as the primary source of channel model parameters.

Table below shows which scenarios are available in the different versions. Note that all the scenarios of Phase I have been updated in Phase II models.

**Table 5-2: Availability of Generic and CDL models**

Scenario		Phase I		Phase II			
		D5.4		D1.1.1		D1.1.2	
		Generic model	CDL	Generic model	CDL	Generic model	CDL
A1	indoor office	yes	yes	yes	yes	yes	yes
A2	indoor-to-outdoor			yes	yes	yes	yes
B1	urban micro-cell	yes	yes	yes	yes	yes	yes
B2	bad urban micro-cell			yes	yes	yes	yes
B3	large indoor hall	yes	yes	yes	yes	yes	yes



B4	outdoor-to-indoor			yes	yes	yes	yes
B5a	stationary feeder		yes		yes		yes
B5b	stationary feeder		yes		yes		yes
B5c	stationary feeder		yes		yes		yes
B5d	stationary feeder		yes				
B5f	stationary feeder				yes		yes
C1	suburban macro-cell	yes	yes		yes		yes
C2	urban macro-cell	yes	yes		yes		yes
C3	bad urban macro-cell				yes		yes
C4	urban macro outdoor-to-indoor						yes
C5	LOS feeder				yes		yes
D1	rural macro-cell	yes	yes	yes	yes	yes	yes
D2a	moving networks			yes	yes	yes	yes
D2b	moving networks					yes	yes

The features of Phase I model and Phase II model are compared in table below.

**Table 5-3: Comparison of Features.**

Feature	Phase I		Phase II			
	D5.4		D1.1.1		D1.1.2	
	generic model	CDL	generic model	CDL	generic model	CDL
Number of main scenarios (see table above)	7	7	13	13	14	14
Number of scenarios including sub-scenarios (a,b,c,...)	10	10	16	16	18	18
Number of scenarios including sub-scenarios and LOS/NLOS versions	15	15	21	21	24	24
Indoor-to-outdoor models			yes	yes	yes	yes
Outdoor-to-indoor models			yes	yes	yes	yes
Bad urban models			yes	yes	yes	yes
Moving networks models			yes	yes	yes	yes
Support of coordinate system	yes		yes		yes	
Support of multi-cell and multi-user simulations	yes		yes		yes	
Support of multihop and relaying simulations	yes	yes*	yes	yes*	yes	yes*
Correlation of large-scale parameters	yes		yes		yes	
Support of interference simulations	yes		yes		yes	
Time evolution			yes		yes	
Reduced variability clustered delay line (CDL) model for calibration,		yes		yes		yes

comparisons, and fast simulations						
CDL analyzed from measured PDP		yes				
CDL based on expectation values of generic model				yes		yes
Intra-cluster delay spread			yes	yes	yes	yes
Far cluster option			yes	yes	yes	yes
Modelling of elevation					yes	yes
LOS as random variable					yes	yes
Moving scatterers					yes	yes

\* With slight modification: AoD and AoA should be adjusted according to the network layout.

Table below shows the difference in parameter values.

**Table 5-4: Comparison of parameters of Phase I and Phase II models**

Parameter	Unit	Phase I		Phase II	
		D5.4		D1.1.1	D1.1.2
		Generic model	CDL	Generic and CDL model	Generic and CDL model
Frequency range	GHz	5	5	2 – 6	2 – 6
Bandwidth	MHz	100	100	100	100
Number of sub-paths per cluster		10	10	20	20
A1 LOS delay spread	ns	39.8	12.9	38.0	40
A1 NLOS delay spread	ns	25.1	24.5	25.1	25
B1 LOS delay spread	ns	36	19.5	41.7	36
B1 NLOS delay spread	ns	76	94.7	81.3	76
B3 LOS delay spread	ns	26.0	18.6	28.2	
B3 NLOS delay spread	ns	45.0	30.0	39.8	
C1 LOS delay spread	ns	1.6	29.6	58.9	59
C1 NLOS delay spread	ns	55.0	61.5	75.9	75
C2 LOS delay spread	ns				41
C2 NLOS delay spread	ns	234.4	313.0	182.0	234
D1 LOS delay spread	ns	15.8	20.4	15.8	16
D1 NLOS delay spread	ns	25.1	27.8	25.1	37
D2 LOS delay spread	ns				39
A1 LOS AoD spread	°	5.5	5.1	43.7	44
A1 NLOS AoD spread	°	20.0	23.2	53.7	53
B1 LOS AoD spread	°	3	5.6	2.5	3
B1 NLOS AoD spread	°	15	12.4	17.4	15

B3 LOS AoD spread	°	26.4	3.7	30.2	
B3 NLOS AoD spread	°	38.0	3.0	39.8	
C1 LOS AoD spread	°	13.8	14.2	13.8	6
C1 NLOS AoD spread	°	3.4	5.0	3.4	8
C2 LOS AoD spread	°				10
C2 NLOS AoD spread	°	8.5	8.0	8.5	8
D1 LOS AoD spread	°	16.6	21.5	16.6	6
D1 NLOS AoD spread	°	9.1	22.4	9.1	9
D2 LOS AoD spread	°				5
A1 LOS AoA spread	°	33.1	32.5	44.7	45
A1 NLOS AoA spread	°	37.2	39.1	46.8	49
B1 LOS AoA spread	°	25	37.1	25.1	25
B1 NLOS AoA spread	°	35	36.4	39.8	35
B3 LOS AoA spread	°	13.1	18.1	14.1	
B3 NLOS AoA spread	°	9.5	18.7	11.7	
C1 LOS AoA spread	°	40.7	45.8	40.7	30
C1 NLOS AoA spread	°	46.8	53.0	46.8	45
C2 LOS AoA spread	°				50
C2 NLOS AoA spread	°	52.5	53.0	52.5	53
D1 LOS AoA spread	°	33.1	24.0	33.1	16
D1 NLOS AoA spread	°	33.1	17.9	33.1	33
D2 LOS AoA spread	°				30
A1 LOS Shadow fading	dB	3.1		3	3
A1 NLOS Shadow fading	dB	3.5		6	6
B1 LOS Shadow fading	dB	2.3		3	3
B1 NLOS Shadow fading	dB	3.1		4	4
B3 LOS Shadow fading	dB	1.4		2	
B3 NLOS Shadow fading	dB	2.1		2	
C1 LOS Shadow fading	dB	4.0 ... 6.0		4 ... 6	4 ... 6
C1 NLOS Shadow fading	dB	8.0		8	8
C2 LOS Shadow fading	dB	8.0		8	4
C2 NLOS Shadow fading	dB				8
D1 LOS Shadow fading	dB	3.5 ... 6.0		4 ... 6	4 ... 6
D1 NLOS Shadow fading	dB	8.0		8	8
D2 LOS Shadow fading	dB				2.5

## 5.6 Approximation of Channel Models

WINNER Generic model is aimed to be applicable for many different simulations and to cover high number of scenarios with several combinations of large-scale and small-scale parameters. Generic model is the most accurate model and is recommended to be used whenever possible. However, in some simulations, channel model can be simplified (approximated) to reduce the simulation complexity. It has to be done very carefully. When approximating the model, reality is reduced, and the impact of the approximation has to be understood. The impact of the approximation depends on, e.g., the transceiver system, algorithms, modulation, coding, multi-antenna technology, and required accuracy of the simulation results. If someone is uncertain whether approximation affects on the simulation results or not, it is better not to approximate. Therefore, the following approximation steps can only be done by the simulation experts.

Firstly, we can approximate the model by assuming all the large scale parameters fixed to median values. Furthermore, we can reduce the model by fixing the delays, but keep angles as random. The third approximation can be done by freezing all propagation parameters to obtain so called Clustered Delay Line (CDL) model. If, from a good reason, correlation model is desired, we can calculate correlation matrices from the CDL model by fixing the antenna structure. Kronecker approach can simplify the model even further, and finally, independent channels make the model very simple, but at the same time very inaccurate. The approximation steps are shown below.

- A) WINNER II Generic Model (D1.1.2)
- B) Fixed large scale parameters
- C) Constant delays, random angles (“CDL with random angles”)
- D) WINNER II CDL Model (D1.1.2)
- E) Tapped Delay Line model (delays are taken from CDL) with MIMO Correlation Matrix
- F) Tapped Delay Line model with TX and RX Correlation Matrix, MIMO correlation is obtained via Kronecker product.
- G) Tapped Delay Line model, zero correlation between MIMO channels.

## 6. Parameter Tables for CDL Models

In the CDL model each cluster is composed of 20 rays with fixed offset angles and identical power. In the case of cluster where a ray of dominant power exists, the cluster has 20+1 rays. This dominant ray has a zero angle offset. The departure and arrival rays are coupled randomly. The CDL table of all scenarios of interest are give below, where the cluster power and the power of each ray are tabulated. The CDL models offer well-defined radio channels with fixed parameters to obtain comparable simulation results with relatively non-complicated channel models.

Delay spread and azimuth spreads medians of the CDL models are equal to median values given in Table 4-8. Intra cluster delay spread is defined in Table 4-2.

### 6.1 A1 – Indoor small office

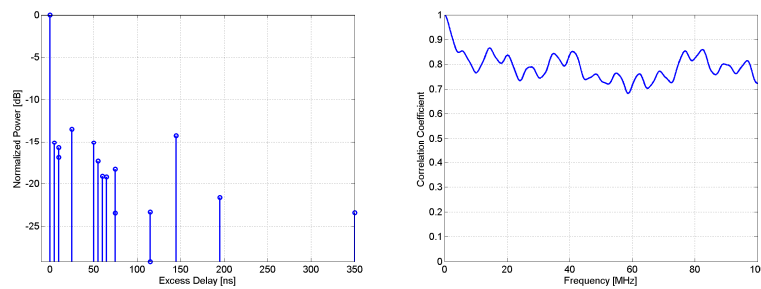
The CDL parameters of LOS and NLOS condition are given below. In the LOS model Ricean K-factor is 4.7 dB.

**Table 6-1 Scenario A1: LOS Clustered delay line model, indoor environment.**

Cluster #	Delay [ns]			Power [dB]			AoD [°]	AoA [°]	Ray power [dB]		Cluster ASD = 5°	Cluster ASA = 5°	XPR = 11 dB
1	0	5	10	0	-15.1	-16.9	0	0	-0.23*	-22.9**			
2	10			-15.8			-107	-110	-28.8				
3	25			-13.5			-100	102	-26.5				
4	50	55	60	-15.1	-17.3	-19.1	131	-134	-25.1				
5	65			-19.2			118	121	-32.2				
6	75			-23.5			131	-134	-36.5				
7	75			-18.3			116	-118	-31.3				
8	115			-23.3			131	-134	-36.4				
9	115			-29.1			146	149	-42.2				
10	145			-14.2			102	105	-27.2				
11	195			-21.6			-126	129	-34.6				
12	350			-23.4			131	-134	-36.4				

\* Power of dominant ray,

\*\* Power of each other ray



**Figure 6-1: PDP and frequency correlation (FCF) of CDL model.**

**Table 6-2 Scenario A1: NLOS Clustered delay line model, indoor environment.**

Cluster #	Delay [ns]	Power [dB]	AoD [°]	AoA [°]	Ray power [dB]	Cluster ASD = 5°	Cluster ASA = 5°	XPR = 10 dB
1	0	-2.2	45	41	-15.2			
2	5	-6.6	77	-70	-19.7			
3	5	-2.1	43	39	-15.1			
4	5	-5.8	72	66	-18.8			
5	15	-3.3	54	-49	-16.3			
6	15	-4.7	-65	59	-17.7			

7	15			-4.1			-60	-55	-17.1			
8	20			-8.2			85	-78	-21.2			
9	20	25	30	-3.0	-5.2	-7.0	0	0	-13.0			
10	35	40	45	-4.6	-6.8	-8.6	-104	95	-14.6			
11	80			-10.0			95	86	-23.0			
12	85			-12.1			-104	95	-25.1			
13	110			-12.4			-105	-96	-25.4			
14	115			-11.8			103	-94	-24.8			
15	150			-20.4			-135	123	-33.4			
16	175			-16.6			-122	-111	-29.6			

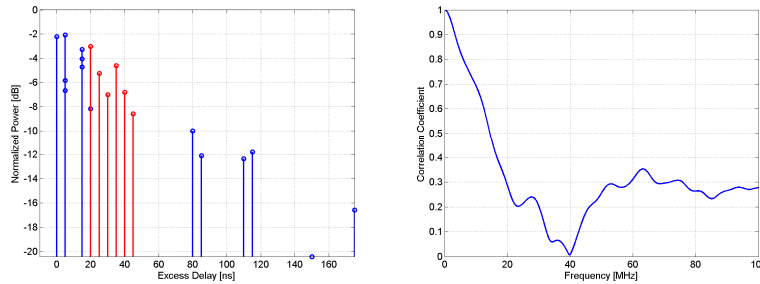


Figure 6-2: PDP and frequency correlation (FCF) of CDL model.

## 6.2 A2/B4 – Indoor to outdoor / outdoor to indoor

Table 6-3 Scenario A2/B4: NLOS Clustered delay line model, indoor to outdoor environment.

Cluster #	Delay [ns]			Power [dB]			*AoD [°]	*AoA [°]	Ray power [dB]	** Cluster ASD = 8°	** Cluster ASA = 5°	XPR = 9 dB
1	0	5	10	-3.0	-5.2	-7.0	0	0	-13.0			
2	0			-8.7			102	32	-21.7			
3	5			-3.7			-66	-21	-16.7			
4	10			-11.9			-119	37	-24.9			
5	35			-16.2			139	-43	-29.2			
6	35			-6.9			91	28	-19.9			
7	65	70	75	-3.4	-5.6	-7.3	157	-49	-13.4			
8	120			-10.3			-111	-34	-23.3			
9	125			-20.7			157	-49	-33.7			
10	195			-16.0			138	43	-29.1			
11	250			-21.0			158	49	-34.0			
12	305			-22.9			165	51	-35.9			

\* AoD refer to angles of the indoor terminal and AoA refer to outdoor terminal

\*\* Cluster ASD refer to indoor terminal and Cluster ASA refer to outdoor terminal

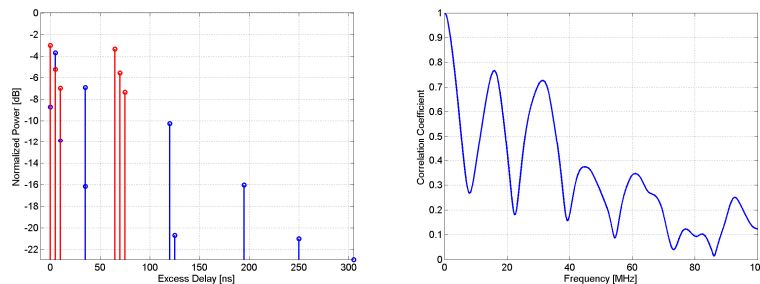


Figure 6-3: PDP and frequency correlation (FCF) of CDL model.

### 6.3 B1 – Urban micro-cell

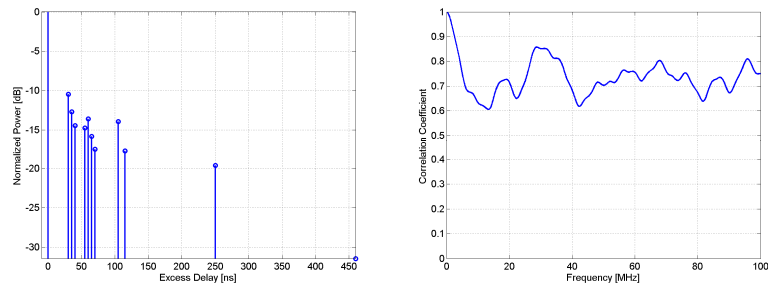
The parameters of the CDL model have been extracted from measurements with chip frequency of 60 MHz at frequency range of 5.3 GHz. In the LOS model Ricean K-factor is 3.3 dB.

**Table 6-4 Scenario B1: LOS Clustered delay line model.**

Cluster #	Delay [ns]			Power [dB]			AoD [°]	AoA [°]	Ray power [dB]		Cluster ASD = 3°	Cluster ASA = 18°	XPR = 9 dB
1	0			0.0			0	0	-0.31 <sup>*</sup>	-24.7 <sup>**</sup>			
2	30	35	40	-10.5	-12.7	-14.5	5	45	-20.5				
3	55			-14.8			8	63	-27.8				
4	60	65	70	-13.6	-15.8	-17.6	8	-69	-23.6				
5	105			-13.9			7	61	-26.9				
6	115			-17.8			8	-69	-30.8				
7	250			-19.6			-9	-73	-32.6				
8	460			-31.4			11	92	-44.4				

\* Power of dominant ray,

\*\* Power of each other ray



**Figure 6-4: PDP and frequency correlation (FCF) of CDL model.**

**Table 6-5 Scenario B1: NLOS Clustered delay line model.**

Cluster #	Delay [ns]			Power [dB]			AoD [°]	AoA [°]	Ray power [dB]	Cluster ASD = 10°	Cluster ASA = 22°	XPR = 8 dB
1	0			-1.0			8	-20	-14.0			
2	90	95	100	-3.0	-5.2	-7.0	0	0	-13.0			
3	100	105	110	-3.9	-6.1	-7.9	-24	57	-13.9			
4	115			-8.1			-24	-55	-21.1			
5	230			-8.6			-24	57	-21.6			
6	240			-11.7			29	67	-24.7			
7	245			-12.0			29	-68	-25.0			
8	285			-12.9			30	70	-25.9			
9	390			-19.6			-37	-86	-32.6			
10	430			-23.9			41	-95	-36.9			
11	460			-22.1			-39	-92	-35.1			
12	505			-25.6			-42	-99	-38.6			
13	515			-23.3			-40	94	-36.4			
14	595			-32.2			47	111	-45.2			
15	600			-31.7			47	110	-44.7			
16	615			-29.9			46	-107	-42.9			

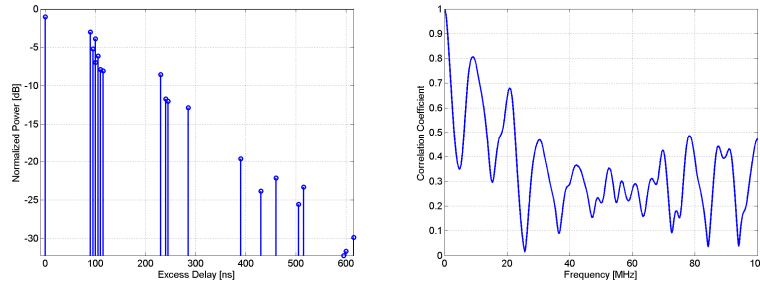


Figure 6-5: PDP and frequency correlation (FCF) of CDL model.

## 6.4 B2 – Bad Urban micro-cell

Table 6-6 Scenario B2: NLOS Clustered delay line model, bad urban, microcell

Cluster #	Delay [ns]			Power [dB]			AoD [°]	AoA [°]	Ray power [dB]	Cluster ASD = 10°	Cluster ASA = 22°	XPR = 8 dB
1	0	5	10	-3.0	-5.2	-7.0	0	0	-13.0			
2	35			-5.4			20	-46	-18.4			
3	135	140	145	-5.0	-7.2	-9.0	40	-92	-15.0			
4	190			-8.2			25	57	-21.2			
5	350			-21.8			40	-92	-34.8			
6	425			-25.5			-44	-100	-38.5			
7	430			-28.7			-46	-106	-41.7			
8	450			-20.8			39	90	-33.8			
9	470			-30.7			-48	-110	-43.7			
10	570			-34.9			-51	-117	-47.9			
11	605			-34.5			-51	-116	-47.5			
12	625			-31.5			-48	-111	-44.5			
13	625			-35.3			-51	-118	-48.3			
14	630			-37.5			53	121	-50.5			
15	1600			-5.7			-110	15	-18.7	3°	3°	
16	2800			-7.7			75	-25	-20.7			

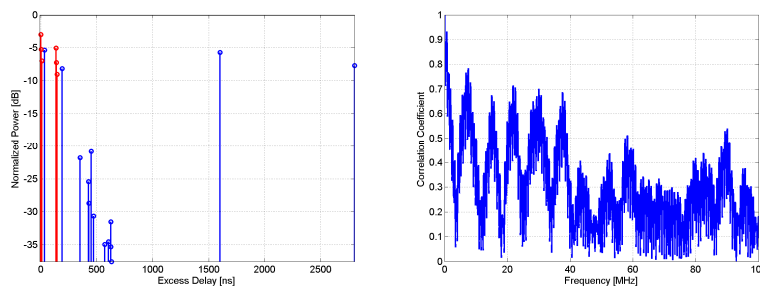


Figure 6-6: PDP and frequency correlation (FCF) of CDL model.

## 6.5 B3 – Indoor hotspot

The CDL parameters of LOS and NLOS condition are given below. In the LOS model Ricean K-factor is 2 dB.

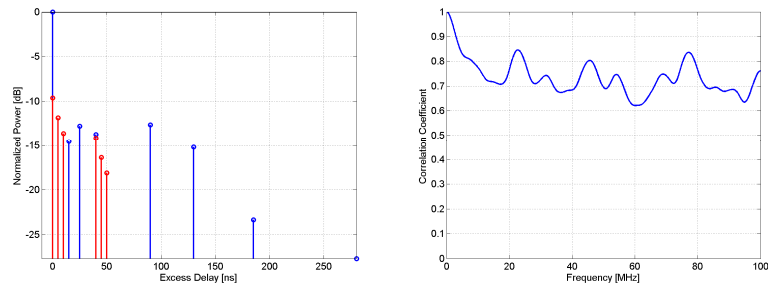


**Table 6-7 Scenario B3: LOS Clustered delay line model.**

Cluster #	Delay [ns]			Power [dB]			AoD [°]	AoA [°]	Ray power [dB]		Cluster ASD = 5°	Cluster ASA = 5°	XPR = 9 dB
1	0			0.0			0	0	-0.32*	-24.5**			
2	0	5	10	-9.6	-11.8	-13.6	-23	-53		-19.6			
3	15			-14.5			-34	-79		-27.6			
4	25			-12.8			-32	-74		-25.8			
5	40			-13.7			33	76		-26.8			
6	40	45	50	-14.1	-16.4	-18.1	-35	80		-24.1			
7	90			-12.6			32	-73		-25.6			
8	130			-15.2			-35	80		-28.2			
9	185			-23.3			-43	-100		-36.4			
10	280			-27.7			47	-108		-40.7			

\* Power of dominant ray,

\*\* Power of each other ray

**Figure 6-7: PDP and frequency correlation (FCF) of CDL model.****Table 6-8 Scenario B3: NLOS Clustered delay line model.**

Cluster #	Delay [ns]			Power [dB]			AoD [°]	AoA [°]	Ray power [dB]	Cluster ASD = 6°	Cluster ASD = 13°	XPR = 5 dB
1	0			-6.6			-16	-73	-19.6			
2	5	10	15	-3.0	-5.2	-7.0	0	0	-13.0			
3	5			-11.0			-21	-94	-24.0			
4	10	15	20	-4.3	-6.5	-8.2	-10	-46	-14.3			
5	20			-7.1			17	75	-20.1			
6	20			-2.7			-10	-46	-15.7			
7	30			-4.3			-13	-59	-17.3			
8	60			-14.1			-24	107	-27.1			
9	60			-6.2			-16	71	-19.2			
10	65			-9.1			19	86	-22.1			
11	75			-5.5			-15	67	-18.5			
12	110			-11.1			-21	95	-24.1			
13	190			-11.8			22	98	-24.8			
14	290			-17.0			-26	117	-30.1			
15	405			-24.9			-32	142	-37.9			

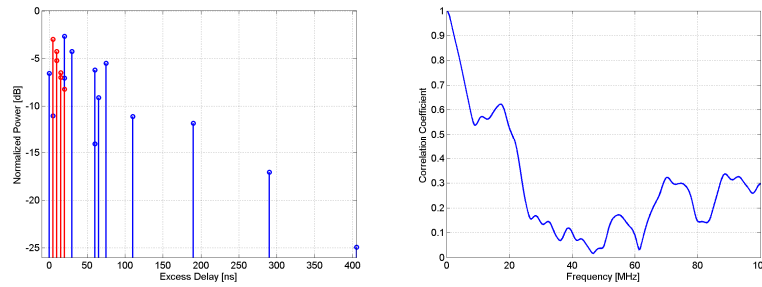


Figure 6-8: PDP and frequency correlation (FCF) of CDL model.

## 6.6 C1 – Urban macro-cell

The CDL parameters of LOS and NLOS condition are given below. In the LOS model Ricean K-factor is 12.9 dB.

Table 6-9 Scenario C1: LOS Clustered delay line model, suburban environment.

Cluster #	Delay [ns]			Power [dB]			AoD [°]	AoA [°]	Ray power [dB]		Cluster ASD = 5° Cluster ASA = 5° XPR = 8 dB
1	0	5	10	0.0	-25.3	-27.1	0	0	-0.02*	-33.1**	
2	85			-21.6			-29	-144	-34.7		
3	135			-26.3			-32	-159	-39.3		
4	135			-25.1			-31	155	-38.1		
5	170			-25.4			31	156	-38.4		
6	190			-22.0			29	-146	-35.0		
7	275			-29.2			-33	168	-42.2		
8	290	295	300	-24.3	-26.5	-28.2	35	-176	-34.3		
9	290			-23.2			-30	149	-36.2		
10	410			-32.2			35	-176	-45.2		
11	445			-26.5			-32	-159	-39.5		
12	500			-32.1			35	-176	-45.1		
13	620			-28.5			33	-165	-41.5		
14	655			-30.5			34	-171	-43.5		
15	960			-32.6			35	177	-45.6		

\* Power of dominant ray,

\*\* Power of each other ray

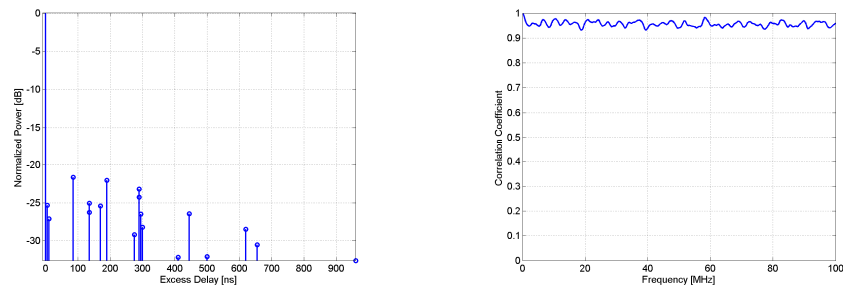
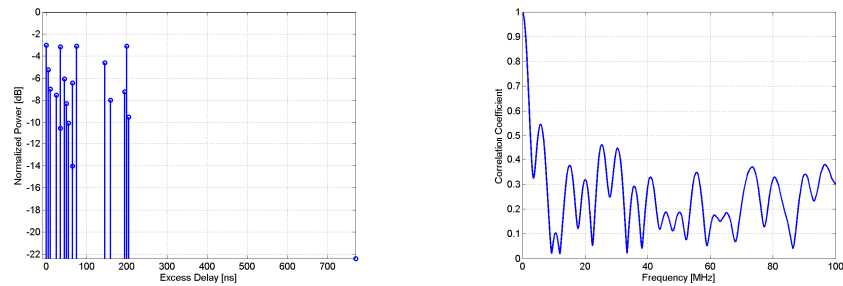


Figure 6-9: PDP and frequency correlation (FCF) of CDL model.

**Table 6-10 Clustered delay-line model for Scenario C1 NLOS**

Cluster #	Delay [ns]			Power [dB]			AoD [°]	AoA [°]	Ray power [dB]	Cluster ASD = 2°	Cluster ASA = 10°	XPR = 4 dB
1	0	5	10	-3.0	-5.2	-7.0	0	0	-13.0			
2	25			-7.5			13	-71	-20.5			
3	35			-10.5			-15	-84	-23.5			
4	35			-3.2			-8	46	-16.2			
5	45	50	55	-6.1	-8.3	-10.1	12	-66	-16.1			
6	65			-14.0			-17	-97	-27.0			
7	65			-6.4			12	-66	-19.4			
8	75			-3.1			-8	-46	-16.1			
9	145			-4.6			-10	-56	-17.6			
10	160			-8.0			-13	73	-21.0			
11	195			-7.2			12	70	-20.2			
12	200			-3.1			8	-46	-16.1			
13	205			-9.5			14	-80	-22.5			
14	770			-22.4			22	123	-35.4			

**Figure 6-10: PDP and frequency correlation (FCF) of CDL model.**

## 6.7 C2 – Urban macro-cell

The CDL parameters of LOS and NLOS condition are given below. In the LOS model Ricean K-factor is 7.0 dB.

**Table 6-11 Scenario C2: LOS Clustered delay line model.**

Cluster #	Delay [ns]			Power [dB]			AoD [°]	AoA [°]	Ray power [dB]		Cluster ASD = 6°	Cluster ASA = 12°	XPR = 8 dB
1	0			0.0			0	0	-0.08*	-30.6**			
2	0	5	10	-16.2	-18.4	-20.2	-24	-120		-26.2			
3	30			-15.3			26	129		-28.3			
4	85			-16.7			-27	-135		-29.7			
5	145	150	155	-18.2	-20.4	-22.2	26	-129		-28.2			
6	150			-18.2			28	141		-31.2			
7	160			-15.3			26	-129		-28.3			
8	220			-23.1			-32	-158		-36.1			

\* Power of dominant ray,

\*\* Power of each other ray

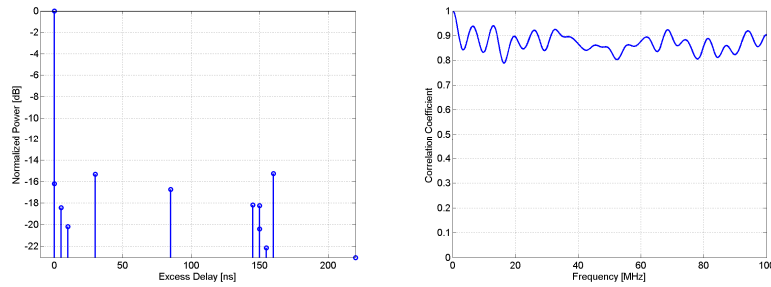


Figure 6-11: PDP and frequency correlation (FCF) of CDL model.

Table 6-12 Scenario C2: NLOS Clustered delay line model.

Cluster #	Delay [ns]			Power [dB]			AoD [°]	AoA [°]	Ray power [dB]	Cluster ASD = 2° Cluster ASA = 15° XPR = 7 dB
1	0			-6.4			11	61	-19.5	
2	60			-3.4			-8	44	-16.4	
3	75			-2.0			-6	-34	-15.0	
4	145	150	155	-3.0	-5.2	-7.0	0	0	-13.0	
5	150			-1.9			6	33	-14.9	
6	190			-3.4			8	-44	-16.4	
7	220	225	230	-3.4	-5.6	-7.4	-12	-67	-13.4	
8	335			-4.6			-9	52	-17.7	
9	370			-7.8			-12	-67	-20.8	
10	430			-7.8			-12	-67	-20.8	
11	510			-9.3			13	-73	-22.3	
12	685			-12.0			15	-83	-25.0	
13	725			-8.5			-12	-70	-21.5	
14	735			-13.2			-15	87	-26.2	
15	800			-11.2			-14	80	-24.2	
16	960			-20.8			19	109	-33.8	
17	1020			-14.5			-16	91	-27.5	
18	1100			-11.7			15	-82	-24.7	
19	1210			-17.2			18	99	-30.2	
20	1845			-16.7			17	98	-29.7	

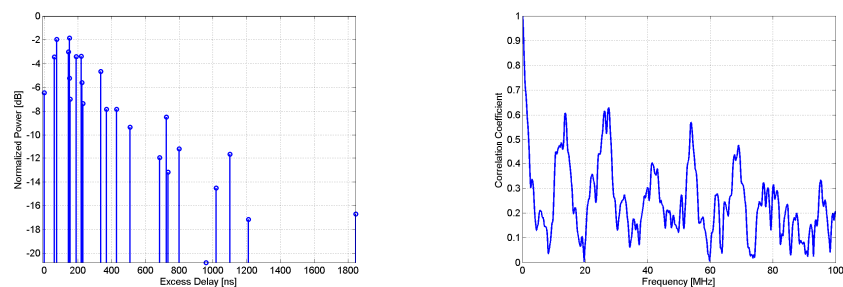


Figure 6-12: PDP and frequency correlation (FCF) of CDL model.

## 6.8 C3 – Bad urban macro-cell

The CDL parameters of NLOS condition are given below.

Table 6-13 Scenario C3: NLOS Clustered delay line model, bad urban, macrocell

Cluster #	Delay [ns]			Power [dB]			AoD [°]	AoA [°]	Ray power [dB]	Cluster ASD = 2°	Cluster ASA = 15°	XPR = 7 dB
1	0			-3.5			-9	-52	-16.5			
2	5			-8.9			14	-83	-22.0			
3	35			-4.6			-10	-60	-17.6			
4	60			-9.2			-14	-85	-22.2			
5	160	165	170	-3	-5.2	-7	0	0	-13.0			
6	180			-1.7			-6	-36	-14.7			
7	240			-2.7			7	46	-15.7			
8	275			-7			-12	74	-20.0			
9	330			-5.9			11	68	-18.9			
10	335			-6.7			-12	-72	-19.7			
11	350	355	360	-4.3	-6.5	-8.3	-10	-62	-14.3			
12	520			-5.3			-10	-64	-18.3			
13	555			-4.9			-10	-62	-17.9			
14	555			-9.4			14	85	-22.4			
15	990			-12.3			16	-98	-25.3			
16	1160			-12.2			16	-97	-25.2			
17	1390			-20.8			21	127	-33.8			
18	1825			-25.4			-23	140	-38.4			
19	4800			-9.7			-135	25	-22.7	2°	2°	
20	7100			-13			80	40	-26.0			

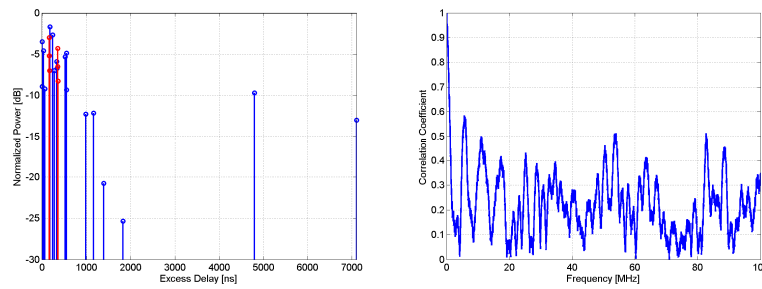


Figure 6-13: PDP and frequency correlation (FCF) of CDL model.

## 6.9 C4 – Outdoor to indoor (urban) macro-cell

The CDL parameters of NLOS condition are given below.

Table 6-14 Scenario C4: NLOS Clustered delay line model, outdoor to indoor (urban) macro-cell

Cluster #	Delay [ns]			Power [dB]			AoD [°]	AoA [°]	Ray power [dB]	Cluster ASD = 5°	Cluster ASA = 8°	XPR = 9 dB
1	0	5	10	-3.0	-5.2	-7.0	0	0	-13.0			
2	15			-6.9			28	-91	-19.9			
3	95			-3.6			-20	65	-16.6			
4	145			-16.2			43	-139	-29.3			
5	195			-8.5			-31	101	-21.5			
6	215			-15.9			43	-138	-28.9			
7	250			-6.9			28	-91	-19.9			
8	445			-14.1			-40	130	-27.1			
9	525	530	535	-3.8	-6.0	-7.8	45	-146	-13.8			
10	815			-13.6			-39	128	-26.6			
11	1055			-17.8			45	-146	-30.8			
12	2310			-32.2			-61	196	-45.2			

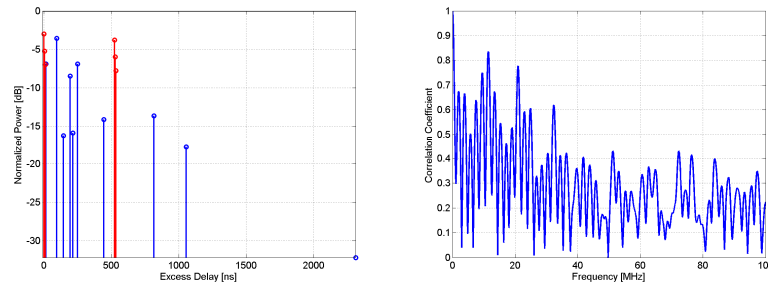


Figure 6-14: PDP and frequency correlation (FCF) of CDL model.

## 6.10 D1 – Rural macro-cell

The CDL parameters of LOS and NLOS condition are given below. In the LOS model Ricean K-factor is 5.7 dB.

Table 6-15 Scenario D1: LOS Clustered delay line model, rural environment.

Cluster #	Delay [ns]			Power [dB]			AoD [°]	AoA [°]	Ray power [dB]	
1	0	5	10	0.0	-15.0	-16.8	0	0	-0.23*	-22.8**
2	20			-15.5			17	44	-28.5	
3	20			-16.2			17	-45	-29.2	
4	25	30	35	-15.3	-17.5	-19.2	18	-48	-25.3	
5	45			-20.5			-19	50	-33.5	
6	65			-18.9			18	-48	-31.9	
7	65			-21.1			-19	51	-34.2	
8	90			-23.6			-20	-54	-36.6	
9	125			-26.1			-22	57	-39.1	
10	180			-29.4			23	-60	-42.4	
11	190			-28.3			-22	59	-41.3	

Cluster ASD = 2°

Cluster ASA = 3°

XPR = 12 dB

\* Power of dominant ray,

\*\* Power of each other ray

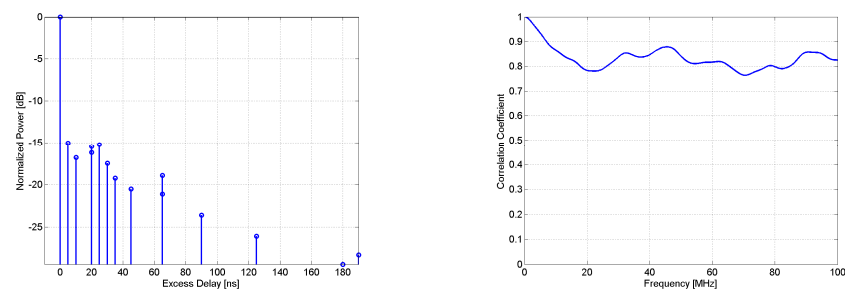
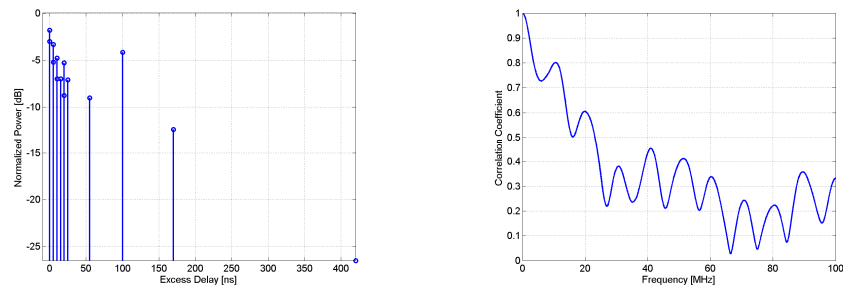


Figure 6-15: PDP and frequency correlation (FCF) of CDL model.

**Table 6-16 Scenario D1: NLOS Clustered delay line model, rural environment.**

Cluster #	Delay [ns]			Power [dB]			AoD [°]	AoA [°]	Ray power [dB]	Cluster ASD = 2°	Cluster ASA = 3°	XPR = 7 dB
1	0	5	10	-3.0	-5.2	-7.0	0	0	-13.0			
2	0			-1.8			-8	28	-14.8			
3	5			-3.3			-10	38	-16.3			
4	10	15	20	-4.8	-7.0	-8.8	15	-55	-14.8			
5	20			-5.3			13	48	-18.3			
6	25			-7.1			15	-55	-20.1			
7	55			-9.0			-17	62	-22.0			
8	100			-4.2			-12	42	-17.2			
9	170			-12.4			20	-73	-25.4			
10	420			-26.5			29	107	-39.5			

**Figure 6-16: PDP and frequency correlation (FCF) of CDL model.**

### 6.11 D2a – Moving networks

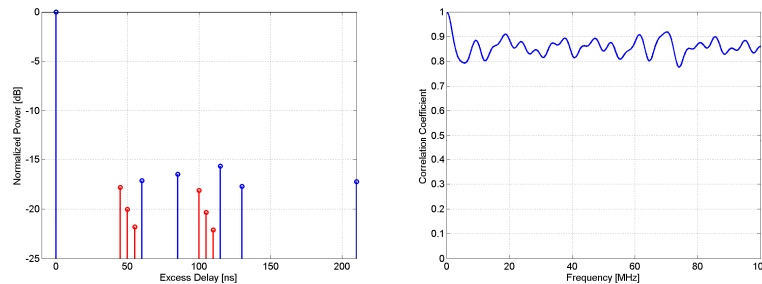
The CDL parameters of LOS condition are given below. In the LOS model Ricean K-factor is 7 dB.

**Table 6-17 Scenario D2: LOS Clustered delay line model, MRS-MS, rural**

Cluster #	Delay [ns]			Power [dB]			AoD [°]	AoA [°]	Ray power [dB]		Cluster ASD = 2°	Cluster ASA = 3°	XPR = 12 dB
1	0			0.0			0.0	0.0	-0.12*	-28.8**			
2	45	50	55	-17.8	-20.1	-21.8	12.7	-80.0		-27.8			
3	60			-17.2			-13.6	86.0		-30.2			
4	85			-16.5			13.4	84.4		-29.5			
5	100	105	110	-18.1	-20.4	-22.1	-13.9	87.5		-28.1			
6	115			-15.7			-13.0	-82.2		-28.7			
7	130			-17.7			-13.9	87.5		-30.8			
8	210			-17.3			13.7	86.2		-30.3			

\* Power of dominant ray,

\*\* Power of each other ray

**Figure 6-17: PDP and frequency correlation (FCF) of CDL model.**

## 6.12 Fixed feeder links - Scenario B5

For the stationary feeder scenarios only CDL models have been created. The CDL models are based on the parameters in the tables below which are derived mostly from literature. Note that the CDL models only approximate the selected parameters. Basically any antenna pattern can be used with the models. However, for the B5 scenario at distances larger than 300 meters the 3 dB beamwidth  $\gamma_{\text{dB}}$  of one of the link ends should be smaller than 10 degrees while the other is smaller than 53 degrees.

### 6.12.1 Scenario B5a

The clustered delay-line model for the rooftop to rooftop case is given in table below. In stationary scenarios, i.e. B5, the Doppler shifts of the rays are not a function of the AoAs. Instead, they are obtained from the movement of the scatterers. In B5 we let one scatterer per cluster be moving while the others are stationary. The Doppler frequency of the moving scatterers is also included in tables below.

**Table 6-18 Parameters selected for scenario B5a LOS stationary feeder: rooftop to rooftop.**

Parameter	Value
Power-delay profile	Exponential (non-direct paths).
Delay-spread	40ns
K-factor	10dB
XPR	30dB
Doppler	A peak centred around zero Hz with most energy within 0.1 Hz.
Angle-spread of non-direct components.	Gaussian distributed clusters with 0.5 degrees intra angle-spread. Composite angle-spread 2 degrees. Same in both ends.

**Table 6-19 LOS Clustered Delay-Line model. Rooftop-to-rooftop.**

cluster #	delay [ns]	Power [dB]	AoD [°]	AoA [°]	Freq. of one scatterer mHz	K-factor [dB]	XPR = 30dB, MS speed N/A							
1	0	-0.39	0.0	0.0	41.6	21.8	Number of rays /cluster = 20 <sup>+</sup>	Ray Power [dB]	-0.42 <sup>*</sup>	-35.2 <sup>**</sup>	cluster AS at MS [°] = 0.5	cluster AS at BS [°] = 0.5	Composite AS at MS [°] = 0.76	Composite AS at BS [°] = 1.13
2	10	-20.6	0.9	0.2	-21.5	-33.61								
3	20	-26.8	0.3	1.5	-65.2	-39.81								
4	50	-24.2	-0.3	2.0	76.2	-37.21								
5	90	-15.3	3.9	0.0	10.5	-28.31								
6	95	-20.5	-0.8	3.6	-20.2	-33.51								
7	100	-28.0	4.2	-0.7	1.3	-41.01								
8	180	-18.8	-1.0	4.0	2.2	-31.81								
9	205	-21.6	5.5	-2.0	-15.4	-34.61								
10	260	-19.9	7.6	-4.1	48.9	-32.91								

<sup>\*</sup> Power of dominant ray,

<sup>\*\*</sup> Power of each other ray

<sup>+</sup> Clusters with high K-factor will have 21 rays.



### 6.12.2 Scenario B5b

The clustered delay-line model for range1, range2 and range3 (i.e. path loss < 85 dB, 85 dB < path loss < 110 dB, path loss > 110dB), is given in tables below.

**Table 6-20 Parameters selected for scenario B5b LOS stationary feeder: street-level to street-level.**

Parameter	Value
Shadow-fading	$\sigma_{\text{free}}=3\text{dB}, r \leq r_b,$ $\sigma_{\text{beyond}}=7\text{dB}, r > r_b$
Range definition	Range 1: Loss <85, Range 2: 85<Loss<110, Range 3: Loss>110.
Power-delay profile	Exponential (of non-direct paths).
Delay-spread	Range 1: 30ns. Range 2: 110ns. Range 3: 380ns.
K-factor	Range 1: 10. Rang2: 2. Range 3: 1.
XPR	9dB.
Doppler	The spectrum has a peak at 0Hz and most of it's power within a few Hz.
Angle-spread of non-direct components.	Clusters are uniform distributed [0,360]. Intra-cluster spread is 2degrees.

**Table 6-21 Clustered delay-line model street-level to street-level range 1.**

cluster #	delay [ns]	Power [dB]	AoD [°]	AoA [°]	Freq. of one scatterer mHz	K-factor [dB]	XPR = 9dB, MS speed N/A									
1	0	-0.37	0.0	0.0	744	20.0	-	8	Number of rays/cluster = 20 <sup>+</sup>	Ray Power [dB]	-0.41 <sup>*</sup>	-33.4 <sup>**</sup>	cluster AS at MS [°] = 2	cluster AS at BS [°] = 2	Composite AS at MS [°] =22.4	Composite AS at BS [°] = 26.2
2	5	-15.9	-71.7	70.0	-5	-28.91										
3	15	-22.2	167.4	-27.5	-2872	-35.21										
4	20	-24.9	-143.2	106.4	434	-37.91										
5	40	-26.6	34.6	94.8	295	-39.61										
6	45	-26.2	-11.2	-94.0	118	-39.21										
7	50	-22.3	78.2	48.6	2576	-35.31										
8	70	-22.3	129.2	-96.6	400	-35.31										
9	105	-29.5	-113.2	41.7	71	-42.51										
10	115	-17.7	-13.5	-83.3	3069	-30.71										
11	125	-29.6	145.2	176.8	1153	-42.61										
12	135	-26.6	-172.0	93.7	-772	-39.61										
13	140	-23.4	93.7	-6.4	1298	-36.41										
14	240	-30.3	106.5	160.3	-343	-43.31										
15	300	-27.7	-67.0	-50.1	-7	-40.71										
16	345	-34.8	-95.1	-149.6	-186	-47.81										
17	430	-38.5	-2.0	161.5	-2287	-51.51										
18	440	-38.6	66.7	68.7	26	-51.61										
19	465	-33.7	160.1	41.6	-1342	-46.71										
20	625	-35.2	-21.8	142.2	-61	-48.21										

\* Power of dominant ray,

\*\* Power of each other ray

+ Clusters with high K-factor will have 21 rays.

**Table 6-22 Clustered delay-line model street-level to street-level range 2.**

cluster #	delay [ns]	Power [dB]	AoD [°]	AoA [°]	Freq. of one scatterer mHz	K-factor [dB]	XPR = 9dB, MS speed N/A									
1	0	-1.5	0.0	0.0	744	13.0	-	8	Number of rays/cluster = 20 <sup>+</sup>	Ray Power [dB]	-1.7 <sup>*</sup>	-27.7 <sup>**</sup>	cluster AS at MS [°] = 2	cluster AS at BS [°] = 2	Composite AS at MS [°] =42.8	Composite AS at BS [°] = 50.2
2	5	-10.2	-71.7	70.0	-5	-23.21										
3	30	-16.6	167.4	-27.5	-2872	-29.61										
4	45	-19.2	-143.2	106.4	434	-32.21										
5	75	-20.9	34.6	94.8	294	-33.91										
6	90	-20.6	-11.2	-94.0	118	-33.61										
7	105	-16.6	78.2	48.6	2576	-29.61										
8	140	-16.6	129.2	-96.6	400	-29.61										
9	210	-23.9	-113.2	41.7	71	-36.91										
10	230	-12.0	-13.5	-83.3	3069	-25.01										
11	250	-23.9	145.2	176.8	1153	-36.91										
12	270	-21.0	-172.0	93.7	-772	-34.01										
13	275	-17.7	93.7	-6.4	1298	-30.71										
14	475	-24.6	106.5	160.3	-343	-37.61										
15	595	-22.0	-67.0	-50.1	-7	-35.01										
16	690	-29.2	-95.1	-149.6	-186	-42.21										
17	855	-32.9	-2.0	161.5	-2288	-45.91										
18	880	-32.9	66.7	68.7	26	-45.91										
19	935	-28.0	160.1	41.6	-1342	-41.01										
20	1245	-29.6	-21.8	142.2	-61	-42.61										

\* Power of dominant ray,

\*\* Power of each other ray

+ Clusters with high K-factor will have 21 rays.

**Table 6-23 Clustered delay-line model street-level to street-level range 3.**

cluster #	delay [ns]	Power [dB]	AoD [°]	AoA [°]	Freq. of one scatterer mHz	K-factor [dB]	XPR = 9dB, MS speed N/A								
1	0	-2.6	0.0	0.0	744	10.0	Number of rays/cluster = 20 <sup>+</sup>	Ray Power [dB]	-3.0 <sup>*</sup>	-26.0 <sup>**</sup>	cluster AS at MS [°] = 2	cluster AS at BS [°] = 2	Composite AS at MS [°] =52.3	Composite AS at BS [°] = 61.42	
2	10	-8.5	-71.7	70.0	-5	-21.51									
3	90	-14.8	167.4	-27.5	-2872	-27.81									
4	135	-17.5	-143.2	106.4	434	-30.51									
5	230	-19.2	34.6	94.8	295	-32.21									
6	275	-18.8	-11.2	-94.0	118	-31.81									
7	310	-14.9	78.2	48.6	2576	-27.91									
8	420	-14.9	129.2	-96.6	400	-27.91									
9	630	-22.1	-113.2	41.7	71	-35.11									
10	635	-10.3	-13.5	-83.3	3069	-23.31									
11	745	-22.2	145.2	176.8	1153	-35.21									
12	815	-19.2	-172.0	93.7	-772	-32.21									
13	830	-16.0	93.7	-6.4	1298	-29.01									
14	1430	-22.9	106.5	160.3	-343	-35.91									

15	1790	-20.3	-67.0	-50.1	-7				-33.31				
16	2075	-27.4	-95.1	-149.6	-186				-40.41				
17	2570	-31.1	-2.0	161.5	-2287				-44.11				
18	2635	-31.2	66.7	68.7	26				-44.21				
19	2800	-26.3	160.1	41.6	-1342				-39.31				
20	3740	-27.8	-21.8	142.2	-61				-40.81				

\* Power of dominant ray,

\*\* Power of each other ray

+ Clusters with high K-factor will have 21 rays.

### 6.12.3 Scenario B5c

Model for B5c scenario is same with B1 LOS. Difference is that in B5c both the environment and both link ends are stationary except two clusters, which represent moving vehicles. In these two clusters all the rays have different non-zero Doppler frequency.

**Table 6-24 B5c Clustered Delay-Line model.**

cluster #	delay [ns]	Power [dB]	AoD [°]	AoA [°]	Freq. of one scatterer [mHz]	K-factor [dB]	XPR = 9dB, MS speed N/A							
1	0	0	0	0	-127	3.3	Number of rays/cluster = 20 <sup>+</sup>	Ray Power [dB]	-1.67*	-18.0**	cluster AS at MS [°] = 18	cluster AS at BS [°] = 3	Composite AS at MS [°] = 45.0	Composite AS at BS [°] = 4.5
2	30	-11.7	5	45	385	-24.71								
3	55	-14.8	8	63	-879	-27.81								
4	60	-14.8	8	-69	++	-27.81								
5	105	-13.9	7	61	+++	-26.91								
6	115	-17.8	8	-69	-735	-30.81								
7	250	-19.6	-9	-73	-274	-32.61								
8	460	-31.4	11	92	691	-44.41								

\* Power of dominant ray,

\*\* Power of each other ray

+ Clusters with high K-factor will have 21 rays.

++ Frequency for 20 scatterers in Hz is {45.0, 45.5, 46.0, 46.5, ..., 54.5}

+++ Frequency for 20 scatterers in Hz is {-55.0, -55.5, -56.0, -56.5, ..., -64.5}

### 6.12.4 Scenario B5f

Model for B5f scenario is NLOS version of B5a model.

**Table 6-25 Parameters selected for scenario B5f NLOS stationary feeder: rooftop to rooftop.**

Parameter	Value
Power-delay profile	Exponential (non-direct paths).
Delay-spread	85ns
K-factor	-∞ dB
XPR	10dB
Doppler	A peak centred around zero Hz with most energy within 0.1 Hz.

**Table 6-26 B5f Clustered Delay-Line model. Rooftop-to-rooftop NLOS.**

cluster #	delay [ns]	Power [dB]	AoD [°]	AoA [°]	Freq. of one scatterer [mHz]	K-factor [dB]	XPR = 10dB, MS speed N/A						
1	0	-0.1	0.0	0.0	41.6	-∞	Number of rays /cluster = 20	Ray Power [dB]	-13.11	cluster AS at MS [°] = 0.5	cluster AS at BS [°] = 0.5	Composite AS at MS [°] = 2.33	Composite AS at BS [°] =2.87
2	10	-5.3	0.9	0.2	-21.5				-18.31				
3	20	-11.5	0.3	1.5	-65.2				-24.51				
4	50	-8.9	-0.3	2.0	76.2				-21.91				
5	90	0.0	3.9	0.0	10.5				-13.01				
6	95	-5.2	-0.8	3.6	-20.2				-18.21				
7	100	-12.7	4.2	-0.7	1.3				-25.71				
8	180	-3.5	-1.0	4.0	2.2				-16.51				
9	205	-6.3	5.5	-2.0	-15.4				-19.31				
10	260	-4.6	7.6	-4.1	48.9				-17.61				

## 7. References

- [3GPPSCM] 3GPP TR 25.996, “3<sup>rd</sup> Generation Partnership Project; technical specification group radio access networks; spatial channel model for MIMO simulations (release 6)”, V6.1.0.
- [AGV98] Pauli Aikio, Ralf Gruber and Pertti Vainikainen, Wideband radio channel measurements for train tunnels. VTC 1998.
- [AHY06] M. Alatossava, V-M. Holappa, J. Ylitalo, “Outdoor to indoor MIMO radio channel measurements at 5.25 GHz – characterization of propagation parameters”, EUCAP, November 2006, Nice, France.
- [AI00] Farrokh Abrishamkar, James Irvine, Comparison of Current Solutions for the Provision of Voice Services to Passengers on High Speed Trains. IEEE VTC-Fall, VTC 2000. 24 - 28 Sept. 2000.
- [APM02] A. Algans, K. I. Pedersen, P.E. Mogensen, “Experimental analysis of the joint statistical properties of azimuth spread, delay spread and shadow fading”, IEEE J. Selected Areas in Comm., Vol. 20, pp.523-531, 2002.
- [AP02] J. B. Andersen and K. I. Pedersen, “Angle-of-arrival statistics for low resolution antennas,” IEEE Trans. Antennas Propagat., vol. 50, pp. 391–395, Mar. 2002.
- [B+03] R. J. C. Bultitude et al., “A propagation-measurement-based evaluation of channel characteristics and models pertinent to the expansion of mobile radio systems to frequencies beyond 2 GHz,” IEEE Trans. VT, vol. 56, no. 2, pp. 382-388, Mar. 2007
- [Bul02] Bultitude, R.J.C., “A Comparison of Multipath-Dispersion-Related Micro-Cellular Mobile Radio Channel Characteristics at 1.9 GHz and 5.8 GHz”, in Proc. ANTEM’02, Montreal, Jul. 31 – Aug. 2, 2002, pp. 623-626.
- [BB89] R.J.C. Bultitude, and G.K.Bedal, “Propagation characteristics on microcellular urban mobile radio channels at 910 MHz,” IEEE J. Select. Areas Commun, vol.7, no. 1, 1989, pp. 31-39.
- [Bul02] R.J.C. Bultitude., “Estimating frequency correlation functions from propagation measurements on fading radio channels: A critical review,” IEEE J. Select. Areas Commun. Vol. 20, no. 6, August, 2002, pp. 1133-1143.
- [BBK04] M.D. Batarie, T.K. Blankenship, J.F. Kepler, T.P. Krauss, “Seasonal variations in path loss in the 3.7 GHz band”, IEEE RAWCON, pp. 399-402, 2004.
- [BBK+02] M.D. Batarie, T.K. Blankenship, J.F. Kepler, T.P. Krauss, I. Lisica, S. Mukthvaram, J.W. Porter, T.A. Thomas, F.W. Vook: “Wideband MIMO mobile impulse response measurements at 3.7 GHz”, IEEE 55<sup>th</sup> VTC, pp. 26-30, 2002.
- [BHS05] D. Baum, J. Hansen, J. Salo, G. Del Galdo, M. Milojvic, P. Kyösti: “An Interim Channel Model for Beyond-3G Systems”, IEEE VTC’05, April 2005.
- [Cal+07] G. Calcev, D. Chizhik, B. Goeransson, S. Howard, H. Huang, A. Kogiantis, A. F. Molisch, A. L. Moustakas, D. Reed and H. Xu, “A Wideband Spatial Channel Model for System-Wide Simulations”, IEEE Trans. Vehicular Techn., March 2007.
- [CBW95] D. J. Cichon, T. C. Becker, W. Wiesbeck, “Determination of Time-Variant Radio Links in High-Speed Train Tunnels by Ray Optical Modeling”. AP-S 1995.
- [Cha03] Ashok Chandra, Propagation of 2000 MHz Radio Signal into A Multi-Storeyed building Through Outdoor-Indoor Interface. The 14<sup>th</sup> IEEE 2003 International Symposium on Personal, Indoor and Mobile Radio Communication Proceedings. 2003.
- [C02] M. Celidonio, “Outdoor-indoor propagation measurements in the 3.6-4.2 GHz band”, IEEE 13th PIMRC, Vol. 2, pp. 644-648, 2002.
- [CG99] T.-S. Chu, and L. J. Greenstein, “A quantification of link budget differences between the cellular and PCS bands,” IEEE Trans VT, vol. 48, no. 1, pp. 60-65, Jan. 1999.
- [CKC03] A. Chandra, A. Kumar, P. Chandra, “Propagation of 2000 MHz radio signal into a multi-storeyed building through outdoor-indoor interface”, Proceedings on 14th PIMRC, Vol. 3, pp. 2983-2987, 2003.

- [COST231] European Commission: European cooperation on the field of scientific and technical research (EURO-COST 231): "Digital mobile radio towards future generation systems", Final report, <http://www.lx.it.pt/cost231/>, Bruxelles, 1999.
- [DDA00] Michael Doehler, Monica Dell' Anna, A. H. Aghvami, Pdf - Transformation for the Outdoor-Indoor Propagation Model. VTC 2000-Spring. 2000, 15 – 18 May 2000 Pages 1646-1650 Vol. 3.
- [deJKH02] Y.L.C.deJong. M.H.J.L Koelen, and M.H.J.Herben, "A building transmission model for improved propagation prediction in urban microcells," IEEE Trans., Veh. Technol., vol. 53, no. 2, 2002.
- [DRX98] G. Durkin, T.S Rappaport, H". Xu."Measurements and models for radio path loss and penetration in and around homes and trees at 5.85 GHz, IEEE Trans. Comm., Vol. 46, pp.1484-1496, 1998.
- [EGT+99] V. Erceg, L.J. Greenstein, S. Tjandra, S. Parkoff, A. Gupta, B. kulic, A. Julius, R. Bianci., "An empirically based path loss model for wireless channels in suburban environments", IEEE J. Sel. Areas Comm., Vol. 17, pp. 1205-1211, 1999.
- [Erc+01] V. Erceg, et al., "Channel Models for Fixed Wireless Applications" (IEEE802.16.3c-01/29r4), IEEE P802.16, Broadband Wireless Working Group, 2001.
- [ESB+04] V. Erceg, P. Soma, D.S. Baum, S. Catreux, "Multiple-input multiple-output fixed wireless radio channel measurements and modeling using dual-polarized antennas at 2.5 GHz" in IEEE Trans. on Wireless Communications, Vol 3, Nov 2006.
- [FDS+94] Foster, H.M.; Dehghan, S.F.; Steele, R.; Stefanov, J.J.; Strelouhov, H.K., "Microcellular measurements and their prediction", IEE Colloquium on "Role of Site Shielding in Prediction Models for Urban Radiowave Propagation" (Digest No. 1994/231), Nov. 1994, pp. 2/1 - 2/6.
- [Fuj03] T. Fujii, "Path loss prediction formula in mobile communication -an expansion of "SAKAGAMI" path loss prediction formula-," Trans. IEICE, Japan, J86-B, 10, pp. 2264-2267, 2003.
- [GEA03] S. Geng et al., "Measurements and Analysis of Wideband Indoor Radio Channels at 60 GHz," Proc. of 3rd ESA Workshop on Millimeter Wave Technology and Applications, Espoo, Finland, May 21-23, 2003.
- [GEY97] L.J. Greenstein, V. Erceg, Y.S. Yeh, M.V. Clark, "A new path-gain/delay spread model for digital cellular channels", IEEE Trans. Veh. Tech., Vol. 46, pp. 477-485, 1997.
- [GRZ07] Guo Rui Zhang, "Measurement and Characterisation of Delay, Angular and Frequency Dispersion and their Evolution at Mobile Receivers in 2.25 GHz Microcells," M.Sc. Thesis. Report, Dept. of Systems and Computer Engineering, Carleton University, Ottawa, to be submitted, spring 2007.
- [GTD+04] M. Ghaddar, L. Talbi, T.A. Denidni, A. Charbonneau, "Modeling human body effects for indoor radio channel using UTD", in Canadian Conference on Electrical and Computer Engineering, Vol. 3, Pages: 1357- 1360, 2-5 May 2004
- [Gud91] M. Gudmundson, "Correlation model for shadow fading in mobile radio systems", Electron. letter, vol. 27, pp. 2145-2146, Nov. 1991.
- [ITU] ITU Rec. ITU-R P.1238-4.
- [ITU-R] Rec. ITU-R P.1546-2, "Method for point-to-area predictions for terrestrial services in the frequency range 30 MHz to 3000 MHz"
- [JHH+05] T. Jämsä, V. Hovinen, L. Hentilä, and J. Iinatti, "Comparisons of Wideband and Ultra-wideband channel measurements " IEEE IWS2005/WPMC2005, Aalborg, Denmark.
- [KeM90] J.M Keenan, A.J. Motley, "Radio coverage in buildings", British Telecom Tech. Journal, vol.8, no.1, Jan. 1990, pp.19-24.
- [KI04] K. Kitao, S. Ichitsubo, "Path loss prediction formula for microcell in 400 MHz to 8 GHz band", Electronics Letters, Vol. 40, No. 11, 2004.
- [KJ07] Pekka Kyösti and Tommi Jämsä, "Complexity Comparison of MIMO Channel Modelling Methods", ISWCS'07, Trondheim, Norway, October 2007.

- [KKM02] J. F. Kepler, T.P. Krauss, S. Mukthvaram: "Delay spread measurements on a wideband MIMO channel at 3.7 GHz", IEEE 56th VTC, pp. 2498-2502, 2002.
- [KBM+06] Sandra Knoerzer, Michael A. Baldauf, Juergen Maurer, Werner Wiesbeck, "OFDM for Multimedia Applications in High-Speed Trains: Channel Model Including Different Antenna Types.", 2006.
- [KMV+05] Sandra Knoerzer, Juergen Maurer, Sven Vogeler, Karl-Dirk Kammeyer and Werner Wiesbeck, "Channel Modeling for a High-Speed Train OFDM Communication Link Supporting High Data Rates". ITST 2005.
- [KP02] M. B. Knudsen, Member, IEEE, and G. F. Pedersen, "Spherical Outdoor to Indoor Power Spectrum Model at the Mobile Terminal", IEEE Journal on Selected Areas in Communications, vol. 20, no. 6, August 2002.
- [KRB00] A. Kuchar, J-P. Rossi, E. Bonek: "Directional macro-cell channel characterization from urban measurements", IEEE Trans. Antennas and Propagation, Vol. 48, pp.137-145, 2000.
- [KSL+02] K. Kalliola, K. Sulonen, H. Laitinen, O. Kivekäs, J. Krogerus, P. Vainikainen: "Angular power distribution and mean effective gain of mobile antenna in different propagation environments", IEEE Trans. Veh. Techn., Vol. 51, pp.823-838, 2002.
- [KZV99] J. Kivinen, X. Zhao and P. Vainikainen, "Wideband Indoor Radio Channel Measurements with Direction of Arrival Estimations in the 5 GHz Band," *Proc. of IEEE Vehicular and Technology Conference (VTC'99)*, pp. 2308-2312, Netherlands, 1999.
- [Lan02] J. Nicholas Laneman "Cooperative Diversity in Wireless Networks: Algorithms and Architectures," PhD thesis, sep. 2002
- [Medav] <http://www.channelsounder.de>
- [MEJ91] P.E. Mogensen, P. Eggers, C. Jensen: "Urban area radio propagation measurements for GSM/DCS 1800 macro and micro cells", ICAP 91, pp. 500-503, 1991.
- [MHA+04] J. Medbo, F. Harryson, H. Asplund, J-E. Berg, "Measurements and analysis of a MIMO macrocell outdoor-indoor scenario at 1947 MHz", IEEE 59th VTC, Vol. 1, pp. 261-265, 2004.
- [MKA02] Masui, H.; Kobayashi, T.; Akaike, M., "Microwave path-loss modeling in urban line-of-sight environments," IEEE Journal on Selected Areas in Communications, Vol. 20, Iss. 6, Aug. 2002, pp. 1151-1155.
- [MOT02] Y. Miura, Y. Oda, T. Taka, "Outdoor-to indoor propagation modelling with the identification of path passing through wall openings", IEEE 13th PIMRC, Vol. 1, pp. 130-134, 2002
- [MRA93] L. Melin, M. Rönnlund, R. Angbratt: "Radio wave propagation – a comparison between 900 and 1800 MHz", IEEE 43<sup>rd</sup> VTC conference, pp. 250-252, 1993.
- [NAP05] H. T. Nguyen, J. B. Andersen, G. F. Pedersen, "Characterization of the indoor/outdoor to indoor MIMO radio channel at 2.140 GHz", Department of Communication Technology, Aalborg, Denmark, 2005.
- [OP04] C. Oestges, and A.J. Paulraj, "Propagation into buildings for Broadband Wireless Access," IEEE Trans. Veh. Techn., vol. 53, No. 2, pp. 521-526, March 2004.
- [OBL+02] J. Ojala, R. Böhme, A. Lappeteläinen and M. Uno, "On the propagation characteristics of the 5 GHz rooftop-to-rooftop meshed network," IST Mobile & Wireless Telecommunications Summit 2002, Jun. 2002, Thessaloniki, Greece.
- [OC07] C. Oestges, and B. Clerckx, "Modeling outdoor macrocellular clusters based on 1.9-GHz experimental data," IEEE Trans. Veh. Tech., vol. 56, No. 6, November 2007.
- [OVC06] C. Oestges, D. Vanhoenacker-Janvier, B. Clerckx, "Channel Characterization of Indoor Wireless Personal Area Networks", in IEEE Transactions on Antennas and Propagation, Vol. 54, Issue 11, Pages:3143 – 3150, Nov. 2006.
- [OKT+04] Ohta, G.I.; Kamada, F.; Teramura, N.; Hojo, H., "5 GHz W-LAN verification for public mobile applications - Internet newspaper on train and advanced ambulance car", Consumer Communications and Networking Conference, 2004. CCNC 2004. First IEEE. Volume , Issue , 5-8 Jan. 2004 Page(s): 569 – 574.

- [OOK+68] Y. Okumura, E. Ohmori, T. Kawano, K. Fukuda: "Field strength and its variability in VHF and UHF land-mobile radio services", Review of the Electrical Comm. Lab., Vol. 16, No 9. 1968.
- [OTT+01] Y. Oda, R. Tsuchihashi, K. Tsunekawa, M. Hata, "Measured path loss and multipath propagation characteristics in UHF and microwave frequency band for urban mobile communications", VTC 2001 Spring, Vol.1, pp. 337-341, 2001.
- [Pab04] Ralf Pabst *et al.*, "Relay based deployment concepts for wireless and mobile broadband radio," IEEE communication magazine, Sep. 2004, pp 80-87.
- [Paj03] P. Pajusco: "Double characterisations of power angle spectrum in macrocell environment", Electronics Letters, Vol. 39, pp. 1565-1567, 2003.
- [Pap05] P. Papazian, "Basic transmission loss and delay spread measurements for frequencies between 430 and 5750 MHz", IEEE Trans. Ant. Propagation, Vol. 53, pp. 694-701, 2005.
- [PCH01] E. Perahia, D. Cox, S. Ho, "Shadow fading cross-correlation between base stations", IEEE VTC, pp. 313-317, May 2001.
- [PLB04] J.W. Porter, I. Lisica, G. Buchwald, "Wideband mobile propagation measurements at 3.7 GHz in an urban environment", IEEE Ant. Propagat. Intern. Symposium, Vol. 4, pp. 3645-3846, 2004.
- [PLN+99] M. Pettersen, P. H. Lehne, J. Noll, O. Rostbakken, E. Antonsen, R. Eckhoff, "Characterization of the directional wideband radio channel in urban and suburban areas", IEEE 50<sup>th</sup> VTC, pp. 1454-1459, 1999.
- [PMF00] K. I. Pedersen, P.E. Mogensen, B.H. Fleury, "A stochastic model of the temporal and azimuthal dispersion seen at the base station in outdoor propagation environments", IEEE Trans. Veh. Technol., Vol. 49, pp. 437-447, 2000.
- [Psound] <http://www.propsim.com>
- [PT00] J. W Porter and J. A Thweatt, "Microwave Propagation Characteristics in the MMDS Frequency Band," in Proc. IEEE ICC'00, Jun. 2000, Vol. 3, pp. 1578-1582.
- [RMB+06] M. Riback, J. Medbo, J.-E. Berg, F. Harrysson, and H. Asplund, "Carrier Frequency Effects on Path Loss," IEEE VTC 2006-Spring, vol. 6, pp. 2717-2721, 2006.
- [RSS90] T. Rappaport, S. Seidel, R. Singh, "900-MHz multipath propagation measurements for U.S. digital cellular radiotelephone", IEEE Trans. Veh. Technol., Vol. 39, pp.132-139, 1990.
- [RKJ05] T. Rautiainen, K. Kalliola, J. Juntunen, "Wideband radio propagation characteristics at 5.3 GHz in suburban environments", PIMRC Berlin, Vol. 2, pp. 868-872, 2005.
- [RJK07] T. Rautiainen, J. Juntunen, K. Kalliola, "Propagation analysis at 5.3 GHz in typical and bad urban macrocellular environments", VTC Dublin, April 2007.
- [RWH02] T. Rautiainen, G. Wölfle, R. Hoppe, "Verifying path loss and delay spread predictions of a 3D ray tracing model in urban environment", IEEE 56<sup>th</sup> Veh. Technol. Conf., Vol. 4, pp. 2470-2474, Sept. 2002.
- [Rudd03] R.F. Rudd, "Building penetration loss for slant-paths at L-, S- and C-band." ICAP 2003, 31.3.-1.4, 2003.
- [Sau99] S. Saunders "Antenna and propagation for communication systems concept and design", Wiley, 1999.
- [SG02] S. Salous, H. Gokalp, "Dual-frequency sounder for UMTS frequency-division duplex channels", IEE Proc. Comm., Vol. 149, pp. 117-122, 2002.
- [SRJ+91] S. Seidel, T. Rappaport, S. Jain, K. Lord, R. Singh, "Path loss, scattering, and multipath delay statistics in four European cities for digital cellular and microcellular radiotelephone", IEEE Trans. Veh. Technol., Vol. 40, pp. 721-730, 1991.
- [SBA+02] Schenk, T.C.W., Bultitude, R.J.C., Augustin, L.M., van Poppel, R.H., and Brussaard, G., "Analysis of Propagation loss in Urban Microcells at 1.9 GHz and 5.8 GHz," in Proc. URSI Commission F Open Symposium on Radiowave Propagation and Remote Sensing, Garmisch-Patenkirchen, Germany, Feb. 2002.



- [SCK05] N. Skentos, Constantinou and A. G Kanatas, "Results from Rooftop to Rooftop MIMO Channel Measurements at 5.2 GHz," COST273 TD(05)59, Bologna, Jan. 19-21.
- [SCT03] A. Seville, S. Cirstea and J.F. Taylor. Effects of propagation between the indoor and outdoor environment. ICAP 2003. 31.3.-1.4. 2003.
- [SG00] T. Schwengler, M. Gilbert:"Propagation models at 5.8 GHz - path loss and building penetration", IEEE Radio and Wireless Conference 10-13 Sep. 2000, pp. 119-124.
- [SJD94] E. Sousa, V. Jovanovic, C. Dainegault, "Delay spread measurements for the digital cellular channel in Toronto", IEEE Trans. Veh. Technol., Vol. 43, pp. 837-846, 1994.
- [SMI+00] H. Shimizu, H. Masui, M. Ishi, K. Sakawa, and T. Kobayashi, "LOS and NLOS Path-Loss and Delay Characteristics at 3.35 GHz in a Residential Environment," IEEE Antennas and Propagation Society International Symposium 2000, Vol. 2, Jul. 2000, pp. 1142 - 1145.
- [SMI+02] K. Sakawa, H. Masui, M. Ishii, H. Shimizu, T. Kobayashi, "Microwave path-loss characteristics in an urban area with base station antenna on top of a tall building", Int. Zurich Seminar on Broadband communications, pp. 31-1 -31-4, 2002.
- [SMJ+99] A. M. Street, J. G. O. Moss, A. P. Jenkins, D. J. Edwards, "Outdoor-indoor wideband study for third generation communication systems", IEE National Conference on Antennas and Propagation, pp. 128-131, 1999.
- [SS01] S. Stavrou, S. R. Saunders, "A deterministic outdoor to indoor propagation modeling approach", IEEE 54th VTC, Vol. 2, pp. 1097-1100, 2001.
- [SMB01] M. Steinbauer, A. F. Molisch, and E. Bonek, "The double-directional radio channel," IEEE Antennas and Propagation Mag., pp. 51-63, August 2001.
- [SV87] A. Saleh, and R. A. Valenzuela, A statistical model for indoor multipathpropagation, IEEE J. Select. Areas Commun., vol. SAC-5, no. 2, Feb. 1987, pp. 128-137.
- [Sva02] Svantesson, T., "A double-bounce channel model for multi-polarized MIMO systems," in Proc. IEEE VTC'02-Fall, Vol. 2, Sep. 2002, pp. 691 - 695.
- [TPE02] S. Thoen, L. Van der Perre, and M. Engels, "Modeling the Channel Time-Variance for Fixed Wireless Communication", IEEE Communication Letters, Vol. 6, No. 8, Aug. 2002.
- [VES00] F. Villanese, N.E. Evans, W.G. Scanlon, "Pedestrian-induced fading for indoor channels at 2.45, 5.7 and 62GHz", in IEEE VTS-Fall VTC 2000, Vol. 1, Pages: 43-48 vol.1, 2000.
- [VKV04] L. Vuokko, J. Kivinen, P. Vainikainen., "Results from 5.3 GHz MIMO measurement campaign", COST273, TD(04)193, Duisburg, Germany, 20.-22.9.2004.
- [WAE+04] S. Wyne, P. Almers, G. Eriksson, J. Karedal, F. Tufvesson, A. F. Molisch, "Outdoor to indoor office MIMO measurements at 5.2 GHz", IEEE 60th VTC, pp. 101-105, 2004.
- [WHL94] J.A. Wepman, J.R. Hoffman, L.H. Loew,"Characterization of macrocellular PCS propagation channels in the 1850-1990 MHz band, 3rd Annual International Conference on Universal Personal Communications, pp. 165-170, 1994.
- [WHL+93] J.A. Wepman, J.R. Hoffman, L.H. Loew, W.J. Tanis, M.E. Hughes: "Impulse response measurements in the 902.928 and 1850.1990 MHz bands in macrocellular environments", 2nd international conference on Universal Personal Communications, Vol. 2, pp. 590-594, 1993.
- [WIN1D54] WINNER1 WP5: "Final Report on Link Level and System Level Channel Models" Deliverable D5.4, 18.11.2005
- [WIN1D72] WINNER WP7, System assessment criteria specification, v1.0.
- [WIN2IR111] WINNER2 WP1: "Propagation Scenarios", Internal Report IR1.1.1, 22.5.2006.
- [WIN2UCM] WINNER2 WP1: "Updated Channel Models", Internal, June 2006.
- [WINNERII] WINNER II Contract, Annex I – "Description of Work", IST-4-027756, 25/10/2005.
- [WAE+04] S. Wyne, P. Almers, G. Eriksson, J. Karedal, F. Tufvesson, and A. F. Molisch, Outdoor to Indoor Office MIMO Measurements at 5.2 GHz. VTC 2004-Fall. 2004 IEEE 60<sup>th</sup> Volume 1, 26-29 Sept. 2004 Pages 101-105 Vol. 1.

- [WH02] J. Weitzen, T. J. Lowe, "Measurement of angular and distance correlation properties of log-normal shadowing at 1900 MHz and its application to design of PCS systems", IEEE transactions on vehicular technology, vol. 51, No. 2, march 2002.
- [WMA+05] S. Wyne, A. F. Molisch, P. Almers, G. Eriksson, J. Karedal, F. Tufvesson, "Statistical evaluation of outdoor-to-indoor office MIMO measurements at 5.2 GHz", IEEE 61st VTC, Vol. 1, pp. 146-150, 2005.
- [WOT99] G. Woodward, I. Oppermann, J. Talvitie, "Outdoor-indoor temporal & spatial wideband channel model for ISM bands", IEEE 50th VTC, Vol. 1, pp. 136-140, 1999.
- [ZEA99] X. Zhao et al, "Diffraction over typical-shaped terrain obstacles," Journal of Electromagnetic Waves and Applications, vol. 13, pp. 1691-1707, 1999.
- [Zet05] P. Zetterberg, "Auto and Multi-Site Correlation of Large Scale Parameters: Model Evolution", Internal WINNER document, Aug. 2005.
- [Xia96] H.H. Xia:" An analytical model for predicting path loss in urban and suburban environments", Seventh IEEE Int. Symposium PIMRC, Vol 1, pp. 19.23, 1996
- [XBM+94] H. Xia, H. Bertoni, L. Maciel, A. Lindsey-Steward, R. Rowe, "Microcellular propagation characteristics for personal communications in urban and suburban environments", IEEE Trans. Veh. Technol., Vol. 43, pp- 743-752, 1994.
- [YIT06] Yonezawa, Ishikawa, Takeuchi, "Frequency range extension of path loss prediction formula for over-rooftops propagation in microwave band", IEEE International Symp. Antennas Propagation, pp. 4747-4750, 2006.
- [YMI+04] K. Yonezawa, T. Maeyama, H. Iwai, H. Harada:" Path loss measurement in 5 GHz macro cellular systems and considerations of extending existing path loss prediction models", IEEE WCNC, Vol. 1, pp. 279-283, 2004.
- [ZKV+02] X. Zhao, J. Kivinen, P. Vainikainen, K. Skog:"Propagation characteristics for wideband outdoor mobile communications at 5.3 GHz", IEEE Sel. Areas Comm., Vol. 20, pp. 507-514, 2002.
- [ZRK+06] X. Zhao, T. Rautiainen, K. Kalliola, P. Vainikainen, "Path-loss models for urban microcells at 5.3 GHz, IEEE Antennas and Propag. Lett., Vol. 5, pp. 152-154, 2006.